

THESIS FOR THE DEGREE OF DOCTOR OF PHILOSOPHY (PhD)

Human SGBS cells can serve for modelling of adipocyte browning

by Ágnes Klusóczki

Supervisor: Prof. Dr. László Fésüs



UNIVERSITY OF DEBRECEN

DOCTORAL SCHOOL OF MOLECULAR CELL AND IMMUNE BIOLOGY

DEBRECEN, 2019

TABLE OF CONTENTS

1. ABBREVIATIONS	5
2. INTRODUCTION	7
2.1. Obesity and adipose tissue	7
2.1.1. White adipose tissue	9
2.1.2. Brown adipose tissue	10
2.2. The development of brown and beige adipocytes	12
2.2.1. The origin of classical brown adipocytes	13
2.2.2. The origin of beige adipocytes	14
2.3. Activators of brown and beige adipocyte development & function	19
2.4. UCP1	21
2.5. Browning inducers which directly target adipose tissue	23
2.6. UCP1 independent mechanisms of thermogenesis	24
2.6.1. SERCA pump	24
2.6.2. Futile cycle of creatine	26
2.6.3. The Glycerol 3-phosphate shuttle	27
2.7. Secreted factors by the adipose tissue	28
2.8. SGBS cells	30
2.9. Transglutaminase 2	33
3. AIMS OF THE STUDY	35
4. MATERIALS AND METHODS	36
4.1. Materials	36
4.1.1. Cell Culture Media	36
4.1.2. Antibodies	36
4.1.3. Cell dyes	36
4.1.4. Reagents, plates	37
4.2. Methods	38
4.2.1. Ethics statement	38
4.2.2. Obtained samples and isolation of hADMSCs	38
4.2.3. Flow cytometry: characterization of adipose tissue-derived stem cells	39
4.2.4. Cell culture and differentiation of human SGBS preadipocytes into mature white and brown adipocytes	39
4.2.5. RNA isolation, TaqMan™ reverse transcription-coupled quantitative (RT-PCR), qPCR	42
4.2.6. Total DNA isolation and mitochondrial DNA quantification	43

4.2.7. Antibodies and immunoblotting	44
4.2.8. Immunofluorescence staining.....	44
4.2.9. Laser scanning cytometry	45
4.2.10. Oxygen consumption and extracellular acidification measurements	46
4.2.11. Determination of cytokine release	47
4.2.12. Genotyping	47
4.2.13. Statistical analysis	48
5. RESULTS.....	48
5.1. SGBS cells express surface markers similarly to primary preadipocytes and are heterozygous for the FTO risk allele Rs1421085.....	49
5.2. SGBS preadipocytes respond to sustained PPAR γ ligand and irisin or BMP7 treatment by inducing either beige or classical brown marker genes.....	52
5.3. Laser scanning cytometry can quantify SGBS adipocyte browning.	63
5.4. Differentiated SGBS adipocytes respond to activation as functional beige cells and can use the creatine phosphate cycle.....	66
5.5. The brown/beige adipocyte phenotype of differentiated SGBS cells is maintained in the absence of the PPAR γ -ligand.	69
5.6. Browning cocktail resulted in increased expression of IL-8, IL-6 and MCP1 cytokines compared to white adipocytes.	74
5.7. Continuous inhibition of the IL-6 receptor resulted in a downregulation of UCP1 and extracellular acidification during browning differentiation.	76
5.8. TG2 is expressed at a higher level in browned adipocytes and as a result of its inhibition both TG2 and UCP1 expression decreased.....	81
6. DISCUSSION	89
1. Distribution of BAT in the human body and studying browning of hADMSCs.....	89
2. Human preadipocyte cell lines exist and have some features consistent with having browning capacity.....	90
3. Interpretation of SGBS adipocyte browning observed by other groups.....	91
4. SGBS cells are able to differentiate into brown or beige adipocytes, and respond to either rosiglitazone, irisin or BMP7.	96
5. FTO locus is connected to beige or “masked beige” potential of adipocytes.	98
6. Cytokine secretion of SGBS cells and hADMSCs.....	99
7. The role of transglutaminase 2 and its inhibitor in SGBS adipocyte differentiation.....	100
7. SUMMARY	102
ÖSSZEFOGLALÁS	104

8. REFERENCES	106
9. KEYWORDS	129
10. ACKNOWLEDGEMENTS	130

1. ABBREVIATIONS

α – MSH: Alpha-Melanocyte-Stimulating Hormone
ADMSC: Adipose tissue-derived mesenchymal stem cells
ANOVA: Analysis of variance
BAT: Brown adipose tissue
 β -GPA: β -guanidinipropionic acid
BMI: Body mass index
BMP: Bone morphogenetic protein
BMP7: Bone morphogenic protein 7
BMP8b: Bone morphogenic protein-8b
BMR: Basal Metabolic Rate
cAMP/cGMP: 3',5'-cyclic adenosine monophosphate/3',5'-cyclic guanosine monophosphate
C/EBP/ β : CCAAT/enhancer binding protein beta
CIDEA: Cell death-inducing DFFA-like effector A
CITED1: Cnp/P300 Interacting Transactivation With Glu/Asp Rich Carboxy-Terminal Domain 1
CKMT1/2: Creatine Kinase, Mitochondrial $\frac{1}{2}$
Ct: Threshold cycle
CREB: cAMP Response Element Binding Protein
CYC1: Cytochrome C1
DHAP: Dihydroxyacetone Phosphate
DKO: Double knock-out
DMEM/F12: Dulbecco's Modified Eagle's Medium/Nutrient Mixture F-12 Ham 1:1 mixture
DMSO: Dimethyl sulfoxide
EBF2: Early B-cell-factor-2
EDTA: Ethylene Diamine Tetraacetic Acid
EGF: Epidermal growth factor
EHMT1: Euchromatic histone lysine methyltransferase 1
ELISA: Enzyme-Linked Immunosorbent Assay
ELOVL3: ELOVL Fatty Acid Elongase 3
EN1: Engrailed-1
EWS: Ewing sarcoma breakpoint region 1
FABP4: Fatty acid binding protein 4
FAD/FADH2: Flavin adenine dinucleotide
FBS: Fetal Bowine Serum
FC: Fold change
 ^{18}F -FDG: [^{18}F]-2-fluoro-D-2-deoxy-D-glucose
FGF21: Fibroblast Growth Factor-21
FNDC5: Fibronectine Type III Domain Containing 5
FOXC2: Forkhead box protein C2
FTO: Fat Mass and Obesity Associated
FXIII: blood coagulation factor XIII A-subunit
GAPDH: Glyceraldehyde-3-phosphate dehydrogenase
GPC-3: Glypican-3
GPDH: Glycerol-3-phosphate dehydrogenase
IMBX: 3-Isobutyl-1-methylxantin
hADMSCs: Human adipose-derived mesenchymal stem cells

HEPES: 4-(2-hydroxyethyl)-1-piperazineethanesulfonic acid
 HFD: High-fat Diet
 HRP: Horseradish Peroxidase
 IL: Interleukin
 IL-6: Interleukin-6
 IL-8: Interleukin-8
 IMM: Internal mitochondrial matrix
 IRX3/5: Iroquois Homebox 3/5
 KLB: FGFR1c/ β Klotho complex
 KNCK3: Potassium Two Pore Domain Channel Subfamily K Member 3
 LCFAs: Long-chain fatty acids
 LSC: Laser Scanning Cytometry
 LPGDS: Lipocalin-type Prostaglandin D Synthase
 MAPK: Mitogen-activated protein kinase
 MCP-1: Monocyte chemoattractant protein-1
 MYF5: Myogenic Factor-5
 NAD⁺/NADH: Nicotinamide adenine dinucleotide
 NE: Norepinephrine
 NGF: Nerve growth factor
 NST: Non-shivering thermogenesis
 NPs: Natriuretic Peptides
 NPRs: Natriuretic Peptide Receptors
 NRG4: Neuregulin 4 (NRG4)
 NST: Non-shivering thermogenesis
 OC: Oxygen consumption
 OCR: Oxygen consumption rate
 PBS: Phosphate Buffered Saline
 PCr: Phospho-creatine
 PCR: Polymerase Chain Reaction
 PDGF α : Platelet-Derived Growth Factor alpha
 PET/CT: Positron emission tomography/computed tomography
 PFA: Paraformaldehyde
 PGC-1 α : PPAR γ coactivator 1 alpha
 PPAR γ : Peroxisome Proliferator Activated Receptor Gamma
 PRDM16: PR Domain Containing 16
 Q-PCR: Quantitative polymerase chain reaction
 RNA: Ribonucleic acid
 RYR1: Ryanodine Receptor 1
 SD: Standard deviation
 SDS: Sodium dodecyl-sulfate
 SERCA: Sarco/endoplasmic reticulum Ca²⁺-ATPase
 SGBS: Simpson-Golabi-Behmel Syndrome
 SLN: Sarcosine
 SNS: Sympathetic Nervous System
 SV: Sum variance
 SVF: Stromal Vascular Fraction
 T2DM: Type 2 diabetes mellitus

T3: 3,3',5-Triiodo-L-thyronine
TBX1: T-box transcription factor 1
TBS: Tris-Buffered Saline
TBS-T: Tris-Buffered Saline and Tween20
TNF α : Tumor Necrosis Factor alpha
TMEM26: Transmembrane Protein 26
UCP1: Uncoupling Protein-1
VEGFA: Vascular Endothelial Growth Factor A
WAT: White adipose tissue
WHO: World Health Organization
WT: Wild Type
ZIC1: Zic Family Member 1
ZFP516: Zinc Finger Protein 516

2.INTRODUCTION

2.1. Obesity and adipose tissue

Obesity and overweight are determined as a systemic disease that displays abnormal and excessive accumulation of body fat leading to harmful health effects. In spite of significant attempts to increase awareness, the epidemic of obesity persists in at a frightening rate (Arroyo et al., 2016). Obesity is connected with higher rates of mortality driven by chronic disorders such as metabolic syndrome, type 2 diabetes mellitus (T2DM), certain types of cancers, hypertension, dyslipidemia, infertility and gastroesophageal reflux (Haslam et al., 2005). There are three possible measures of obesity often used in several studies; however, the most commonly used is body mass index (BMI) which equals the ratio of body weight in kilograms divided by height in meters squared (kg/m^2). The classes are the followings: normal (BMI: 18.5-24.9 kg/m^2), overweight (BMI: 25-29.9 kg/m^2) and obese (BMI: $>30 \text{ kg/m}^2$) determined by WHO (World Health Organization, 2000).

In Europe, more than half of the population is overweight and up to 30% is obese; moreover, the prevalence of obesity has doubled since 1980 (GBD Obesity Collaborators, 2015). In Hungary, these numbers are very similar, 60% of the population is overweight, and half of them are obese. Unfortunately it is attributable to the lack of exercise, genetic predisposition, unhealthy diet and habits like smoking or alcohol consumption (Barness et al., 2007). The Hungarian National Health Insurance spent more than 680 million EUR for the treatment of obesity in 2012. Notwithstanding, outlays can be even higher as a result of a higher prevalence rate of overweight and obesity and the development of co-morbidities with higher costs (Wilkin et al., 2004). It is a well known fact that in many cases obesity is preventable, although the pathogenesis of obesity is an exceedingly complex and is far from being revealed. The key modulator of obesity is, however, the long-term dysregulation of energy balance, containing reduced energy expenditure and increased energy intake. In spite of continuous research and developments in the understanding of the regulators of energy balance, there is only limited data and limited number of drugs that can be useful for the

effective treatment of obesity. Studies, targeting specific components of the neuroendocrine regulation, such as leptin or neuropeptides, have been unsuccessful yet. However, new alternatives focusing on adipose tissue functions e.g. heat production as a result of thermogenesis, can potentially have therapeutic relevance in the future (Poher et al., 2015). Adipose tissue is a complex organ with profound effects on the physiology and pathophysiology of the organism, serving as a calorie storage after feeding and as the source of circulating free fatty acids during fasting. This is the first tissue that is affected by several changes in response to obesity (Rosen et al., 2014). Traditionally, two types of adipose tissue have been described: white adipose tissue (WAT) and brown adipose tissue (BAT). Both tissues are able to accumulate lipids in intracellular droplets. WAT functions as an energy store, mainly in the form of triglycerides and releases fatty acids upon fasting. On the other hand, BAT contains highly specialized cells with high number of mitochondria which can dissipate energy in the form of heat through activation of Uncoupling Protein-1 (UCP1) (Rosen et al., 2014).

2.1.1. White adipose tissue

WAT is a heterogeneous tissue which contains various cell types in the stromal vascular fraction (SVF): endothelial cells, fibroblasts, pre-adipocytes, macrophages and histiocytes. In addition to its function as an energy store, WAT has an important role as an active endocrine organ, plays a role in the modulation of physiological functions such as energy expenditure, immunity, inflammation, appetite or insulin sensitivity (Shoelson et al., 2007). WAT releases the stored energy as free fatty acids (FFA) and glycerol (these are the products of major secretory function) (Trayhurn et al., 2001). Moreover, several important proteins have been described to be secreted by WAT, including: leptin, adiponectin, resistin, tumor necrosis factor-alpha (TNF- α), interleukin-

6 (IL-6), angiotensinogen as well as others (Trayhun et al., 2001; Federico et al., 2010; Clément et al., 2004).

WAT is widely dispersed in humans and divided into different depots, mainly subcutaneous and visceral adipose tissue (Wajchenberg et al., 2000). Subcutaneous WAT is located under the skin and plays an important role as a barrier against dermal infection; it also prevents loss of heat and protects the body against external mechanical stress (Kwok et al., 2016). Moreover, it is 4-5 times larger than the visceral adipose tissue (Wajchenberg et al., 2000; Márin et al., 1992). The subcutaneous adipose tissue stores 80-90% of the total body fat (in abdominal, subscapular, gluteal, femoral areas) – meanwhile, smaller percentage of the body fat is located visceraally in the abdomen (Márin et al., 1992).

2.1.2. Brown adipose tissue

The number of studies focusing on the therapeutic potential of BAT against obesity has increased over the last decade (Lynes et al., 2015). Two types of thermogenic adipocytes exist in mammals: the classical brown and beige/brite adipocytes (Ishibashi et al., 2010; Petrovic et al., 2010). Evolutionary, brown adipocytes appear only in placental mammals (Hayward et al., 1992). Interestingly, ‘protoendothermic’ mammals, like pregnant mammals also have BAT to make them able to maintain endothermy during carrying their fetus (Oelkrug et al., 2013). Human infants have significant brown fat depots, in order to provide heat in the cold environment in the post-natal period. Previously, it was proposed that adult humans are mostly lacking of brown fat, unless they are exposed to chronic cold or to state of catecholaminergic excess (Huttunen et al., 1981; English et al., 1973). The existence of significant classical brown fat in adult humans was proven by ^{18}F -FDG radiolabeled metabolic substrates. Such scans for cancer diagnosis, like PET/CT revealed

positive depots of BAT mostly in the supraclavicular and spinal regions of patients. As a result of the positive PET/CT scans, these regions were tested for immunohistochemical analysis of UCP1 (Cypess et al., 2009; van Marken Lichtenbelt et al., 2009; Virtanen et al., 2009). Nevertheless, a negative association between BMI and the amount of detected ^{18}F -FDG positive BAT was found. The glucose-uptake by BAT and its mass also showed a negative correlation with BMI (Ouellet et al., 2011; Matsushita et al., 2014; Chondronikola et al., 2014). Energy expenditure in mammals is inversely correlated with the body size. The whole body basal metabolic rate (BMR) is 1-2 W/kg in humans. Studies focusing on this thermogenic fat depots showed that BAT activity has been forecasted for 2,7-5% of BMR in humans, which can result in more than 4 kg of weight loss per year (Virtanen et al., 2009; van Marken Lichtenbelt et al., 2011). The benefits of BAT activation could potentially be a therapeutic approach to reduce elevated triglyceride concentrations and fighting against obesity in humans (Bartelt et al., 2011; Ouellet et al., 2012).

UCP1-expressing adipocytes also exist in WAT, with thermogenic capacity, in response to various stimuli (Vitali et al., 2012), namely the beige adipocytes (brite=brown in white). Beige adipocytes can be typified by their multilocular lipid droplets, high mitochondrial content and expression of brown and white fat-specific genes. In spite of the common appearance, brown and beige adipocytes have many distinguishable characteristics and should be regarded as distinct cell types (**Figure 1**).

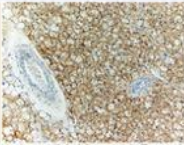
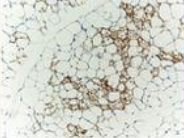
	Immunohistochemistry with anti-Ucp1	Location in humans	Location in mice	Developmental origin in mice	Enriched markers	Key transcription factors	Activators
Brown		Neck Interscapular (newborns) (Perirenal?)	Interscapular Cervical Axillary Perirenal (Endocardial?)	Myf5 ⁺ cells (dermomyotome)	<i>Zic1</i> <i>Lhx8</i> <i>Eva1</i> <i>Pdk4</i> <i>Epsti1</i> <i>miR-206, miR-133b</i>	<i>C/ebpβ</i> <i>Prdm16</i> <i>Pgc-1α</i> <i>Ppar-α</i> <i>Ebf2</i> <i>TR</i>	Cold Thiazolidinediones Natriuretic peptides Thyroid hormone Fgf21, Bmp7, Bmp8b Orexin
Beige		Supraclavicular (Paraspinal?)	Interspersed within WAT subcutaneous fat > visceral fat	Myf5 ⁻ cells <i>Pdgfr-α</i> ⁺ (perigonadal)	<i>Cd137</i> <i>Tbx1</i> <i>Tmem26</i> <i>Cited1</i> <i>Shox2</i>	<i>C/ebpβ</i> <i>Prdm16</i> <i>Pgc-1α</i> (<i>Ppar-α</i> ?)	Cold Thiazolidinediones Natriuretic peptides (Thyroid hormone?) Fgf21 Irisin

Figure 1. Differences between Brown and Beige adipocytes. Figure adapted from: Harms et al., 2013

The figure shows immunohistochemistry analysis of adipocytes: brown adipocytes express high levels of UCP1 under basal conditions, meanwhile beige adipocytes can be recognized interspersed within WAT after cold or β -adrenergic stimuli. Many enriched markers have been identified yet in mice, as classical brown: *Zic1* (Petrovic et al., 2010), *Lhx8* (Petrovic et al., 2010, Jespersen et al., 2013), *Eva1* (Wu et al., 2012) and *Epsti1* (Sharp et al., 2012) or as beige markers: *Cd137* (Wu et al., 2012), *Tmem26* (Wu et al., 2012), *Tbx1* (Petrovic et al., 2010; Wu et al., 2012), *Cited1* (Sharp et al., 2012) and *Shox2* (Lidell et al., 2013). Several activators have been identified as inducers for the development of brown and beige adipocytes, such as cold or thiazolidinediones; however, irisin represents a beige, but not a brown inducer. In addition, the developmental origin of beige adipocytes is distinct from brown adipocytes (Myf5^{+/+}) in mouse subcutaneous depots (Seale et al., 2008).

2.2. The development of brown and beige adipocytes

It was presumed for a long time that brown and white adipocytes have a common precursor (Rosen et al., 2000; Gesta et al., 2007), because a large number of similarities exist between the two cell types. Nonetheless, data gained from the last decade have shown that classical brown

fat is considered to be related to myocytes and originates from a common myogenic factor 5 (Myf5+) positive precursor (Seale et al., 2008). Meanwhile, inducible beige adipocytes together with white adipocytes are believed to arise from a separate lineage (Myf5-) (Timmons et al., 2007; Seale et al., 2008; Petrovic et al., 2010). However, tracing studies found some Myf5+ precursors also in WAT, which indicates that white and beige cells may be derived from both lineages (Sanchez-Gurmaches et al., 2012; Shan et al., 2013). Beige adipocytes can be activated by cold or other inducers, but after the cold challenge is removed, these cells return to the resting state and assume the morphology of white adipocytes (Rosen et al., 2014).

2.2.1. The origin of classical brown adipocytes

In spite of the differences in the developmental origins of white and brown adipocytes, both differentiation pathways have similar transcriptional cascades. Firstly, Peroxisome Proliferator Activated Receptor Gamma (PPAR γ) plays an important role in the differentiation of both white and brown adipocytes (Tontonoz et al., 1994; Barak et al., 1999; Rosen et al., 1999; Rosen et al., 2001; Nedergaard et al., 2005). Brown adipocyte differentiation requires PPAR γ , but this factor alone is not sufficient to regulate the program of mesenchymal cells to brown adipocytes. Secondly, members of the C/EBP family of transcription factors also take part in activating and maintaining the expression of adipogenic genes (Tontonoz et al., 1994; Freytag et al., 1994). In mouse brown adipocytes, myogenin-expressing central dermomyotome gives rise to dorsal dermis, skeletal myocytes and BAT but not WAT (Atit et al., 2006). This multipotent precursor population is typified by the expression of key transcription factors like Pax7, Myf5 and Engrailed-1 (En1) (Seale et al., 2008; Lepper et al., 2010; Sanchez-Gurmaches et al., 2012; Wang et al., 2014). In addition, Early B-Cell Factor-2 (*Ebf2*) was shown as an important marker

gene of embryonic brown preadipocytes (Wang et al., 2014). Studies focusing on PRDM16 revealed that it acts primarily through binding to, then modulating the activity of several transcriptional factors like PPAR γ Coactivator-1 α (PGC1- α), C/EBP β , PPAR α or PPAR γ . Additionally, it converts white adipocyte precursor cells and myoblasts into thermogenic, UCP1-containing adipocytes (Hondares et al., 2006; Seale et al., 2007; Seale et al., 2008; Kajimura et al., 2009). The expression of PRDM16 in white adipocytes not only activates the browning program, but also represses the white or muscle-directed gene program (Seale et al., 2007; Seale et al., 2008; Kajimura et al., 2008). Cold or β 3-adrenergic stimulation (Collins et al., 1997; Guerra et al., 1998; Himms-Hagen et al., 2000; Vitali et al., 2012) results in brown adipocyte differentiation and vascularization of BAT which is promoted by PRDM16 and FOXC2 (Cederberg et al., 2001). Together PRDM16 and FOXC2 drive an increased expression of PGC1 α (Kim et al., 2005; Seale et al., 2007). PGC1 α was originally described as a coactivator of PPAR γ and it was shown to promote brown adipocyte differentiation and fatty acid oxidation (Puigserver et al., 1998; Wu et al., 2007). PGC1 α is induced in muscle, as a result of exercise and stimulates many of the beneficial events which happen in muscle, e.g. mitochondrial biogenesis, angiogenesis (Handschin et al., 2008). As a result of cold or β 3-adrenergic stimulation, PGC1 α is a key regulator of the browning process, it interacts with IRF4 (Boström et al., 2012; Kong et al., 2014).

2.2.2. The origin of beige adipocytes

Brown-like adipocytes, these so-called beige (Ishibashi et al., 2010) or “brite” adipocytes (Petrovic et al., 2010) have multilocular morphology and express UCP1, can be found in depots of WAT (Young et al., 1984; 1997; Guerra et al., 1998; Himms-Hagen et al., 2000; Vitali et al., 2012; Collins et al., 2014; Cinti et al., 2009) as a result of cold or other inducers. Beige

adipocytes do not derive from the same precursor cells (Pax7+, Myf5+) like classical brown adipocytes, as they do not express *Myf5* (Seale et al., 2008; Sanchez-Gurmaches et al., 2012). Even though several studies suggest that a large percentage of the thermogenic fat in adult humans mostly consist of beige cells, there is only limited data about the origin and regulators of beige adipocytes in the literature (Wu et al., 2012; Lee et al., 2014; Shinoda et al., 2015). It seems that the mechanism for beige adipocyte induction in inguinal WAT is different from that seen in epididymal WAT (Lee et al., 2012) (**Figure 2**).

Two major theories exist about the origin of beige cells. Firstly, one group said that these adipocytes are derived through a transdifferentiation program of existing mature white adipocytes. This idea came from observations in which β 3-adrenergic stimuli or cold exposure did not result in cell proliferation in the newly browned cells (Himms-Hagen et al., 2000; Vitali et al., 2012).

Secondly, others state that beige cells derive from unique precursor cells within the white fat depots, and these cells can be identified and isolated using sorting or cloning (Vegiopoulos et al., 2010; Schutz et al., 2011; Wu et al., 2012; Lee et al., 2012). However, two genetic tracing studies revealed the possible development of beige cells. The first study showed that new adipogenesis is required for beige adipocyte development upon cold exposure (Wang et al., 2013). The second study used specific markers to investigate if beige adipocytes appear as a result of an initial period of cold exposure. They examined gene expression pattern of white adipocyte markers and took pictures to investigate the morphology of adipocytes. Moreover, after cold exposure they used warm conditions (Rosenwald et al., 2013), then replaced it in the cold for some seconds which resulted in the reinducement of the thermogenic program in many of these cells.

A number of mouse studies indicate that beige cells have a distinct precursor from classical brown adipocytes, and the differentiation program is induced as a result of several stimuli (e.g. cold), which is regulated by β 3-adrenergic pathway (Federico et al., 2010; Petrovic et al., 2010; Seale et al., 2011; Lee et al., 2012; Wu et al., 2012; Harms et al., 2013). These inducible cells are mostly differentiated from preadipocytes in subcutaneous WAT, during a so-called “browning” process (Ishibashi et al., 2010; Petrovic et al., 2010; Seale et al., 2011; Berry et al., 2013; Wang et al., 2014; Stine et al., 2016). When the thermogenic stimuli stops, “masked” beige adipocytes resemble a white adipocyte-like morphology *in vivo* (Wang et al., 2013; Rosenwald et al., 2013). These results indicate that the thermogenic capacity of beige adipocytes is reversible and adrenergic stimulus is required for maintaining of the thermogenic profile. Additionally, these studies demonstrate that mature adipocyte conversion and *de novo* differentiation of precursors also contribute to beige fat biogenesis and the balance between these mechanisms may depend on the environment.

EBF2, the brown preadipocyte marker is expressed in many adipogenic precursor cells, isolated from mouse inguinal WAT (Wang et al., 2014). Cells exposed to cold responded by increasing amount of EBF2⁺ precursor cells in the SVF. However, when EBF2⁺ and EBF2⁻ cells undergo a differentiation process, only the EBF2⁺ cells are able to activate a thermogenic program as a result of rosiglitazone, which suggest that EBF2 is a typical marker of beige-fat specific precursors in WAT.

In epididymal WAT, Platelet-Derived Growth Factor alpha (PDGFR α)⁺ precursor cells undergo proliferation as a result of β 3-adrenergic stimuli and are differentiated into UCP1⁺ beige adipocytes (Lee et al., 2012). Moreover, clonal analyses showing that adipogenic cells that are PDGFR α ⁺ have a biopotent function, as they are able to differentiate into both white and beige adipocytes (Lee et al., 2012).

In addition, thiazolidinediones (PPAR γ agonists) are also able to induce a brownig program in mouse and human WAT-driven adipogenic precursor cells (Elabd et al., 2009; Petrovic et al., 2010; Qiang et al., 2012; Ohno et al., 2012; Bartesaghi et al., 2015).

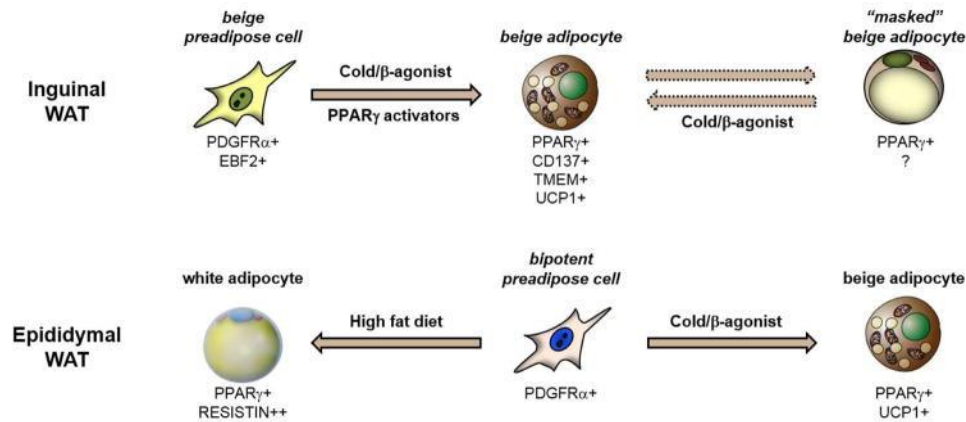


Figure 2. Beige adipocyte development in mouse system. *Figure adapted from: Kajimura et al., 2015*

The balance between the energy-storing white and energy-dissipating beige adipocytes is determined during the initial differentiation of mesenchymal precursor cells into adipocyte subtypes (Wang et al., 2013; Kajimura et al., 2015; Claussnitzer et al., 2015; Lynes et al., 2015). The mechanism regulating this process was described in the recent years and contributes to the better understanding of beige adipocyte commitment.

Genomewide association studies can be used to identify disease-relevant genomic regions; Obesity-Associated gene (*Fto*) was investigated by this method in humans. (Frayling et al., 2007; Scuteri et al., 2007). There can be a T-to-C conversion at Rs1421085 position, which has an effect on a mesenchymal superenhancer site. Individuals carrying the risk-allele of the FTO locus demonstrate a diminished rate of beige cell differentiation from adipocyte progenitors – therefore,

this SNP has a strong genetic association with obesity. When carrying a healthy genotype, a repressor binds to a super enhancer in one of the intronic region of *Fto* gene, resulting in decreased *Irx5* and *Irx3* expression levels during the early differentiation. Meanwhile, a developmental shift may occur towards more energy-dissipating beige adipocytes (**Figure 3**)(Claussnitzer et al., 2015).

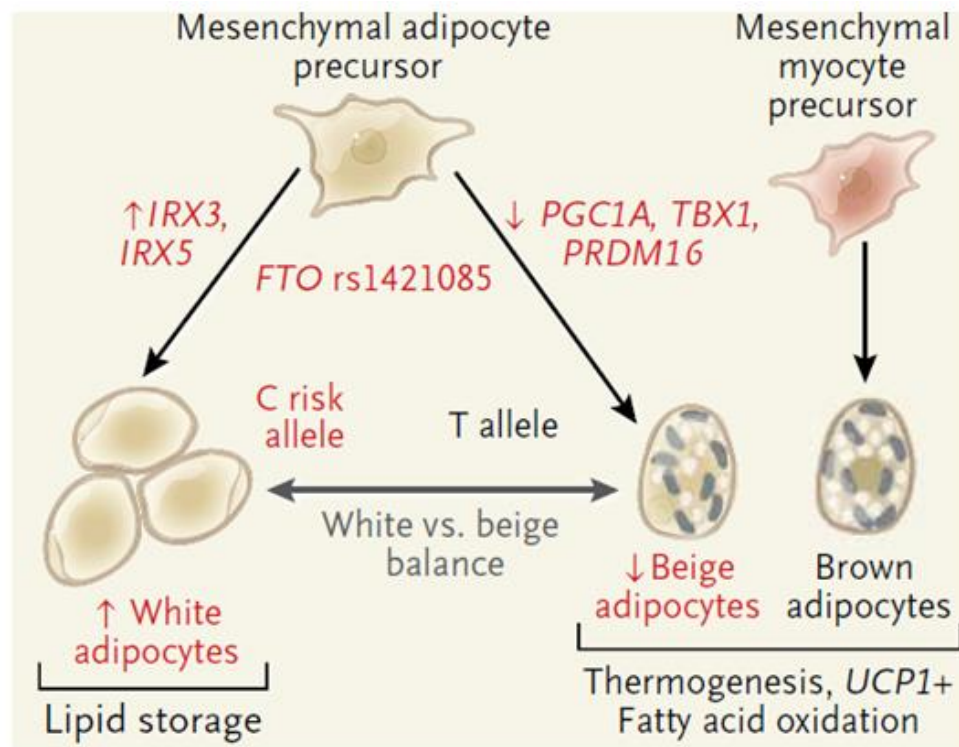


Figure 3. Mechanistic model of the FTO rs1421085 locus association with obesity. *Figure adapted from: Claussnitzer et al., 2015*

2.3. Activators of brown and beige adipocyte development & function

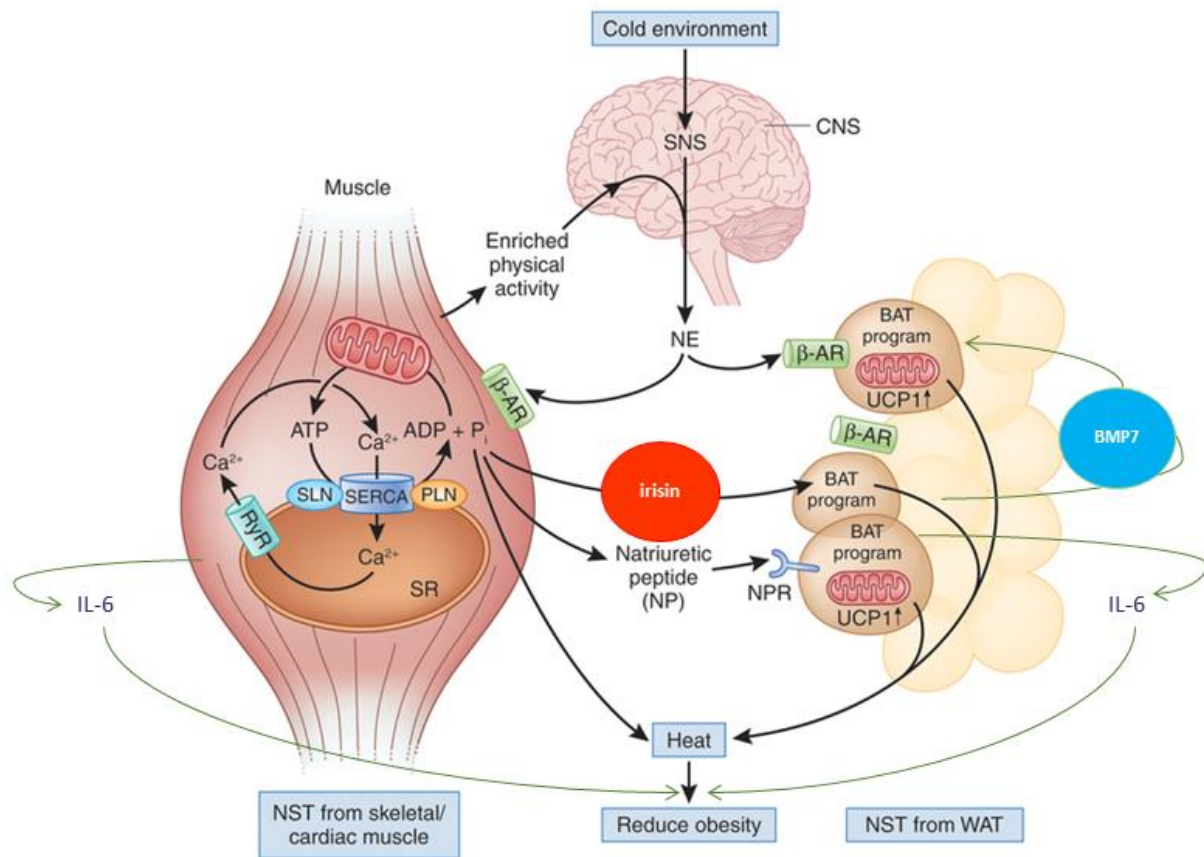


Figure 4. Regulation of non-shivering thermogenesis by muscle and brown or beige adipose tissue in rodents. *Figure adapted from then modified: Kozak et al., 2012*

The sympathetic nervous system (SNS) is involved in regulating both the development and the thermogenic functions of brown adipocytes (Bartness et al., 20120; Morrison et al., 2012). It has also been documented that the presence of sensory neurons in BAT are likely to participate in regulating the functions of brown adipocytes (Vaughan et al., 2012; Ryu et al., 2015) in which heat production is under the control of hypothalamus, where the control of temperature and feeding status are integrated. Via the SNS, the outgoing signal is transmitted to the direction of BAT (Cannon et al., 2004). In response to stimuli (for example cold exposure), norepinephrine (NE) is

released from the SNS, which acts primarily on the β_3 -adrenergic receptor. β_3 -adrenergic receptors are coupled to adenylyl cyclase (AC), which induces the production of a secondary messenger, cyclic adenosine monophosphate (cAMP). During the last decade it was described that cAMP stimulates protein kinase A (PKA) and hormone-sensitive lipase (Shih et al., 1995). β -adrenergic signaling cascade is controlled via AC activation, then cAMP and PKA transmit the thermogenic signal (Granneman et al., 1988; Bouřová et al., 2000; Chaudhry et al., 1996). PKA activation directly stimulates lipolysis and leads to gene expression changes (e.g. UCP1 upregulation), facilitated by the induced MAP kinase pathways (e.g. p38) or the phosphorylation of cAMP response element binding protein (CREB) (Holm et al., 1987; Lindquist et al., 2000; Cao et al., 2001; Wang et al., 2001).

It is a well-known fact that physical exercise has beneficial metabolic effects and protects against several pathological conditions, such as metabolic syndrome, cancer or neurodegenerative disorders (Brandt et al., 2010; Mathur et al., 2008). Skeletal and cardiac muscle cells secrete various hormones in humans and mice as well, which are named as “myokines”, in response to physical activity (Pedersen et al., 2012; Febbraio et al., 2002). These myokines markedly contribute to the crosstalk between muscle, brain and adipose tissue, by which “browning” is also regulated (Gamas et al., 2015; Contreras et al., 2015) (**Figure 4.**) Several rodent studies showed increased activity of BAT and browning of WAT during exercise (De Matteis et al., 2013; Peppler et al., 2017; Aldiss et al., 2018). An exercise-induced mediator, irisin, has been discovered in mice in the last decade. Irisin is a myokine, which is released by skeletal muscles, whose levels increase following exercise (Boström et al., 2012). In humans, mass spectrometry-based analysis confirmed the presence of irisin in human blood plasma (Jedrychowski et al., 2015). When irisin is released by skeletal muscle, it can be a potent inducer of browning.

2.4. UCP1

In BAT, brown adipocytes are filled with mitochondria that contain UCP1, which uncouples ATP synthesis from the respiratory chain activity and reduces the proton gradient through the inner mitochondrial membrane (IMM) produced by the electron transfer system (Nicholls et al., 1976; Ricquier et al., 1979, Lin et al., 1980, Jacobsson et al., 1985). In line with this, mitochondria in BAT contain high amounts of the mitochondrial respiratory chain enzymes but remarkably low amount of the F_1F_0 -ATPase. The latter is probably caused by the low expression level of the nuclear ATP5G1 gene, which encodes the mitochondrial membrane-bound c subunit of F_o oligomer (Lindberg et al., 1967; Cannon et al., 1977; Houstek et al., 1995; Kramarova et al., 2008). UCP1 increases IMM conductance for H^+ to dissipate the mitochondrial H^+ gradient and convert the energy of substrate oxidation into heat (Nicholls et al., 1984) (**Figure 5**).

When thermogenesis is physiologically required, NE is released by surrounding sympathetic fibers that activates lipolysis, which in turn increases the level of free fatty acids in brown adipocyte mitochondria. Long-chain free fatty acids (LCFAs) are not only substrates for oxidation but also activate UCP1, and they are cleaved by the hormone-sensitive lipase from triglycerides in the cytoplasmic lipid droplets upon β_3 -adrenergic stimulation of BAT (Shih et al., 1995; Prusiner et al., 1968; Chaudry et al., 1999; Matthias et al., 2000; Cannon et al., 2004).

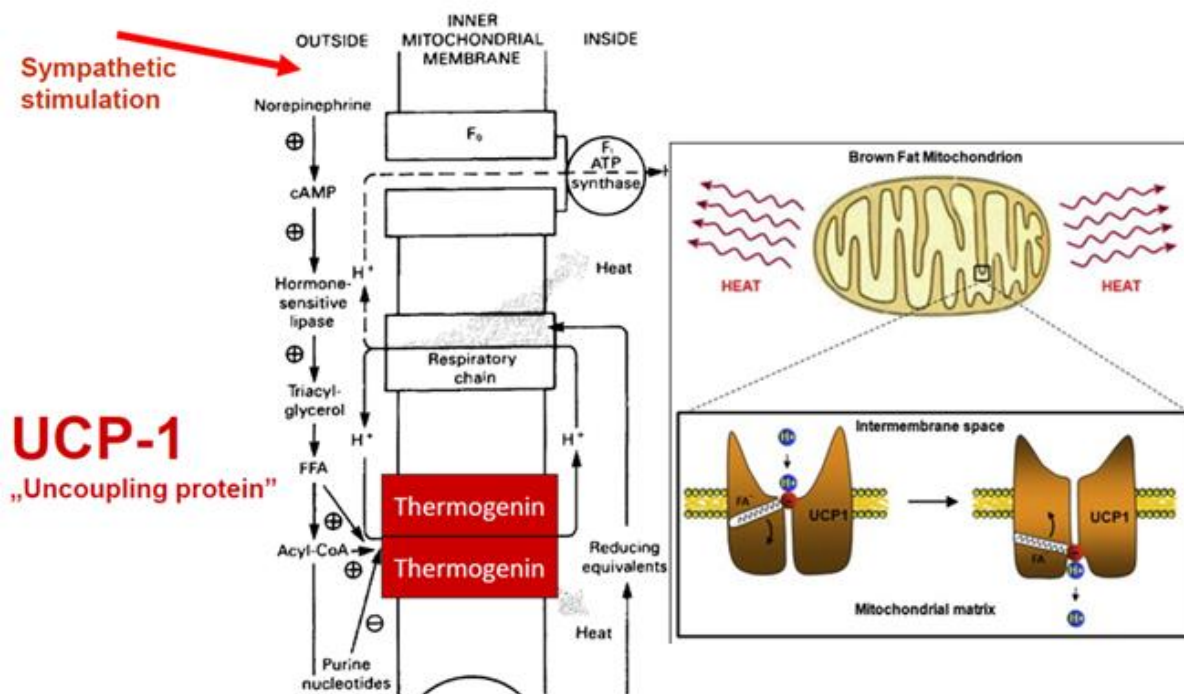


Figure 5. Thermogenesis by UCP1 in mammalian organisms and fatty acid shuttling model of UCP1-dependent thermogenic proton leak. Figures adopted from then modified: Fesüs et al., 2014; Federenko et al., 2012

It has been discovered recently that UCP1 is an LCFA anion/H⁺ symporter; hence, LCFA cannot dissociate from UCP1 due to hydrophobic interactions. LCFA is associated with UCP1, while UCP1 effectively operates as an H⁺ carrier through the IMM, then protons are released in the mitochondrial matrix (Fedorenko et al., 2012). This mechanism leads to the dissipation of energy generated by β -oxidation of fatty acids mainly as heat. Acutely activated BAT thermogenesis is determined by a relevant increase in mitochondrial reactive oxygen species (ROS) levels and the key target is Cys253 of UCP1 which is sulfenylated during the process. This study identified BAT mitochondrial ROS in mice as a mechanism that drives UCP1-dependent thermogenesis (Chouchani et al., 2016).

2.5. Browning inducers which directly target adipose tissue

As a result of certain stimuli, e.g. Bone Morphogenic Protein-7 (BMP7), which was shown to play a crucial role in BAT development, drives both classical brown adipogenesis and recruit beige adipocytes in mice (Tseng et al. 2008; Schulz et al., 2011). In addition, loss of BMP7 leads to a near-complete absence of BAT development (Tseng et al., 2008; Schulz et al., 2013).

Additionally, liver also plays a crucial role in the activation of BAT, via the production of bile acids. On one hand, it was demonstrated that bile acids are secreted after meal-induced BAT thermogenic activity, through the induction of 5'-deiodinase. This effect requires a G protein-coupled bile acid receptor, TGR5 (Watanabe et al., 2006), which is present in high levels in brown adipocytes (Thomas et al., 2009). On the other hand, an important hepatic factor, fibroblast growth factor-21 (FGF21), was recently identified as one of the regulators of BAT. It induces the thermogenic program in brown adipocytes by interacting with FGF receptor/b-Klotho complexes (KLB) at the cell surface, then inducing mitochondrial uncoupled respiration (Hondares et al., 2010). In neonates, FGF21 directly activates the heat production by BAT, while in adults, FGF21 promotes the browning of WAT depots (Kleiner et al., 2012).

The other recognized thermogenic activator is bone morphogenic protein-8b (BMP8b) that acts through both central nervous system (CNS) and periphery in mice (Whittle et al., 2012). It sensitizes the brown adipocytes to the action of NE.

Heart also plays a significant role in the activation of BAT, by producing natriuretic peptides (NPs) in mouse and human adipocytes (Bordicchia et al., 2012), which induce thermogenesis through the interaction with NP receptors (NPRs). On the surface of brown adipocytes, NPRs interact with natriuretic peptides and activate cGMP-dependent protein kinase (PKG), which results in the

induction of p38 MAP-kinase activity. It is known that the activation of p38 MAP kinase leads to induction of thermogenic gene expression program.

IL-6 is considered to be far from a standard pro-inflammatory cytokine and is known to be released by skeletal muscle as a result of exercise in humans (Ikeda et al., 2016). IL-6 as a myokine has been shown to activate beige adipocyte development and is also required for exercise-induced WAT beige-ing in mice (Knudsen et al., 2014). IL-6 targets several tissues like the liver, pancreas, brain, WAT and BAT; moreover, it balances between catabolic pathways to mediate glycemic control (Steensberg et al., 2000; Kelly et al., 2009; Ellingsgaard et al., 2011; White et al., 2014). Based on the above observations, IL-6 is responsible for several beneficial effects of physical exercise and non-shivering thermogenesis. However, the effect of IL-6 on the differentiation of human adipocytes is still unclear.

2.6. UCP1 independent mechanisms of thermogenesis

- 1. SERCA pump**
- 2. Futile cycle of creatine-phosphate**
- 3. Glycerol-3-phosphate shuttle**

UCP1-independent heat-producing mechanisms were described as a beige specific feature (Kajimura et al., 2015), besides the UCP1 dependent thermogenesis.

2.6.1. SERCA pump

During the last decade, several *in vivo* studies have revealed different nonshivering thermogenic (NST) mechanisms. Bal et al. showed that sarcolipin (SLN) is a key regulator of the sarcoendoplasmic reticulum Ca^{2+} ATPase (SERCA) pump (Asahi et al., 2003; Asahi et al., 2004;

Babu et al., 2005; Babu et al., 2006; Babu et al., 2007) which is necessary for muscle-mediated thermogenesis in mice (Bal et al., 2012). When they challenged SLN ^{-/-} mice (Babu et al., 2007) to acute cold (4°C), it resulted in hypothermia, because mice were not able to maintain their core body temperature (37°C). Overexpression of SLN in the SLN^{-/-} mice resulted in totally restored muscle-mediated thermogenesis, suggesting that SLN is the basis of SERCA-mediated heat production. They also established that ryanodine receptor 1 (RYR-1)-mediated Ca²⁺ leak is a key mechanism for the heat generation by SERCA activation. Additionally, SLN can proceed to interact with SERCA in the presence of calcium. These results suggest that SLN-mediated non-shivering thermogenesis is essential during metabolic overload (**Figure 4**).

Rowland et al. also demonstrated that SLN is an uncoupler of the SERCA pump and it may contribute to the heat production by the skeletal muscle. They wanted to answer an important question, how loss of SLN or UCP1 is compensated during cold exposure. Thus, they generated a double-knock-out (DKO) mouse model and exposed DKO and single KO mice to acute and long-term cold. The results clearly showed that in UCP-KO mice there is an upregulation of SLN; moreover, loss of SLN is compensated by elevated expression of UCP1 and browning of WAT. DKO mice were able to survive step-by-step cold challenge, but they lost large amount of weight and depleted their fat stores. DKO mice were viable at thermoneutrality; however, when they were challenged to acute cold, they became extremely cold-sensitive. Altogether these data suggest that SLN and UCP1 are both required to maintain an optimal thermogenesis and loss of them may threaten the survival of mice under cold exposure (Rowland et al., 2015).

Researchers in a different laboratory found a robust UCP1 independent thermogenesis in beige fat that involved increased ATP-dependent Ca²⁺ cycling by sarco/endoplasmic reticulum Ca²⁺-ATPase 2b (SERCA2b) and ryanodine receptor 2 (RYR2). Inhibition of SERCA2b resulted in marred NST

in humans and mice. Reciprocally, increased Ca^{2+} cycling by activation of the adrenergic receptor or the SERCA2b-RYR1 pathway urges UCP1 independent thermogenesis. In the absence of UCP1, beige fat expends glucose for ATP-dependent thermogenesis, through the SERCA2b pathway (Ikeda et al., 2017).

These results collectively demonstrate the existence of UCP1 independent thermogenesis, although numerous processes remain questionable in beige fat.

2.6.2. Futile cycle of creatine

Several years ago, a creatine-phosphate futile cycle was recognized, which requires coupled ATP synthesis to enhance energy expenditure through stimulation of mitochondrial ATP turnover in humans and mice (Kazak et al., 2015 and 2017). Mitochondrial creatine kinase 1 or 2 (CKMT1/2) catalyzes the phosphorylation of creatine, while using ATP to create phospho-creatine (PCr) and ADP. In the futile cycle PCr is immediately dephosphorylated, leading to heat production (Jacobus et al., 1973; Berlet et al., 1976; Terblanche et al., 1998; Kazak et al., 2015). This is further supported by data demonstrating that reduction of endogenous creatine levels by the usage of β -guanidinopropionic acid (β -GPA) results in blunted adrenergic activation of metabolic rate, as shown in Figure 6. Since most of the data regarding this futile cycle comes from experiments in mice, additional studies are needed to validate its importance in humans.

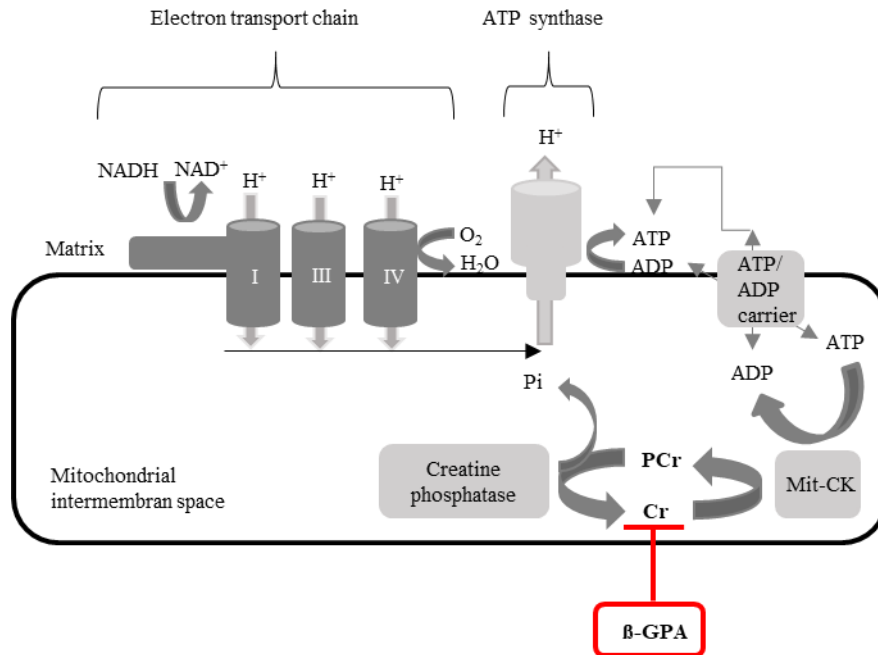


Figure 6. Model of creatine-driven futile cycle. *Modified figure adopted from: Kazak et al., 2015*

2.6.3. The Glycerol 3-phosphate shuttle

The research of mitochondrial glycerol-3-phosphate dehydrogenase (mGPDH) has been started more than 80 years ago (Green et al.; 1936), and there are still many unanswered questions. Firstly, cytosolic GPDH converts dihydroxyacetone phosphate (DHAP) to glycerol-3-phosphate by oxidizing one molecule of NADH to NAD⁺ - the NADH is usually derived from glycolysis. Then, glycerol-3-phosphate is converted back to DHAP by mitochondrial GPDH, which localizes to the IMM, and reduces one molecule of FAD to FADH₂ (Anunciado-Koza et al., 2008). The glycerol-3-phosphate shuttle has been advanced as a source of metabolic disorganization, because of the production of 2, instead of 3 ATPs/mol of NADH generated by glycolysis (Lardy et al., 1990; Koza et al., 1996). In interscapular BAT of mice, the protein levels of GPDH gene and cytoplasmic GPDH are much higher than in any other tissues (Ratner et al., 1981; Koza et al., 1996; Anunciado-

Koza et al., 2008). This suggests that the heat production by the glycerol phosphate shuttle is a parallel pathway that could supplement UCP1-mediated thermogenesis independently.

2.7. Secreted factors by the adipose tissue

Since the last century, when leptin was discovered, the original concept that WAT has only a storage function has changed significantly (Zhang et al., 1994). Leptin is a circulating hormone exclusively secreted by adipocytes, which serves as an essential regulator of body weight. Additionally, it increases BAT thermogenesis via hypothalamic pathways (Minokoshi et al., 1999; Commins et al., 2001). The number of proteins found to be produced and released from adipose tissue is steadily increasing, and the current list of WAT-secreted factors consist of more than a hundred proteins and other molecules (Trayhurn et al., 2004; Fischer-Posovszky et al., 2007; Sakurai et al., 2013). The abovementioned list covers a broad range of protein families as well as fatty acids, prostaglandins, adipokines, chemokines and inflammatory cytokines (Figure 7.) (Hauner et al., 2005).

Since WAT secretes many adipokines, it is rightful to think that brown and beige adipocytes may secrete “batokines” with various functions, although only limited information exist about them. Many of the WAT-secreted adipokines and inflammatory cytokines are moderately expressed in BAT of mammals (Cannon et al., 2004; Ortega et al., 2011); however, the secretory profile of BAT is quite distinct.

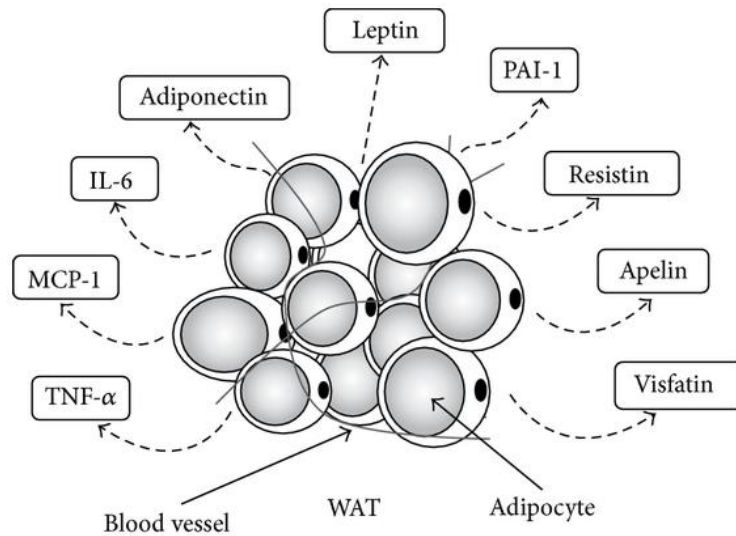


Figure 7. Adipokines secreted by WAT in mammals. *Figure adopted from: Sakurai et al., 2013*

During the process of adipocyte differentiation or thermogenic activation, several molecules are released by BAT or brown and beige adipocytes. Although limited evidence is available about the existence of the specific actions of “batokines”, their general biological functions suggest that some may have autocrine and/or paracrine roles. Brown and beige adipocytes are able to secrete several autocrine factors, which leads to inhibited (sLR11) or increased (FGF21, BMP8b, endothelin-1, IL-6, LPGDS) thermogenic activity. Thermogenic activation of BAT induces the expression and release of FGF21 (Chartoumpekis et al., 2011; Hondares et al., 2011), which is regulated by noradrenergic, cAMP-mediated mechanisms (Hondares et al., 2011). As an autocrine regulator, FGF21 itself promotes thermogenesis and metabolite oxidation in BAT (Hondares et al., 2010; Kleiner et al., 2012).

BMP8b is produced mainly by mature brown adipocytes and its expression is enhanced as a result of thermogenic and nutritional factors, like cold exposure or high-fat diet (HFD). These findings of FGF21 and BMP8b suggest a paracrine or autocrine “batokine” function.

The expression of Angiopoietin-like 8 (ANGPTL8) or lipasin, is induced as a result of cold in BAT (Fu et al., 2013), whereas the secretion of vascular endothelial growth factor A (VEGFA) targets endothelial cells and can subserve the vascularization process of BAT itself (Asano et al., 1999; Xue et al., 2009). Lastly, it has been shown recently that Neuregulin 4 (NRG4), which is a member of the Epidermal growth factor (EGF) family, is secreted by brown adipocytes and is induced during adipocyte differentiation (Rosell et al., 2014; Wang et al., 2014).

2.8. SGBS cells

Contrary to detailed studies in rodents, there is only limited data about regulatory networks that drive human brown or beige adipocyte differentiation. Therefore, human cell line models are needed in order to investigate key molecular elements of browning and to find targets of novel pharmacological treatments that can enhance browning. A non-immortalized human preadipocyte cell line, namely the Simpson-Golabi-Behmel syndrome (SGBS) cell strain was described in the last decade by our collaborating partners (Wabitsch et al., 2001). The SGBS is an X-linked, rare, congenital overgrowth syndrome, which is characterized by pre- and postnatal growth disturbances, craniofacial dysmorphia, congenital heart diseases, and visceral and skeletal abnormalities (Tenorio et al., 2014). Affected people with SGBS have an increased risk of developing embryonal type tumors, (Wilms and liver- tumors, Lapunzina et al., 2015). SGBS is caused by point mutations or deletions in the glypican-3 (*Gpc-3*) gene which encodes for a membrane associated heparin sulfate proteoglycan. This protein might play a crucial role in the control of cell division and growth (Bhowmik et al., 2015). SGBS cell line was found to be a proper model for white adipocyte differentiation (Fischer-Posovszky et al., 2008; Allott et al., 2012; Schlottmann et al., 2014; Palominos et al., 2015; Sárvári et al., 2015). Wabitsch et al. found that SGBS cells behave very similarly to human primary preadipocytes without any differentiation;

moreover, *in vitro* differentiated SGBS adipocytes are functionally indistinguishable from human adipocytes. Additionally, they demonstrated that SGBS cells have a doubling time of 38 hours \pm 1 hour, which is higher than the doubling time of SVF (Stromal Vascular Fraction) from three healthy infants. Originally SGBS cells and SVF were cultured in adipogenic media, supplemented with insulin, cortisol, T3, which resulted in mature adipocytes within 20 days, as most cells accumulated lipid droplets. Researchers in our group have used essentially the same protocol to differentiate SGBS cells (Doan-Xuan et al., 2013). The SGBS started to accumulate lipid droplets after one week of the differentiation process. In addition, at day 14 they were completely full of triacylglycerols, as shown in Figure 8.

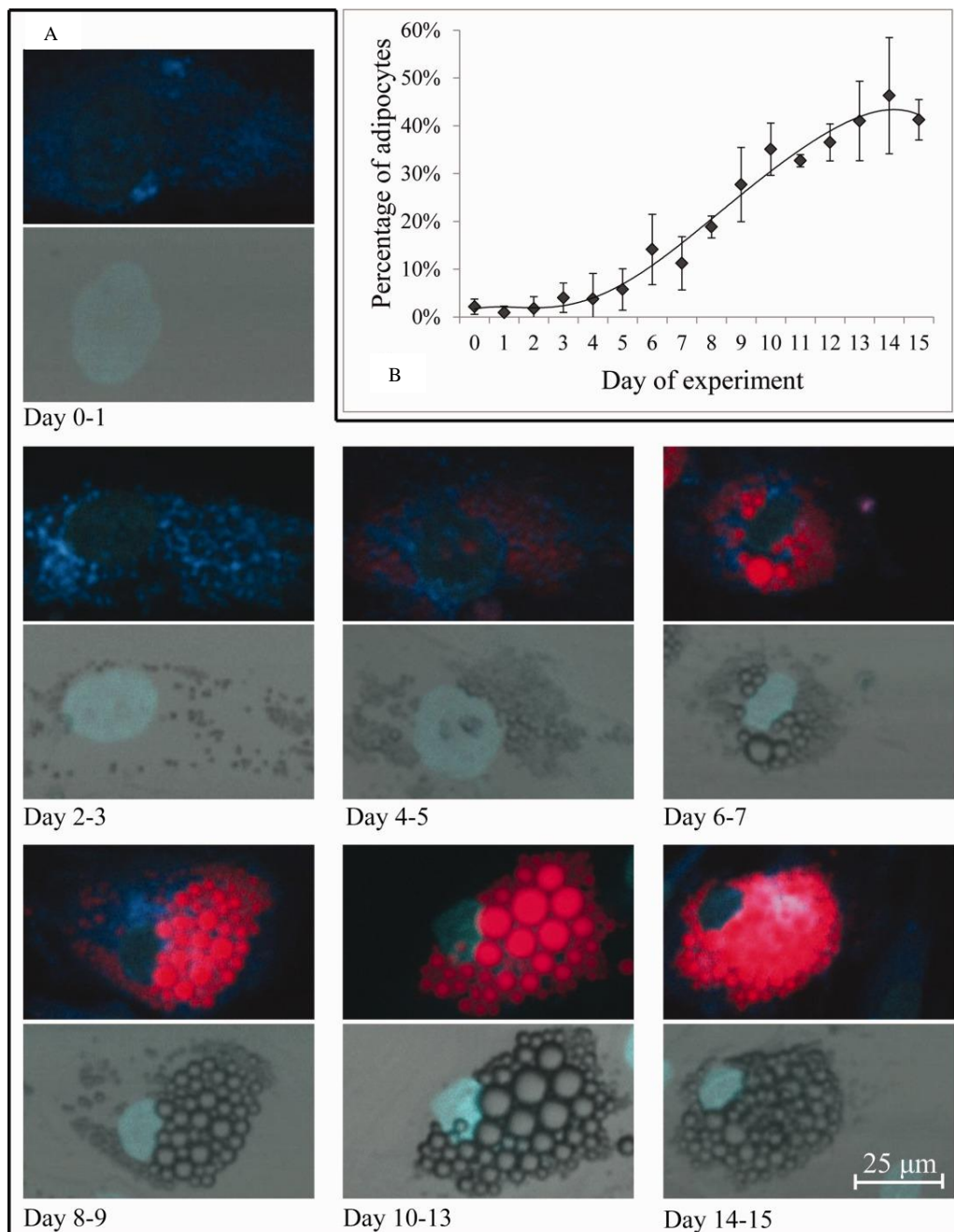


Figure 8. Inspection of SGBS adipocyte differentiation. Representative SGBS cells at different cell ages (A); Kinetics of the ratio of adipocytes matured over total number of cells (B). *Figure adapted from: Doan-Xuan et al., 2013*

2.9. Transglutaminase 2

Transglutaminases (TGs) are widely distributed enzymes with several functions. In mammals, nine members have been identified: keratinocyte (TG1), tissue (TG2), epidermal (TG3), prostate (TG4), type 5 (TG5), neuronal (TG6), type 7 (TG7), blood coagulation factor XIII A-subunit (FXIII-A) and the erythrocyte band 4.2 protein which is catalytically inactive (Griffin et al., 2002). TGs belong to a family of functionally and structurally related enzymes which catalyze posttranslational modification of proteins in a Ca^{2+} -dependent manner by introducing protein-protein cross-links, site-specific deamidation and amine incorporation (Greenberg et al., 1991; Lorand et al., 2003).

This multifunctional protein, TG2, has different cellular localization and plays a role in several physiological (regulation of cell survival - cell death processes, migration, cell adhesion, proliferation, signal transduction) and pathological processes (neurodegenerative disorders, coeliac disease, inflammatory diseases, metabolic diseases, cancer, fibrosis). Moreover, TG2 is known to take part in the differentiation processes of several cell types (Fesus et al., 2002; Iismaa et al., 2009; Wang et al., 2012; Eckert et al., 2014; Király et al., 2016).

Apart from acting as transglutaminase, TG2 also possesses GTPase, protein kinase and protein disulphide isomerase activities (Nakaoka et al., 1991; Fesus et al., 2002). TG2 is expressed in almost all cell compartments, including the mitochondria, cytoplasm, nucleus and recycling endosomes. It can be found on the cell surface, as well as being secreted into the extracellular matrix via non-classical mechanisms (Belkin et al., 2011). The structure of TG2 consists of four domains: catalytic core domain, N-terminal β -sandwich and two C-terminal β -barrel 1-2 domains. When Ca^{2+} is bound to the enzyme, the protein can exist in an opened active conformation; moreover, it can also be in a closed conformation in the presence of GTP (Pinkas et al., 2007). TG2 covalently cross-links proteins by producing an isopeptide bond between lysine and glutamine

residues (Folk et al., 1977). TG2 is able to incorporate primary amines into glutamine residues of proteins and it can cleave the produced cross-links by its isopeptidase activity (Király et al., 2016). Previously, a TG2 KO mouse model was generated to uncover the complex biological functions of TG2 (De Laurenzi et al., 2001). The researchers found that TG2 KO mice were viable and had normal size and body weight, and no apparent abnormalities were visible in organ functions. However, other research groups revealed that TG2 participated in a crosstalk between phagocytic and dying cells in order to maintain tissue integrity (Sarang et al., 2007; Szondy et al., 2003; Tóth et al., 2009). Moreover, it is also required for the differentiation and bacterial killing of neutrophils (Balajthy et al., 2006; Csomos et al., 2010). Later on, researchers from another laboratory have done more detailed examinations which revealed several abnormalities and important changes that were studied under stress and pathological conditions (Fesus et al., 2002). The lack of TG2 led to diabetes (Bernassola et al., 2002), impaired wound healing (Sarang et al., 2009) and autoimmunity (Sarang et al., 2011).

3. AIMS OF THE STUDY

1. To investigate whether brown or beige adipocyte differentiation can be induced in SGBS cells, by

- gene expression profile analysis
- analysis of the cell morphology by laser scanning cytometry
- functional Seahorse measurements

2. To learn the effect of irisin and BMP7 on SGBS cells

3. To test the involvement of the newly identified creatin-kinase/phosphatase substrate cycle in the heat production of SGBS derived adipocytes (β -GPA treatment during Seahorse measurements)

4. To clarify whether beige differentiation can be reversed to white adipocytes or they maintain their beige morphology

5. To quantify the secretion of cytokines (“batokines”) by SGBS adipocytes

6. To examine the effect of the secreted IL-6 on the beige adipocyte differentiation of primary cells

7. To examine TG2 gene and protein expression both in white and browning SGBS adipocytes

4. MATERIALS AND METHODS

4.1. Materials

4.1.1. Cell Culture Media

Apo-Transferrin human (Sigma-Aldrich, T2252); Biotin (Sigma-Aldrich, B4639); Cortisol (Sigma-Aldrich, H0888); Dexamethasone (Sigma-Aldrich, D1756); Dulbecco's Modified Eagle's Medium (DMEM)/Nutrient Mixture F-12 Ham (Sigma-Aldrich, D8437); Fetal Bovine Serum (FBS) (Gibco, 10270); 3-Isobutyl-1-methylxanthin (IBMX) (Sigma-Aldrich, I5879); Insulin solution human (Sigma-Aldrich, I9278); Rosiglitazone (Cayman Chemicals, 71740); 3,3',5-Triiodo-L-thyronine sodium salt (T3) (Sigma-Aldrich, T6397); Penicillin-Streptomycin (Sigma-Aldrich, P4333); Pantothenic acid (Sigma-Aldrich, P5155).

4.1.2. Antibodies

Anti-Glyceraldehyde-3-Phosphate Dehydrogenase (GAPDH) Antibody, clone 6C5 (Sigma-Aldrich, MAB374); Anti-mouse IgG (H+L) antibody [HRP] (Covalab, lab0252); Anti-rabbit IgG (H+L) antibody [HRP] (Covalab, lab0273); Anti-UCP-1 antibody produced in rabbit (Sigma-Aldrich, U6382); Anti-UCP-1 antibody (Thermo Fisher Scientific, PA1-24894); Anti-UCP-1 antibody (R&D Systems, MAB6158); Anti-OXPHOS (Abcam, ab110411); Anti-TG-2 antibody (Zedira, T002); Goat anti-Rabbit IgG (H+L) Secondary Antibody, Alexa Fluor® 488 conjugate (Thermo Fisher Scientific, A-11034); Human IL-6/R alpha antibody (R&D Systems, MAB227); IgG1 mouse isotype control antibodies (Sigma-Aldrich, M5284).

4.1.3. Cell dyes

Hoechst 33342, Trihydrochloride, Trihydrate (Thermo Fisher Scientific, H1399)

4.1.4. Reagents, plates

2-mercaptoethanol (Sigma-Aldrich, M6250); 3-Guanidinopropionic acid (β -GPA) (Sigma-Aldrich, G6878); 5% skimmed milk (Sigma, 1153639010); Dimethyl sulfoxide (DMSO) (Sigma-Aldrich, D2650); DuoSet ELISA (R&D Systems, DY 201, DY206, DY208, DY210, DY279); Ethylenediaminetetraacetic acid disodium salt dehydrate (EDTA) (Sigma-Aldrich, E5134); High Capacity cDNA Reverse Transcription Kit (Applied Biosystems, 4368813); GeneJET Genomic DNA Purification Kit (Thermo Scientific, K0721); iCys Research Imaging Cytometer (Thorlabs Imaging Systems); Immobilon® Western Chemiluminescent HRP Substrate (Merck-Millipore, WBKLS0500); Immobilon®-P PVDF Membrane (Merck-Millipore, IPVH00010); Irisin (human recombinant) (Cayman Chemicals, 11451); LightCycler 480 (Roche); Maxima SYBR Green/ROX qPCR Master Mix (2X) (Thermo Fisher Scientific, K0221); N₆,2'-O-Dibutyryladenine 3',5'-cyclic monophosphate sodium salt (dibutyryl-cAMP) (Sigma-Aldrich, D0627); NucleoSpin® Gel and PCR Clean-up kit (Macherey-Nagel,); Oligomycin (Enzo Life Sciences, ALX-380-037); Paraformaldehyde (Sigma-Aldrich, P6148); PCR Mycoplasma Test Kit I/C (PromoKine, PK-CA91) Protease inhibitor (Sigma, P1860); PVDF Immobilon®-P Transfer Membrane (Merck-Millipore, IPVH00010); Recombinant Human BMP-7 Protein (R&D systems, 354-BP); Saponin (Sigma-Aldrich, 47036); Taq DNA Polymerase, recombinant (5 U/ μ L) (Thermo Fisher Scientific, EP0401); TaqMan™ reverse transcription reagents kit (Applied Biosystems, N8080234); TRI Reagent (Molecular Research Center, TR118); Triton X-100 (Sigma-Aldrich, T8787); Trizol reagent (Invitrogen Life Technologies, 15596026); Trypsin-EDTA solution (Sigma-Aldrich, T3984); TWEEN® 20 (Sigma-Aldrich, P1379); XF96 FluxPak mini (Seahorse Biosciences, 102312-100); μ -slide 8 well plate (Ibidi GmbH, 80826).

4.2. Methods

4.2.1. Ethics statement

Before the surgical procedure, written informed consent from all participants was obtained. The study protocol was approved by the Medical Research Council of Hungary (20571-2/2017/EKU). All experiments were carried out according to the approved ethical guidelines and regulations.

4.2.2. Obtained samples and isolation of hADMSCs

Human adipose-derived mesenchymal stem cells (hADMSCs) were obtained from subcutaneous abdominal adipose tissue of healthy volunteers, aged 20-65 years who underwent a planned surgical treatment (herniotomy). Patients with known diabetes, abnormal thyroid hormone levels, or malignant tumor at the time of surgery, were excluded. Selection was made based on BMI < 29.9, but not on gender. The adipose tissue samples (1-10 ml) were immediately transported to the laboratory after being removed. Adipose tissue specimens were dissected from fibrous materials and blood vessels, minced into small pieces and digested in Phosphate Buffered Saline (PBS) with 120 U/ml collagenase for 60 min in a 37 °C water bath. Then, the completely disassembled tissue was filtered to remove any remaining tissue, by a filter with pore size of 140 µm. As a next step, cell suspension was centrifugated at 1300 rpm for 10 minutes. The pellet of hADMSCs was re-suspended in DMEM-F12 medium supplemented with 10% FBS, 100 U/ml penicillin-streptomycin, 33 µM biotin and 17 µM pantothenic acid.

hADMSCs were seeded into Ibidi eight-well µ-slides or 6-well plates at 37°C in 5% CO₂ to attach, at a density of 3×10^4 cells/cm² and cultured in the same medium. After 24 hours, floating cells were washed away with PBS and the remaining hADMSCs were cultured until they became

confluent (Kristóf et al., 2015; and 2016). The absence of mycoplasma was tested by polymerase chain reaction (PCR) analysis.

4.2.3. Flow cytometry: characterization of adipose tissue-derived stem cells

To investigate the phenotype of the undifferentiated SGBS preadipocytes, a multiparametric analysis of surface antigen expression was performed by three-color flow cytometry using fluorochrome-conjugated antibodies with isotype matching controls. After harvesting the cells with 0,025% trypsin-EDTA, they were washed once with normal medium. Then, cells were washed two more times with FACS buffer. Cells were incubated with FACS buffer and fixed in 1% PFA/PBS. Analysis was carried out within one day. Samples were measured using FACS Calibur BD flow cytometer and data were analyzed using BD Multiset software.

4.2.4. Cell culture and differentiation of human SGBS preadipocytes into mature white and brown adipocytes

For our experiments hADMSCs and Simpson Golabi Behmel Syndrome (SGBS) preadipocytes have been used as adipocyte progenitors. SGBS human cell line was kindly provided by our collaborating partners, Pamela Fischer-Posovszky and Martin Wabitsch who previously developed it.

SGBS preadipocytes were seeded in 12-well plates or Ibidi-chamber slides at a density of $1,5 \times 10^4$ cells/cm² and cultured in DMEM-F12 medium containing 100 U/ml penicillin/streptomycin, 33 µM biotin, 17 µM pantothenic acid, and 10% FBS at 37°C in 5% CO₂ to getting attached. Cells were cultured in this FBS-containing medium until they completely reach confluency.

The absence of mycoplasma was checked by polymerase chain reaction (PCR) analysis.

To induce a white adipogenic differentiation, cells were incubated in serum-free medium for 4 days, supplemented with 100 U/ml penicillin/streptomycin, 33 μ M biotin, 17 μ M pantothenic acid, 2 μ M rosiglitazone, 20 nM human insulin, 25 nM dexamethasone, 10 μ g/ml human apo-transferrin, 500 μ M 3-isobutyl-1-methylxanthine, 100 nM cortisol and 200 pM triiodothyronine. The medium was changed after the fourth day; and rosiglitazone, dexamethasone and 3-isobutyl-1-methylxanthine were removed from the differentiation media during the remaining 10 days of differentiation. In every fourth day, the differentiation cocktail was replaced (Fischer-Posovszky et al., 2008).

PPAR γ -driven browning differentiation was induced for four days using serum-free DMEM/F12 medium supplemented with 100 U/ml penicillin/streptomycin, 33 μ M biotin, 17 μ M pantothenic acid, 0,85 mM human insulin, 1 μ M dexamethasone, 10 μ g/ml human apo-transferrin, 500 μ M 3-isobutyl-1-methylxanthine and 200 pM triiodothyronine. From the fifth day, cells were further cultured in DMEM/F12 serum-free medium, for the following ten days adding 500 nM rosiglitazone while dexamethasone and 3-isobutyl-1-methylxanthine were omitted (Elabd et al., 2009). In long-term experiments either the same culture conditions were applied for 21 and 28 days or it was replaced by the white differentiation medium without rosiglitazone, 3-isobutyl-1-methylxanthine and dexamethasone. In every fourth days, the differentiation cocktail was changed.

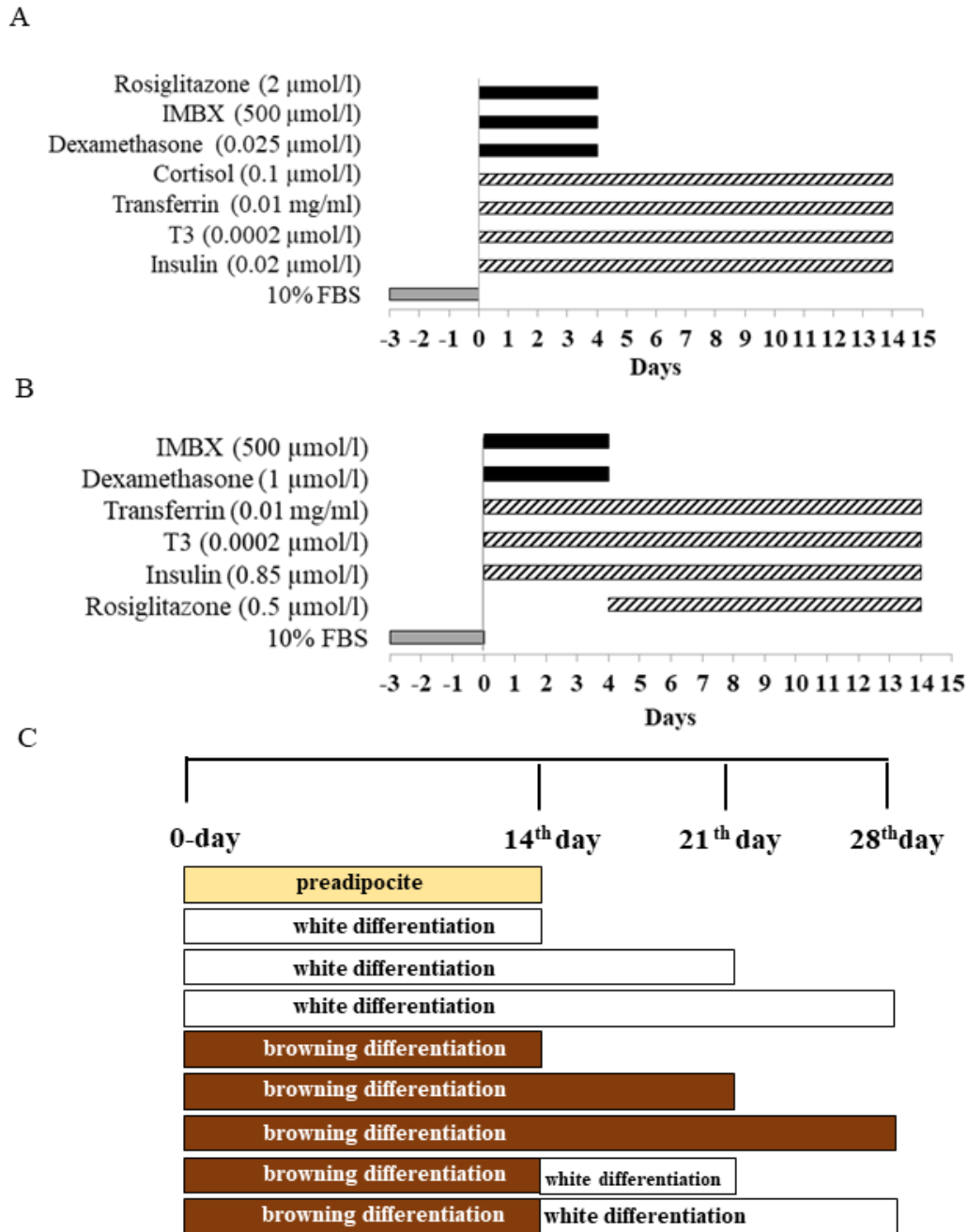


Figure 9. Schematic figure of differentiation process: white cocktail (A), PPAR γ -driven browning cocktail (B) and long-term differentiation (C) of SGBS cells.

Human recombinant irisin was administered at 250 ng/ml concentration, and human recombinant BMP7 was used at 50 ng/ml concentration (Raschke et al., 2013; Kristóf et al., 2015). 12-hours-long irisin or BMP7 treatment was applied after the two weeks-long differentiation program to examine the short term effect of them. Where indicated, the browning inducers mentioned above were added to the differentiating cells in increasing concentrations.

Where indicated, primary adipocytes were treated with human IL-6R alpha or IgG Isotype control antibody at 5 µg/ml every day during the whole differentiation.

To examine the short-term effect of NC9, 9 hours treatment was applied after the two weeks-long (14 days) white and PPAR γ -driven browning differentiation, then the cells were collected. Paralelly, we were curious about the long-term effect of NC9. During the whole differentiation (21 days) NC9 was administered in every fourth day, when the media was replaced and after 21 days cells were collected.

4.2.5. RNA isolation, TaqMan™ reverse transcription-coupled quantitative (RT-PCR), qPCR

Differentiated SGBS adipocytes were collected and total RNA was extracted from the samples by using Trizol reagent. RNA concentrations were quantified by spectrophotometry. To generate cDNA, high-capacity TaqMan™ reverse transcription reagents kit was used according to the manufacturer's instructions. Applied Biosystems designed the gene primers and probes. Quantitative real-time PCR (qPCR) was performed in a LightCycler 480 with the program of 10 seconds at 94°C, followed by 40 cycles of 12 seconds at 94°C and 30 seconds at 60°C. All samples were measured in triplicates. Normalized gene expressions values were calculated by the comparative delta cycle threshold (ΔC_t) method. This method is able to correct the differences

between RNA samples in which the Ct of target genes were normalized to Ct of *Gapdh*, which was used as an endogenous control (Taube et al., 2015). Normalized gene expression levels equal $2^{-\Delta Ct}$. As all genes were measured at the same time in the same assay for each RNA sample, relative quantification was utilized. Using the ΔCt values, the comparative cycle threshold method was used to calculate the fold-change of the different genes, relative to untreated control used as a calibrator. Calibrator is assigned a value of 1. The fold changes for target genes presented in Figures were calculated as the ratio of expression levels of the untreated control and treated / differentiated adipocytes.

4.2.6. Total DNA isolation and mitochondrial DNA quantification

Total DNA was isolated from differentiated SGBS adipocytes by the phenol-chloroform extraction, using Trizol reagent. During the qPCR we were using diluted samples (100 ng DNA), 10 μ M from each primer; human mitochondrial DNA specific primers:

forward 5'CTATGTCGCAGTATCTGTCTTTG-3'

reverse 5'-GTTATGATGTCTGTGTGGAAAG-3'

nuclear specific primers (SIRT1 gene):

forward 5'CTTTGTGTGCTATAGATGATATGGTAAATTG-3'
--

reverse 5'GATTAAACAGTGTACAAAAGTAG-3'

and Maxima SYBR Green/ROX qPCR Master Mix. LightCycler 480 was used with the program of 20 minutes at 95°C, and 50 cycles of 15 seconds at 95°C, 20 seconds at 58°C, 20 seconds at 72°C. Relative mitochondrial DNA content was determined from the difference between the

threshold cycle (Ct) values for mitochondrial DNA and nuclear specific amplification. Results show mitochondrial genomes per diploid nuclei (Szántó et al., 2011; Kristóf et al., 2015; and 2016).

4.2.7. Antibodies and immunoblotting

Differentiated SGBS adipocytes and undifferentiated control cells were collected and washed once with PBS, and then homogenized in 5x Laemmli loading buffer and boiled for 10 min at 100°C. Equal amounts of protein were loaded onto a 12 %-SDS-polyacrylamide gel. Proteins were transferred onto a PVDF Immobilon-P Transfer Membrane. Then the membranes were blocked in Tris-buffered saline containing 0,05% Tween-20 (TBS-T) and 5% skimmed milk for 1 hour.

The membranes were then probed at 4°C with primary antibodies overnight: polyclonal anti-UCP1 (1:500, Sigma, U6382; 1:500, Thermo Scientific, PA1-24894), monoclonal anti-UCP1 (1:1000, R&D Systems, MAB6158), anti-OXPHOS (1:1000, Abcam, UK, ab110411) and anti-TG2 (1:1000; Zedira). All of them were diluted into TBS-T containing 1 % non-fat skimmed milk, followed by the incubation with horseradish-peroxidase (HRP)-conjugated species-specific secondary antibodies for 1 hour at room temperature. For loading control, rabbit polyclonal antibody against β -actin (1:10000, Sigma, A2066) was used overnight at 4°C in TBS-T containing 1% skimmed milk. Immunoreactive proteins were visualized by Immobilon western chemiluminescence substrate. ImageJ software was used to carry out the densitometry measurements.

4.2.8. Immunofluorescence staining

SGBS cells and hADMSCs were plated on eight-well ibidi micro slides and differentiated as described in 4.2.4. On the day of measurement, cells were washed once with PBS, then fresh medium was added. Cells were stained with Hoechst 33342 (50 μ g/ml) for 20 minutes. Next, cells

were washed with PBS and fixed in 4% paraformaldehyde for 5 minutes. Then, blocking step was carried out with 5% skimmed milk for 2 hours and staining with anti-UCP1 (Sigma, U6382; 1:500) for 6 hours at room temperature. As a secondary antibody, Alexa 488 goat anti-rabbit IgG was applied. Between and after antibody usage, washing steps were carried out in the presence of 0.1% saponin in PBS, to make cells more permeable.

4.2.9. Laser scanning cytometry

Scanning was done by an iCys Research Imaging Cytometer (iCys, Thorlabs Imaging Systems, Sterling, VA, USA). Imaging Cytometer equipped with 405-nm, 488-nm and 633-nm solid-state lasers, photodiode forward scatter detectors and photomultiplier tubes with three filters in front. The images were processed and analyzed (n=3, 2000 cells per SGBS sample / hADMSCs) by our high-throughput automatic cell-recognition protocol, which was developed by Doan-Xuan et al. (2013) with some modifications using the iCys companion software (iNovator Application Development Toolkit version 7.0, CompuCyte Corporation, Westwood, MA, USA). Cells were identified in accordance with their Hoechst 33342 nuclear staining. Sample slides were mounted on a computer-controlled stepper motor-driven stage. An area with optimal confluence was selected in low-resolution scout scan with 10x magnification objective and 10 μ m scanning step. Subsequently, high-resolution images were taken by using 40x objective (NA 0.75) and a 0.25- μ m scanning step. The size of a pixel was regulated to 0.25 μ m x 0.245 μ m at 40x magnification. Laser lines were separately operated, namely a 405-nm diode laser was used to excite Hoechst 33342 and a solid-state 488-nm laser was used for Alexa 488 goat anti-rabbit IgG. Emissions of Hoechst was detected at 450 ± 20 nm and Alexa 488 at 530 ± 15 nm. Transmitted laser light was captured by diode photodetectors in which light loss and shaded relief signals were measured to gain information about light absorption, light scattering and texture of the objects. Then, images were

processed and analyzed by our high throughput automatic cell recognition protocol using the iCys companion software (iNovator Application Development Toolkit, CompuCyte Corporation) and CellProfiler (The Broad Institute of MIT).

The hereunder process was used to determine adipocytes in the mixed cultures. Hoechst-stained nuclei were identified first and marked as primary objects. To characterize the lipid droplet content of the cells, texture feature was used, therefore cells which contained lipids above a present threshold value were considered as adipocytes and they were included in further analysis. On texture “sum variance” (SV) vs. UCP1 expression plots undifferentiated progenitor segregated from the rest of the cells and were narrowly confined around the (0, 0) coordinates. Image regions occupied by these cells were excluded from further analysis.

Next, the fluorescence signal intensity of the UCP1 immunostaining and the texture sum variance of the light scatter signal of lipid droplets were quantified in each cell within the 30-pixel immediate outward vicinity of the nucleus contour by the Cell Profiler software. Afterwards, based on these fluorescence and light scatter signal of single cells, a semi-automated classification and enumeration of the differentiated white and brown adipocytes and undifferentiated preadipocytes was carried out applying the trained classification “Fast Gentle Boosting” of the Cell Profiler Analyst software.

4.2.10. Oxygen consumption and extracellular acidification measurements

Real-time oxygen consumption and extracellular acidification rates were measured by using an XF96 oximeter (Seahorse Biosciences, North Billerica, MA, USA). SGBS cells and hADMSCs were seeded onto 96-well XF96 cell culture microplates. Cells were kept in growth medium at the longest for 24 hours and then the differentiation process started as described in 4.2.4. On the days

of measurement, after recording the baseline oxygen consumption (OC) and extracellular acidification rate (ECAR) for 30 minutes, cells received a single bolus of dibutyl-cAMP at 500 μ M concentration to induce adrenergic stimulation. Then, stimulated OC was measured in every 30 minutes. The final reading took place at 6 h post-treatment. Differentiated adipocytes were treated with 2 mM β -guanidinopropionic acid to block the creatine-driven substrate cycle (Kazak et al., 2015). In addition, proton leak respiration was measured by oligomycin treatment at 2 μ M concentration, which blocks the ATP synthase. As a last step, for baseline correction, cells received a single bolus of Antimycin A treatment at 10 μ M concentration. After the measurements, oxygen consumption rate (OCR) and ECAR was normalized to protein content. For statistical analysis, the fold change of OC and ECAR levels were determined comparing basal, cAMP stimulated and oligomycin inhibited (both in unstimulated and stimulated cells) OCRs/ECARs of each sample to the basal OCR/ECAR of untreated white adipocytes (Kristóf et al., 2016).

4.2.11. Determination of cytokine release

In SGBS cell experiment, supernatants were harvested every fourth day during regular replacement of differentiation media and stored for cytokine measurements. The concentration of IL-6, IL-1 β , IL-8, TNF α and MCP-1 was measured from the collected media using ELISA DuoSet Kit (Sárvári et al., 2014; and 2015).

4.2.12. Genotyping

Genomic DNA was purified with GeneJET Genomic DNA Purification Kit according to the manufacturer's protocol. Rs1421085 SNP (single nucleotide polymorphism) was genotyped by qPCR using TaqMan genotyping assays and by DNA sequencing. To amplify the corresponding genomic region, we designed the following primer pair:

Forward: 5'GATGACACACACCATGAGCC
Reverse: 5'TAACAGTGGAGGTCAGCACA

Following PCR amplification, we purified the PCR product with NucleoSpin® Gel and PCR Clean-up kit. Then the quality of the product was investigated by 2% agarose gel electrophoresis. DNA was sequenced by Sanger sequencing method.

4.2.13. Statistical analysis

Results are expressed as the mean \pm SD for the number of assays indicated. The normality of distribution of the data was tested by Kolmogorov-Smirnov test. For multiple comparisons of groups statistical significance was calculated and evaluated by one-way ANOVA followed by Tukey post-hoc test. To compare two groups, two-tailed paired Student's t-test was used.

5. RESULTS

5.1. SGBS cells express surface markers similarly to primary preadipocytes and are heterozygous for the FTO risk allele Rs1421085.

Firstly, to investigate the phenotype of the undifferentiated SGBS cells used in our experiments, a multiparametric analysis of surface antigen expression was performed by three-color flow cytometry using the following fluorochrome-conjugated antibodies against: CD18, CD29, CD31, CD34, CD36, CD44, CD45, CD47, CD49a, CD49d, CD54, CD73, CD90, CD44, CD105, CD146, CD325, CD338, HLA-DR and integrin β 1. We found that hematopoietic/monocyte markers (CD34, CD47), endothelial markers (CD54), fibroblast markers (CD73, CD90), integrins and CAMs (integrin β 1, CD44, CD325) were expressed on the surface of undifferentiated SGBS preadipocytes. Previously, in our laboratory, the surface antigen expression of human adipose-derived stem cells (hADMSC) was characterized (Sárvári et al., 2014). As a next step, we made a comparison in the surface antigen expression pattern of SGBS preadipocytes to hADMSC cells isolated from human abdominal subcutaneous fat. Most of the examined markers were expressed similarly in SGBS and primary preadipocytes as shown in Table 1. However, CD34, CD44, CD146 and HLA-DR expression levels were higher in SGBS preadipocytes, while CD105, CD49a and CD31 antigens were expressed at a lower level as compared to primary preadipocytes.

		Percentage of positive cells (SGBS)	Percentage of positive cells (adipocyte-derived stem cells)
	CD34	91.50	3.23

Hematopoietic/ Monocyte markers	CD45	0.00	0.00
	CD47	94.44	99.31
	CD338 (ABCG2)	11.81	not determined
	HLA-DR	87.25	3.73
Endothelial markers	CD31 (PECAM)	0.00	6.69
	CD54 (ICAM-1)	74.64	not determined
MSC/Fibroblast markers	CD73	98.73	98.37
	CD90 (Thy-1)	98.74	95.05
	CD105 (Endoglin)	80.32	93.20
Integrins and CAMs	CD18	0.00	not determined
	CD29 (Integrin β 1)	98.40	99.81
	CD36	80.76	not determined
	CD44 (H-CAM,Hermes)	94.92	78.79
	CD49a (Integrin α 1)	74.39	99.52
	CD49d (Integrin α 4)	0.00	not determined
	CD146 (MCAM)	85.70	65.27
	CD325	96.36	not determined

Table 1. Analysis of the surface antigen pattern of SGBS preadipocytes and hADMSCs preadipocytes. *Expression of 18 markers was determined in undifferentiated SGBS preadipocytes by flow cytometry. Four groups of markers were tested: hematopoietic/monocyte, endothelial, MSC/fibroblast markers, integrins and CAMs. The numbers represent the percentage of positive cells. Data of adipose derived stem cells were adopted from Sárvári et al., 2014. The analysis was carried out by Dr. Zoltán Veréb.*

Next, we tested the presence of the C risk-allele of the rs1421085 locus; DNA sequencing and qPCR-based genotyping analysis determined that SGBS cells are heterozygous for the C risk allele (**Figure 10.A, B**).

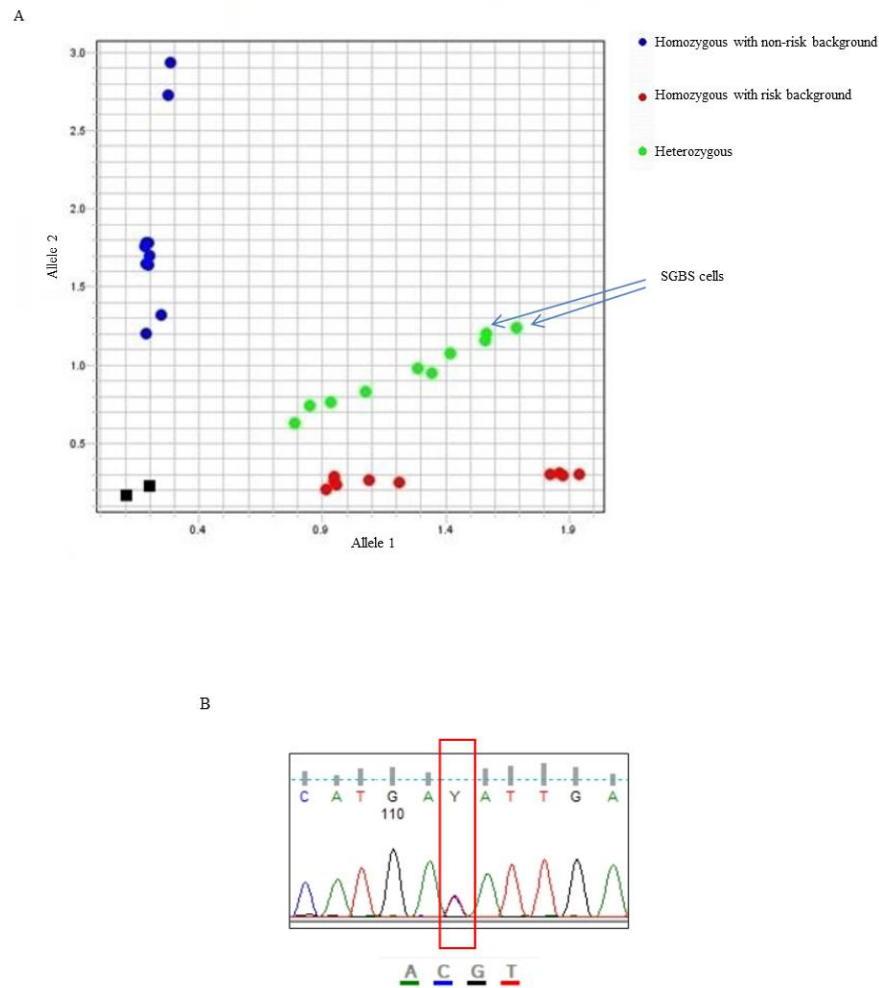


Figure 10. Analysis of rs1421085 SNP of SGBS preadipocytes. *Different genotypes of primary adipocytes and SGBS cells displayed by allele distribution plots, analyzed with Applied Biosystems QuantStudio 12 K Flex Software v1.2.2. (Fig.10.A). Sequence of the rs1421085 locus in the FTO gene showing that SGBS cells are heterozygous for the presence of the C risk allele (Fig.10.B). DNA was sequenced by the Sanger sequencing method. Genotyping was carried out by Attila Vámos, Sequencing was carried out by Dr. Szilárd Póliska.*

5.2. SGBS preadipocytes respond to sustained PPAR γ ligand and irisin or BMP7 treatment by inducing either beige or classical brown marker genes.

The previously described white (initiated by four days treatment with the PPAR γ -ligand rosiglitazone; Fischer-Posovszky et al., 2008) and browning (with the continuous presence of rosiglitazone during differentiation; Elabd et al., 2009) differentiation regimes were applied to differentiate SGBS preadipocytes.

In the two settings, we selected to examine the expression of core set of BAT-specific genes (*Ucp1*, *Cidea*, *Elovl3* and *Pgc1 α*) (**Figure 11**). The beige selective (*Tbx1*, *Cited1*) and “classical brown” adipocyte marker genes (*Zic1*, *Pdk4*) were also examined (**Figure 12**). The expression of *C/ebp β* which is a key transcriptional regulator of browning was also measured. A marker of mitochondrial enrichment (*Cyc1*) and relative mitochondrial DNA content were investigated as well (**Figure 11**). Finally, key drivers of the adipogenic program (*Ppar γ*) and general (*Lep*, *Fabp4*) adipocyte marker genes were investigated (**Figure 12**).

The browning cocktail highly induced *Ucp1* mRNA expression. Similarly, the presence of human recombinant irisin or BMP7 resulted in increased *Ucp1* mRNA expression on the top of the white differentiation protocol; while the presence of irisin or BMP7 in the browning cocktail did not enhance *Ucp1* expression further (**Figure 11**).

In line with the upregulation of *Ucp1* gene, we found that mRNA of brown-fat specific genes, like *Cidea* and *Elovl3* were also enriched during the administration of the browning cocktail and when irisin was added to the white differentiation cocktail. The master regulator of mitochondrial biogenesis, *Pgc1 α* was expressed significantly higher in browned SGBS cells as compared to white adipocytes and irisin treatment had the same effect (**Figure 11**).

On the contrary, we observed decreased expression of the white adipocyte marker gene, *Lep*, in response to the browning differentiation (the effect of irisin and BMP7 was not remarkable in that respect) (**Figure 12**). The expression level of other adipogenic markers, *Cebpb* and *Pparg*, did not differ between white and browned SGBS adipocytes. *Fabp4* expression was significantly increased in case of browned adipocytes as compared to the white ones. Out of these markers, only the expression of *Pparg* was enhanced in response to irisin or BMP7 treatment (**Figure 12**).

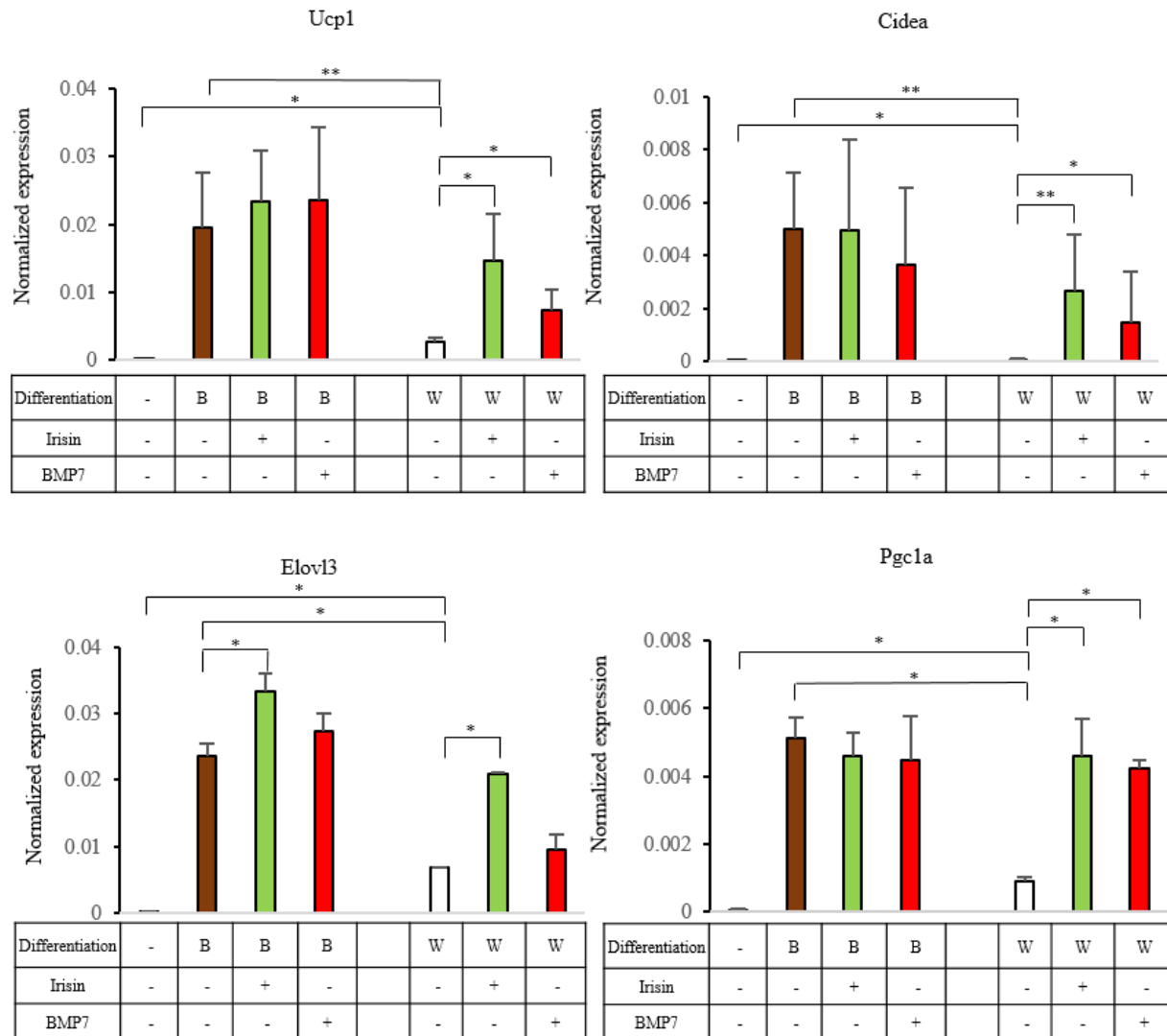


Figure 11. Browning of SGBS cells is induced by PPAR γ -driven differentiation cocktail, irisin or BMP7 treatment. Normalized expression of *Ucp1*, *Cidea*, *Elovl3* and *Pgc1a* genes in SGBS adipocytes. SGBS preadipocytes were differentiated to white (W) or beige (B) for two weeks; human recombinant irisin treatment at 250 ng/ml concentration (green bars) or BMP7 treatment at 50 ng/ml concentration (red bars) were applied to induce browning of SGBS cells from day 1. Gene expression was determined by RT-qPCR and target genes were normalized to *Gapdh*. For multiple comparisons of groups statistical significance was evaluated by one-way ANOVA followed by Tukey post-hoc test $n=5$ * $p<0.05$; ** $p<0.01$

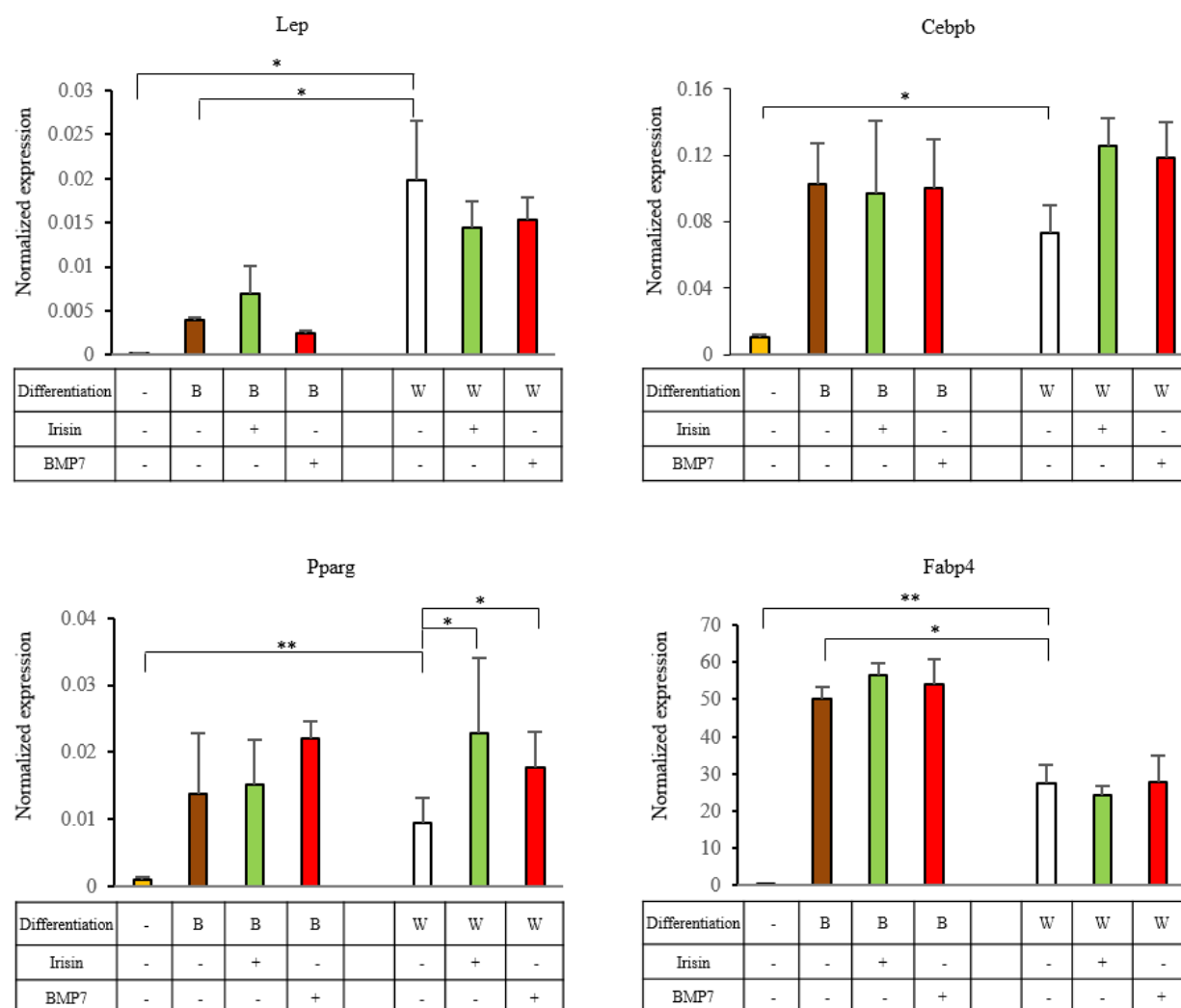


Figure 12. Expression of adipogenic markers in SGBS adipocytes. *Normalized expression of Lep, Cebpb, Pparg and Fabp4 genes in SGBS adipocytes. SGBS cells were differentiated and treated, gene expression was determined as in Figure 11. For multiple comparisons of groups statistical significance was evaluated by one-way ANOVA followed by Tukey post-hoc test. n=5 *p<0.05; **p<0.01*

The expression level of the mitochondrial enrichment marker, *Cyc1*, was significantly higher in browned adipocytes compared to white ones. Moreover, irisin treatment resulted in similar effect on white adipocytes. Undifferentiated SGBS preadipocytes contained high mitochondrial DNA

(mtDNA). In case of white adipocytes we could detect relatively low mitochondrial DNA amount and Irisin treated white adipocytes also have significantly elevated level of it, however, the effect of BMP7 was moderate. The mitochondrial DNA content was the highest in the case of browned cells after the administration of the PPAR γ -driven browning differentiation cocktail (**Figure 13**).

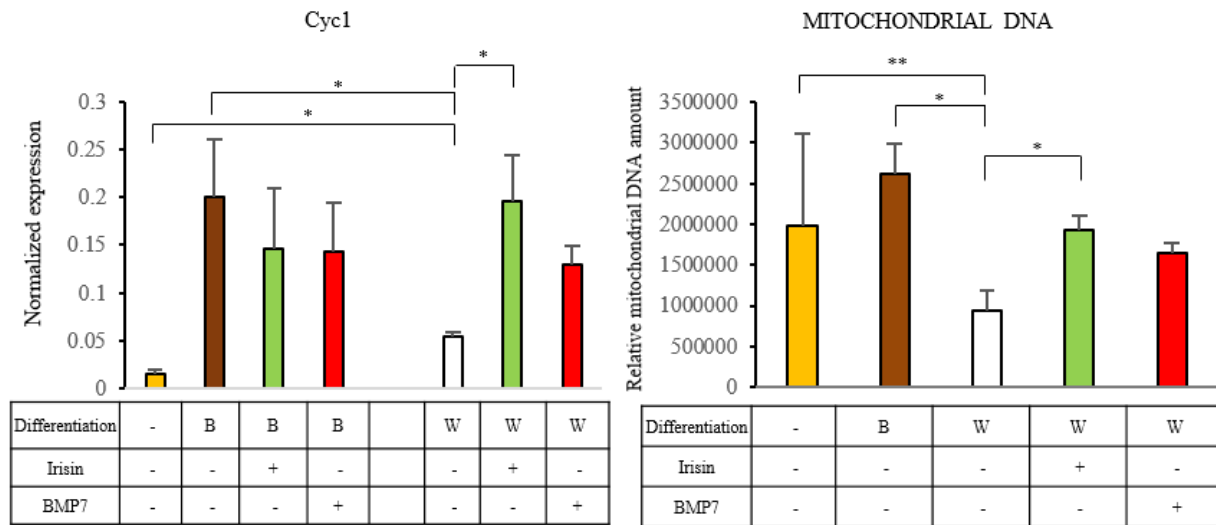


Figure 13. Browning of SGBS cells is induced by PPAR γ -driven differentiation cocktail, irisin or BMP7 treatment. Normalized expression of *Cyc1* gene and relative mitochondrial DNA amount of SGBS adipocytes. SGBS cells were differentiated and treated as in Figures 11-12. Gene expression was determined by RT-qPCR and target gene was normalized to *Gapdh*. Relative mitochondrial DNA content of preadipocytes and differentiated SGBS cells was determined by quantitative PCR. For multiple comparisons of groups statistical significance was evaluated by one-way ANOVA followed by Tukey post-hoc test. $n=5$ * $p<0.05$; ** $p<0.01$

As a next step, we intended to ask a question whether the beige-selective marker genes, including *Tbx1* (Wu et al., 2012) and *Cited1* (Sharp et al., 2012) or classical brown adipocyte markers, like *Zic1* (Cypess et al., 2013) were induced in SGBS cells. In line with the increased *Ucp1* expression, we found that irisin or the browning protocol resulted in marked upregulation of *Tbx1* and *Cited1*

but no *Zic1* induction. We could detect no further increase in the expression of *Tbx1* and *Cited1* when irisin was added on top of the browning protocol. BMP7, on the other hand, only upregulated *Zic1* markedly and even prevented *Tbx1* induction when it was combined with the browning differentiation cocktail (**Figure 14**). The expression of *Tmem26* and *Shox2*, proposed beige-markers (Perdikari et al., 2018) reported in mouse studies, remained at a low level in the browned SGBS adipocytes compared to the white ones (**Figure 15**). Interestingly, *Pdk4*, originally described as a classical brown marker in mice (Cheng et al., 2018), showed a similar expression pattern as the beige-selective *Tbx1* and *Cited1*, in SGBS adipocytes (**Figure 14**).

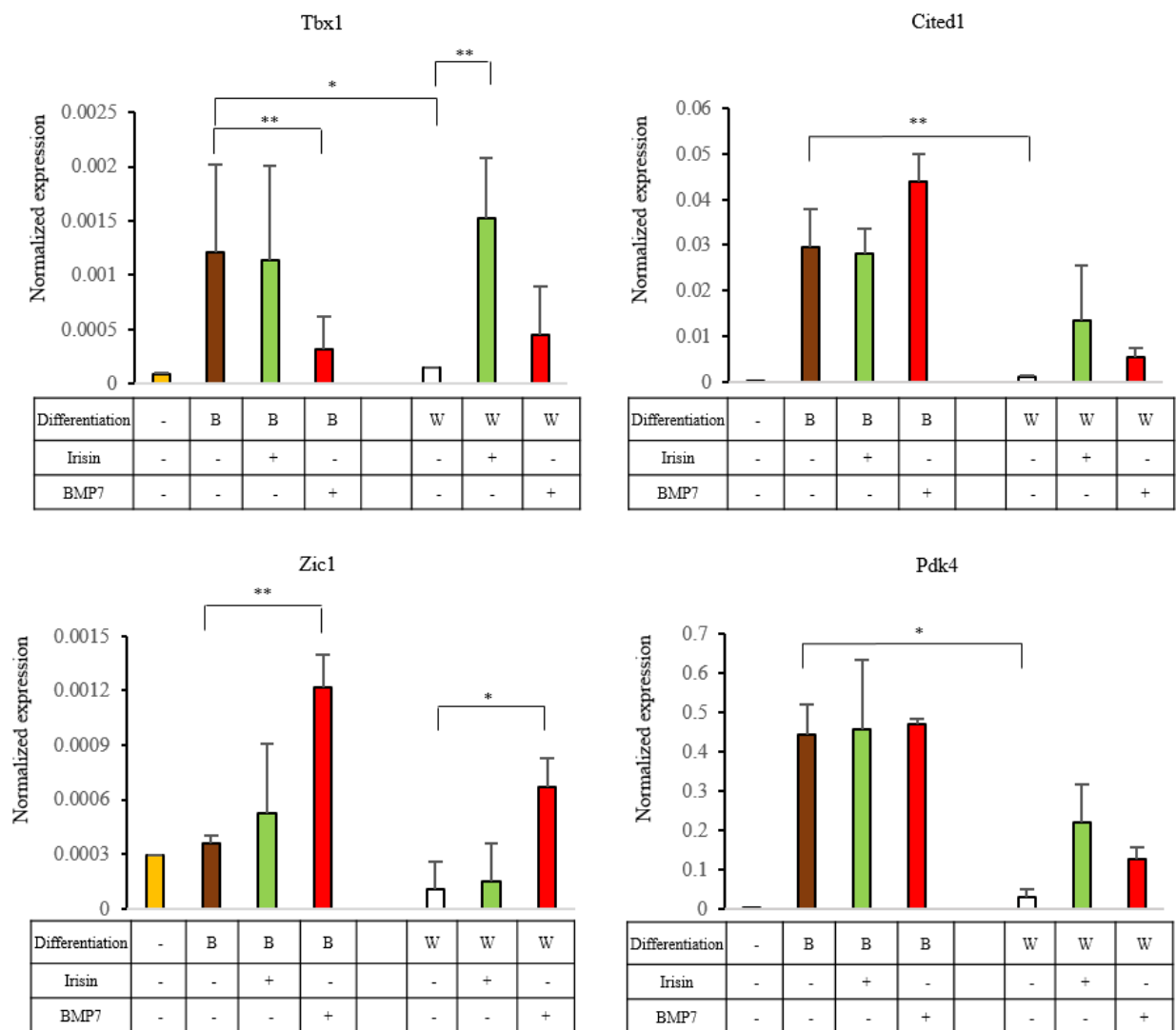


Figure 14. Browning of SGBS cells is induced by PPAR γ -driven differentiation cocktail, irisin or BMP7 treatment. *Normalized expression of Tbx1, Cited1, Zic1 and Pdk4 genes in SGBS adipocytes. SGBS cells were differentiated and treated as in Figures 11-13. (Gene expression was determined by RT-qPCR and target genes were normalized to Gapdh.) For multiple comparisons of groups statistical significance was evaluated by one-way ANOVA followed by Tukey post-hoc test. n=5 *p<0.05; **p<0.01*

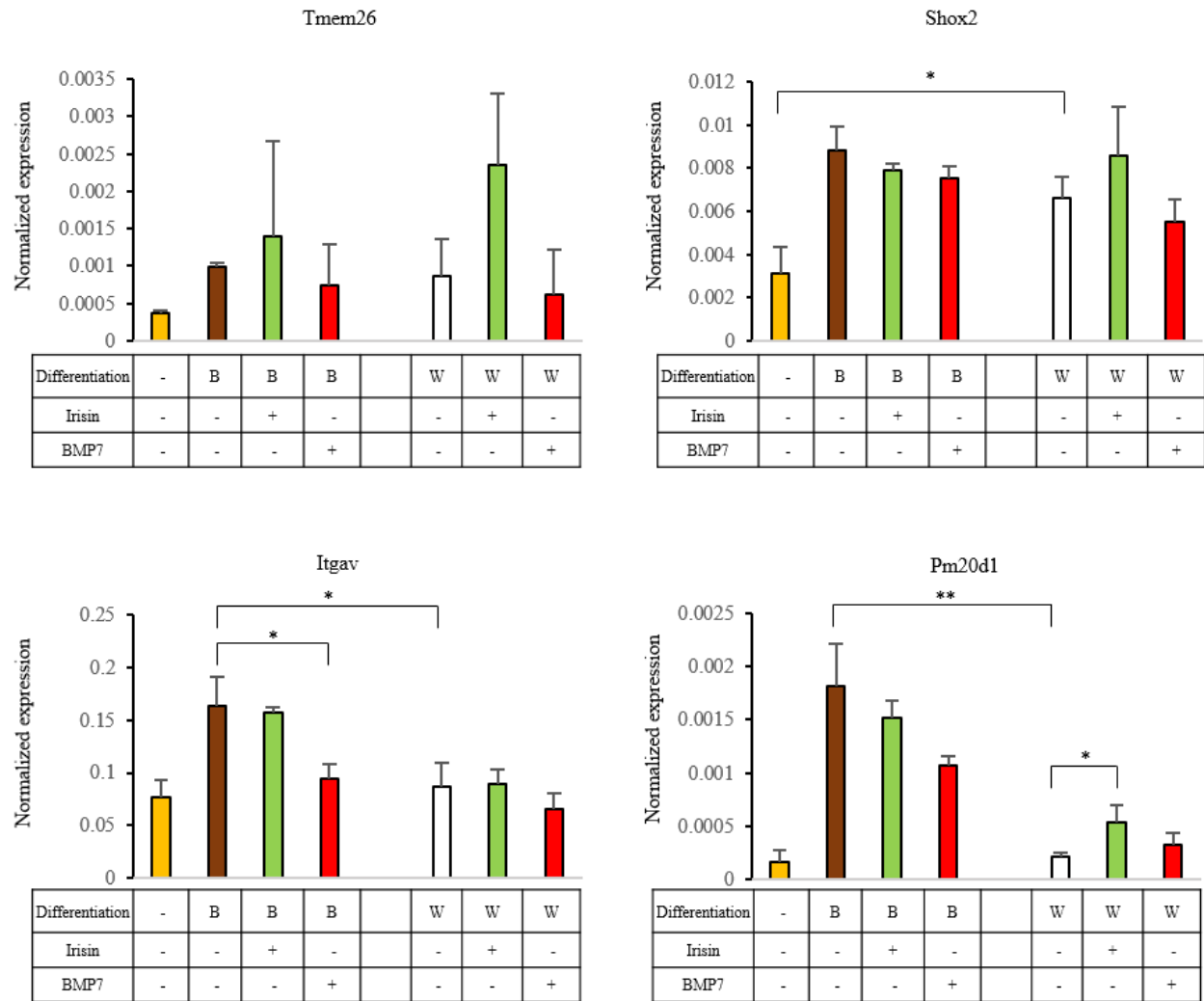


Figure 15. Expression of beige markers in SGBS adipocytes. *Normalized expression of Tmem26, Shox2, Itgav and Pm20d1 genes in SGBS adipocytes. SGBS cells were differentiated and treated as in Figures 11-14. (Gene expression was determined by RT-qPCR and target genes were normalized to Gapdh.) For multiple comparisons of groups statistical significance was evaluated by one-way ANOVA followed by Tukey post-hoc test. n=5*
**p<0.05; **p<0.01*

Then, we investigated the concentration dependence of the irisin and BMP7 effects during white adipocyte differentiation in SGBS cells. In rodents, irisin plasma concentrations were detected (Boström et al., 2012) more than 10-fold higher ($> 100 \text{ ng}/\mu\text{l}$) than in humans, which was investigated by Jedrychowski et al. They found that irisin was present at 3-4 ng/ml concentration in human blood plasma in the case of sedentary life; however, it increased to 4-5 ng/ml in response to aerobic exercise (Jedrychowski et al., 2015).

Itgav, the gene which encodes the specific subunit of the recently discovered irisin receptor (Kim et al., 2018) is expressed both in undifferentiated SGBS preadipocytes and in differentiated adipocytes to the same extent. *Pm20d1* which encodes the secreted enzyme peptidase M20 domain containing 1 (Long et al., 2016) was significantly higher in browned adipocytes, as well as irisin treated white adipocytes, as compared to control ones (**Figure 15**). This means that browned SGBS adipocytes are able to produce N-acyl amino acids which can function as endogenous uncouplers of UCP1-independent thermogenesis.

Only a slight increase could be observed in *Ucp1* expression at 5 ng/ml concentration of irisin as compared to untreated cells. Although, irisin treatment was efficient above 50 ng/ml concentrations on the induction of *Ucp1*. The same trend was observed when the expression of *Tbx1*, *Cyc1*, *Elovl3* and *Pgc1a* was analyzed (**Figure 16**).

The administration of BMP7 to the white adipogenic differentiation cocktail in increasing concentrations resulted in upregulated expression of *Ucp1* and *Cidea* brown marker genes as compared to the untreated white adipocytes. Contrarily, we observed downregulation of *Lep* at 100 ng/ml BMP7 concentration. However, no significant changes were observed in the expression of *Tbx1*, *Cyc1* and *Elovl3* as a result of BMP7 treatment (**Figure 17**).

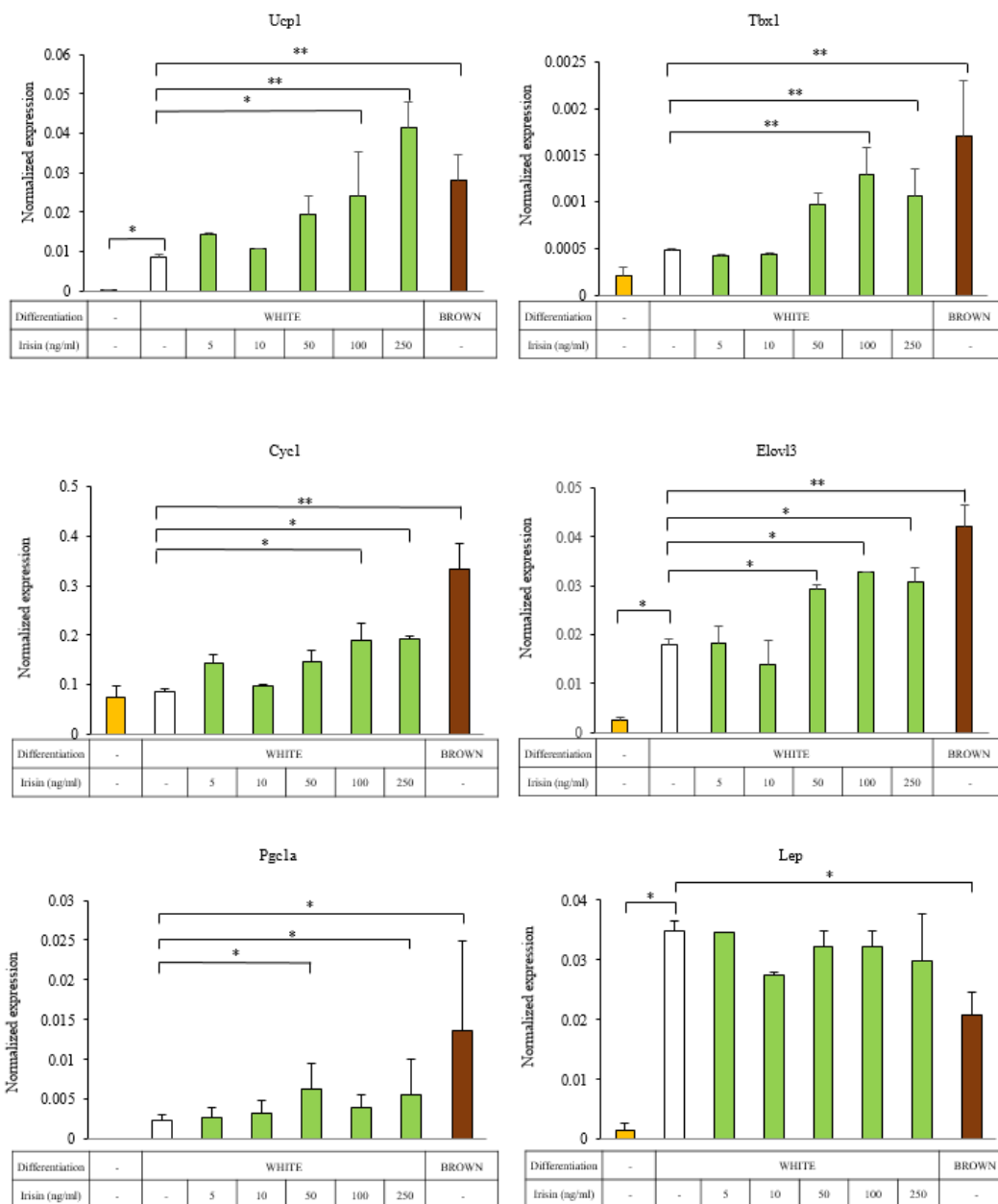


Figure 16. Concentration dependence of the Irisin effect during the white adipocyte differentiation program of SGBS cells *Normalized expression of Ucp1, Tbx1, Cyc1, Elovl3, Pgc1a and Lep genes in SGBS adipocytes which were harvested after 14 days differentiation as described in Figure 11. Gene expression was determined by RT-qPCR and genes were normalized to Gapdh. For multiple comparisons of groups statistical significance was evaluated by one-way ANOVA followed by Tukey post-hoc test * $p < 0.05$; ** $p < 0.01$, $n = 3$*

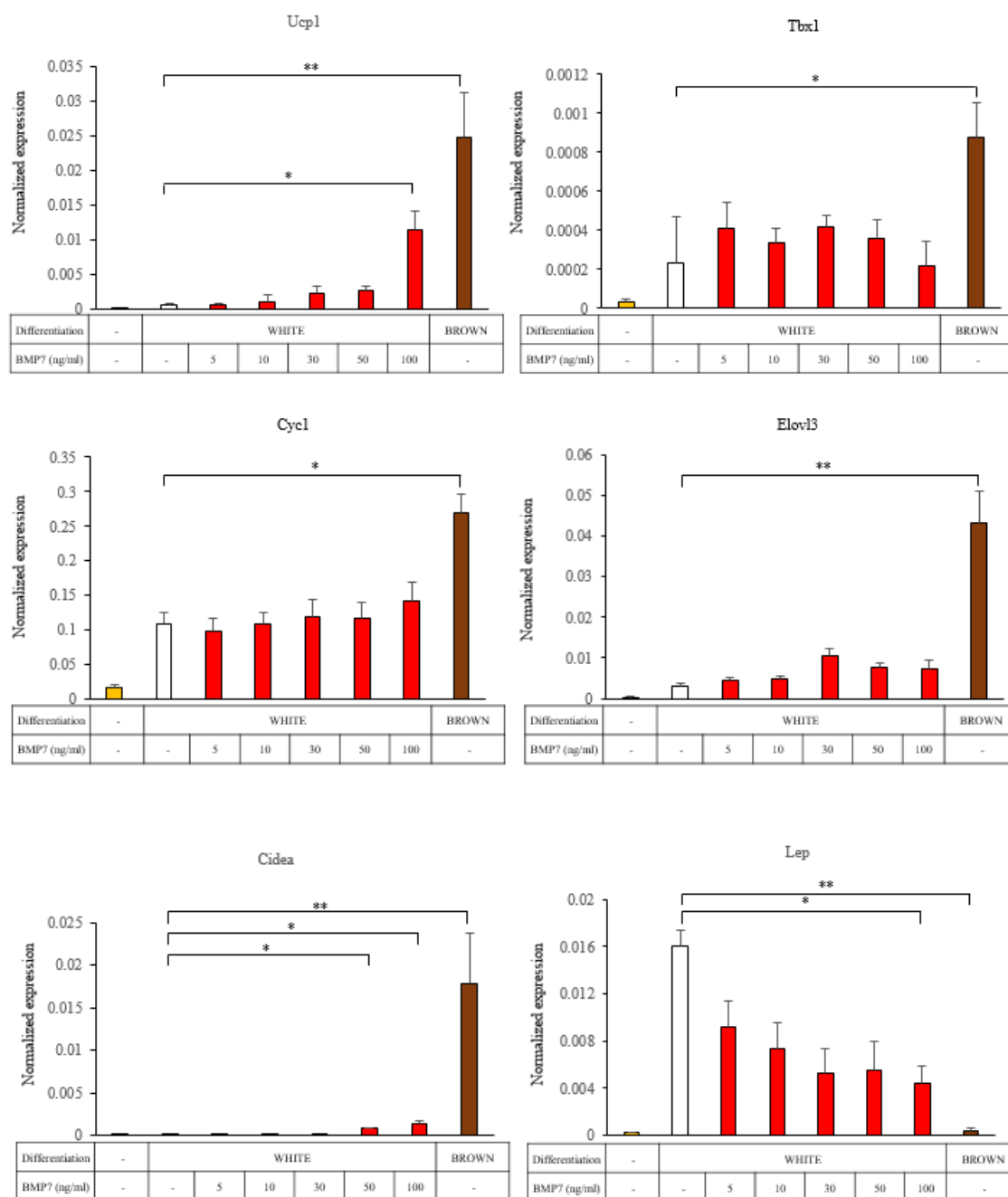


Figure 17. Concentration dependence of the BMP7 effect during the white adipocyte differentiation program of SGBS cells. *Normalized expression of Ucp1, Tbx1, Cyc1, Elovl3, Cidea and Lep genes in SGBS adipocytes which were harvested after 14 days differentiation as described in Figure 11. Gene expression was determined by RT-qPCR and genes were normalized to Gapdh. For multiple comparisons of groups statistical significance was evaluated by one-way ANOVA followed by Tukey post-hoc test * $p < 0.05$; ** $p < 0.01$, $n = 3$*

5.3. Laser scanning cytometry can quantify SGBS adipocyte browning.

Next, we investigated the morphological characteristics of the white and browned SGBS cells by assessing the textural parameters and UCP1 protein content of the individual adipocytes using laser scanning cytometry (LSC). SGBS adipocytes are able to accumulate lipid droplets as a result of 14-day-long adipocyte differentiation, formerly this phenomenon was quantified using LSC by Doan-Xuan et al. (2013). Applying image analysis, single cells were identified based on their nuclei and classified according to their UCP1 content and lipid droplet structure (**Figure 18**). An overview image of a sample of browning differentiation can be found in the **Figure 19**. As a result of the 14-day-long PPAR γ -driven browning differentiation, we found higher UCP1 content either in single SGBS adipocytes or in total cell lysates, as compared to white. In addition, we detected enhanced UCP1 protein content in response to irisin or BMP7 supplementation.

Next, we plotted texture sum variance and UCP1 protein content for each differentiated adipocyte (undifferentiated cells were omitted from the analysis). Adipocytes with morphological characteristics of browning were detected as they contained smaller lipid droplets and had high levels of UCP1 as compared to white adipocytes. On the other hand, white adipocytes had larger lipid droplets and contained low amount of browning marker protein. Our results indicate that the population of differentiated adipocytes remains heterogeneous regardless of whether white or browning protocol was applied. Furthermore, we could detect a significant amount of adipocytes with the characteristic morphological features of browning even in response to the white differentiation. In contrast to primary adipocytes (Kristóf et al., 2015; Abdul.Rahman et al., 2016) the texture sum variance did not decrease significantly during the induction of browning marked by elevated UCP1 expression (**Figure 20**).

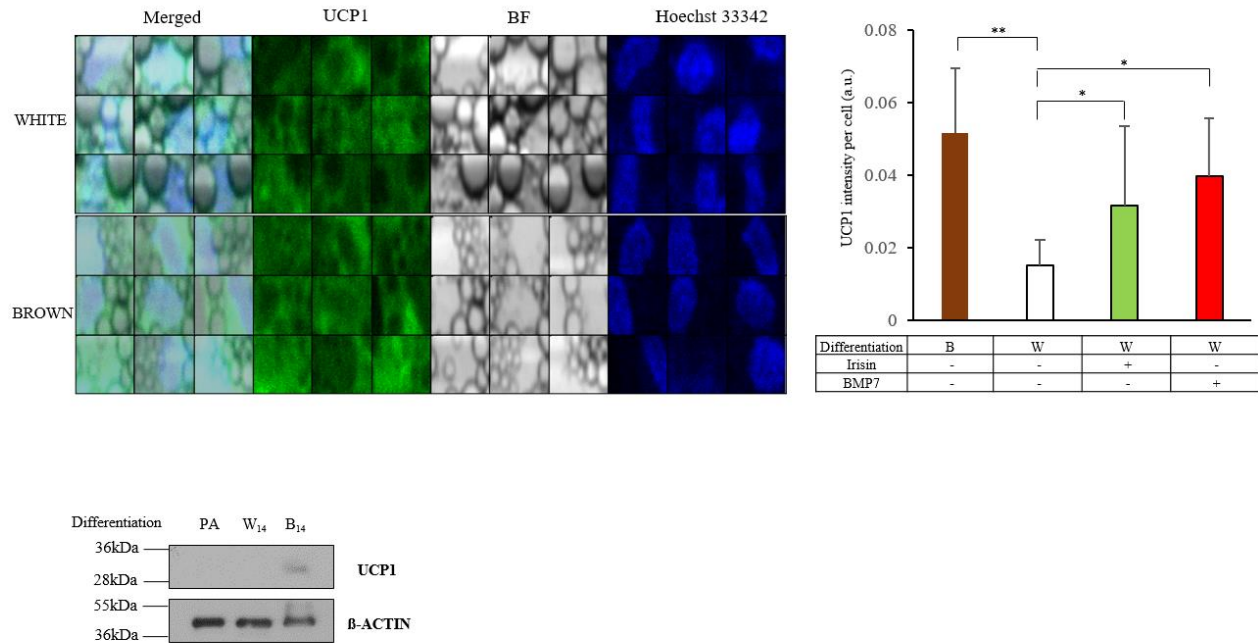


Figure 18. Morphological features of browning SGBS adipocytes that were induced by PPAR γ -driven differentiation cocktail, irisin or BMP7 treatment. *UCP1* content, lipid droplets and nuclei are shown in gallery images ($N=9$) of selected cells within the white and brown differentiated adipocytes. SGBS preadipocytes were differentiated and treated as described in Figure 11. $n=3$, 1000-2000 cells per each sample. *UCP1* protein content of browning induced adipocytes (PPAR γ -driven differentiation cocktail, irisin or BMP7 treatment) as compared to white adipocytes. Expression of *UCP1* at protein level in SGBS adipocyte lysates detected by immunoblotting (c). * $p<0.05$; ** $p<0.01$ Image analysis was carried out by Dr. Zsolt Bacsó.

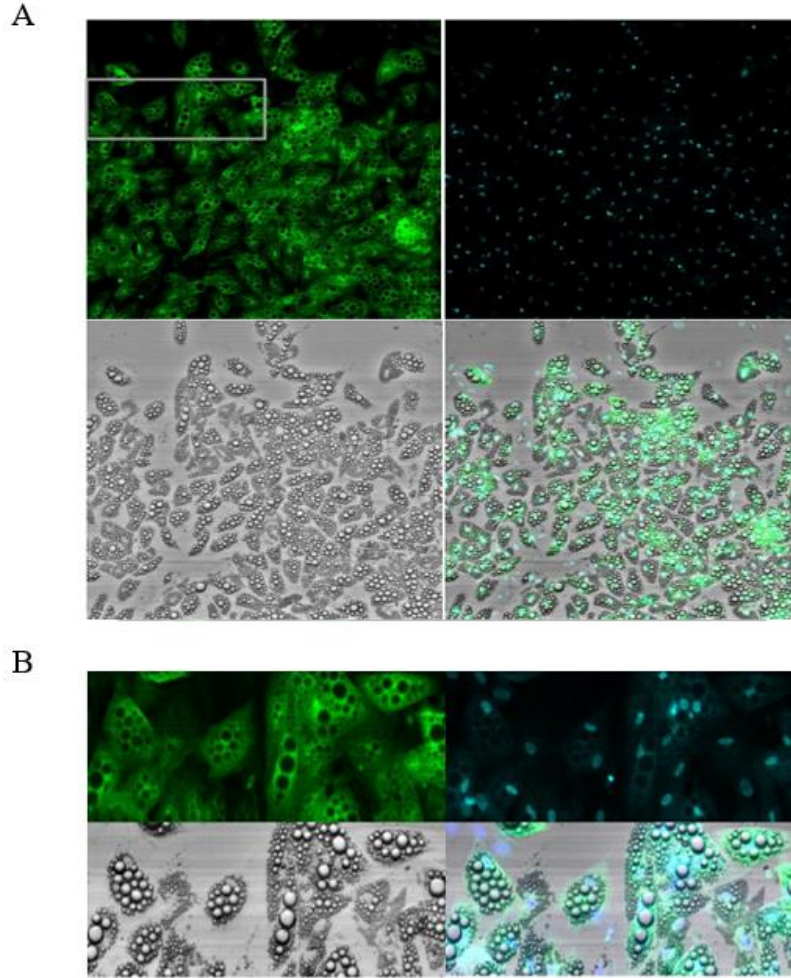


Figure 19. Well images (size: width = 996 μm , height = 957 μm , four images in the upper panel) **and field images** (four images in the bottom panel) **of the green** (UCP1 – Alexa-488 labeled indirect immunostaining, upper left image in both panels), **blue** (nuclei - Hoechst 33342 staining, upper right images) **and light scatter** (bottom left images) **channels and merged images of the previous three channels** (bottom right images) **captured by the iCys laser-scanning cytometer.** This well image, which is an overview image of an appropriately selected area of the sample is composed of 2 x 5 higher resolution field images in the three channels (A). One of these higher resolution field images in each channel is shown in the bottom panel (B). The original location of this field image is indicated by the grey rectangular line in the top left UCP1 channel well image. In every imaging measurements, approximately 5-20 well images were manually selected and automatically recorded. In the image analysis step, individual cells were identified and classified and in the Figure 18. mosaic image 9 of these single cells are shown. Image analysis was carried out by Dr. Zsolt Bacsó.

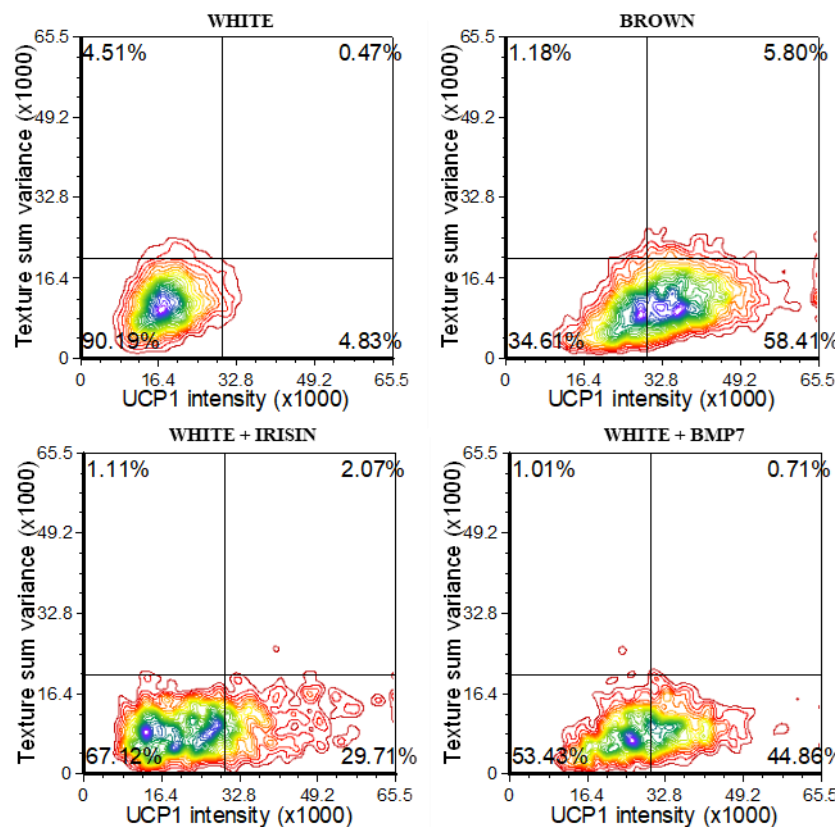


Figure 20. Density plot figures show texture sum variance and UCP1 protein content of differentiated single cells in one representative SGBS replicate. SGBS cells were differentiated as in Figure 11. Density plot images showing texture sum variance and Ucp1 content of differentiated cells in one representative SGBS replicate. Browning adipocytes can be identified as cells containing small lipid droplets and high levels of UCP1 protein. Density plot figures was carried out by Dr. Zsolt Bacsó.

5.4. Differentiated SGBS adipocytes respond to activation as functional beige cells and can use the creatine phosphate cycle.

Next, we intended to investigate the functional capacity of human SGBS adipocytes. Cells were differentiated in the presence of browning-inducers and mitochondrial oxygen consumption rate (OCR) was measured. In accordance with the gene expression and morphological changes, we

found higher basal OCR after the browning was induced by either PPAR γ ligand, irisin or BMP7. We stimulated the adipocytes by a single bolus dose of cell permeable dibutyryl-cAMP. OCR of browning adipocytes was elevated more robustly as compared to the white adipocytes (**Figure 21**). A similar trend was observed when ATP synthase activity was inhibited as a result of oligomycin treatment which is an inhibitor of ATP synthase, and can be used to quantify proton leak respiration. Both basal and cAMP-stimulated proton leak OCRs were significantly higher in browned than in white adipocytes (**Figure 21**).

In parallel, we detected significantly increased extracellular acidification rate (ECAR) both in untreated and cAMP-stimulated browned adipocytes as compared to white cells (**Figure 22**).

Furthermore, we found it important to examine what proportion of cAMP induced OCR is related to the UCP1 independent creatine phosphate futile cycle, a characteristic feature of beige adipocytes, utilizing β -guanidinopropionic acid (β -GPA) which is an inhibitor of this cycle (Kazak et al., 2015). In case of the browned SGBS cells, the creatine-cycle related OCR was appreciably elevated in contrast to untreated white adipocytes, and the same trend was observed as a result of irisin or BMP7 treatment on white adipocytes (**Figure 22**). Mitochondrial creatine kinases, *Ckmt1a* and *Ckmt2*, were expressed at a significantly higher level in the browned SGBS adipocytes as compared to those which were differentiated to white. In undifferentiated preadipocytes the expression level of these genes was below the detection limit (**Figure 22**). This suggests that the creatine phosphate futile cycle is present and active in browned SGBS adipocytes induced either by PPAR γ -driven browning differentiation or by the administration of irisin and BMP7 during white differentiation, demonstrating that the browned SGBS adipocytes functionally resemble beige cells.

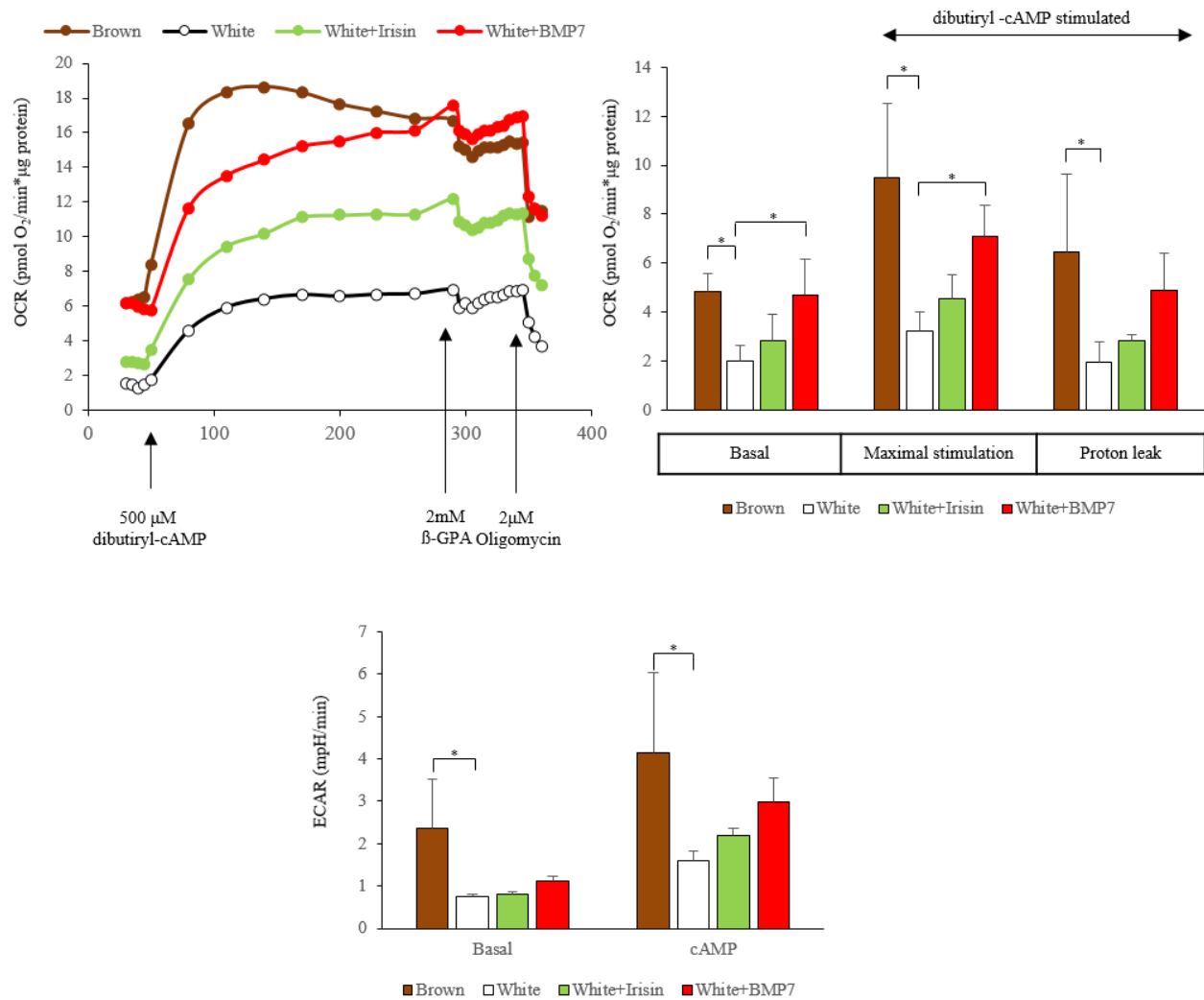


Figure 21. Functional measurements detect high oxygen consumption and significant involvement of the creatine substrate cycle in Rosiglitazone, irisin and BMP7 differentiated browning adipocytes. SGBS preadipocytes were differentiated and treated as in Figure 11. Mitochondrial oxygen consumption rate (OCR) of differentiated SGBS cells of one representative measurement determined by a Seahorse XFe96 analyzer. Basal, dibutyryl-cAMP-stimulated and oligomycin-inhibited oxygen consumption levels in SGBS cells, as compared to basal OCR of white-directed adipocytes. Extracellular acidification rate (ECAR) of differentiated SGBS cells measured by a Seahorse XFe96 analyzer $n=4$ $*p<0.05$.

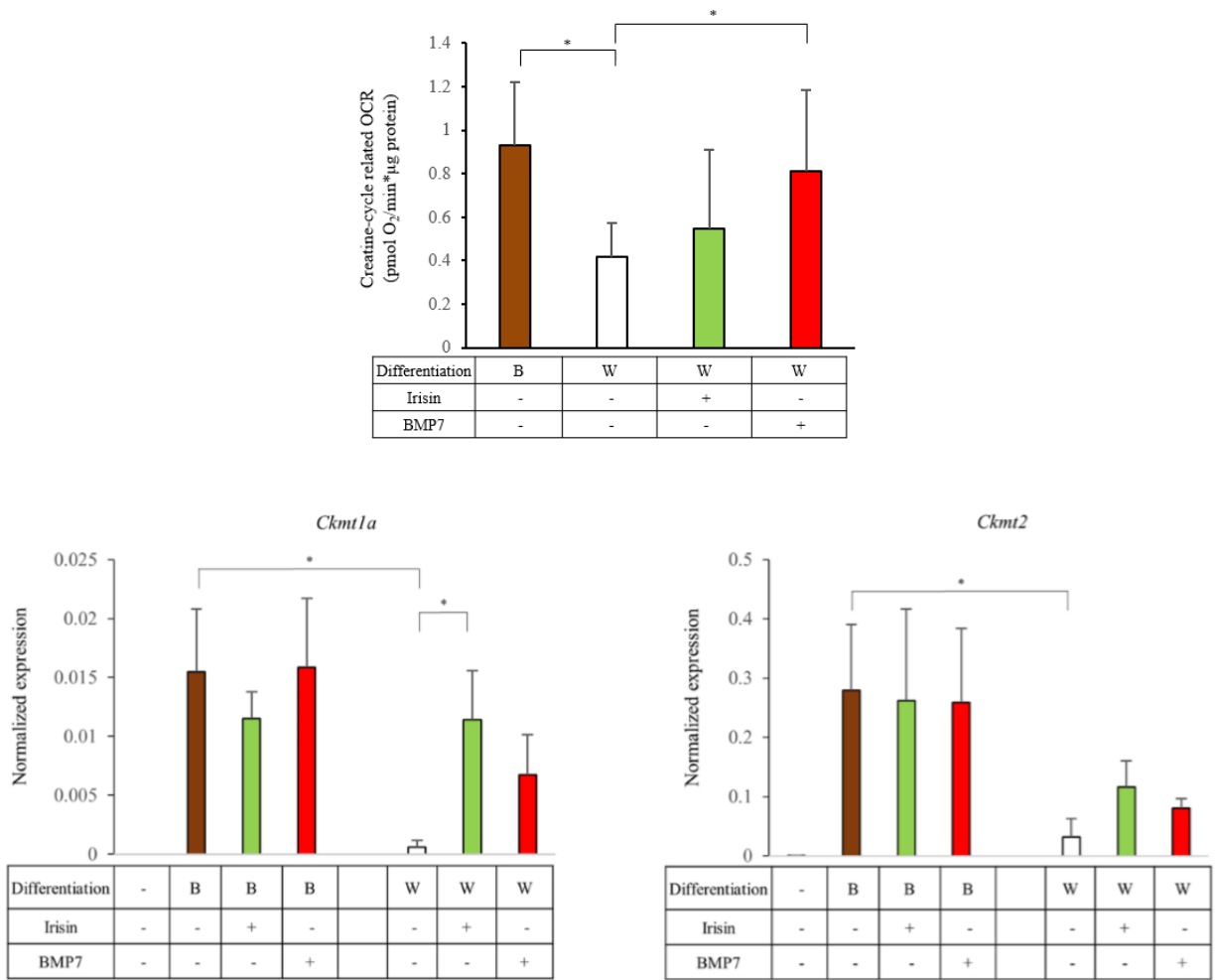


Figure 22. Functional analysis of differentiated SGBS cells treated with irisin or BMP7 and expression of mitochondrial creatine kinases (Ckmt1a and Ckmt2) in SGBS adipocytes. *SGBS preadipocytes were differentiated and treated as in Figure 11. Inhibitory effect of β -guanidiopropionic acid (β -GPA) (at 100mg/ml concentration) on the oxygen consumption of SGBS adipocytes. $n=4$ * $p<0.05$; ** $p<0.01$. Gene expression was determined by RT-qPCR and target genes were normalized to Gapdh. $n=3$ * $p<0.05$*

5.5. The brown/beige adipocyte phenotype of differentiated SGBS cells is maintained in the absence of the PPAR γ -ligand.

In order to determine whether the PPAR γ -driven differentiation could maintain a beige phenotype in a longer time frame, we performed a long-term experiment after 2 weeks altogether for 21 or 28

days; and in parallel samples the browning cocktail was replaced by the white differentiation cocktail for the third (B14,W7) and the fourth week (B14,W14).

We could detect the highest expression of *Ucp1* at day 28, at the end of the long-term browning differentiation program. When we replaced the browning cocktail to white, *Ucp1* mRNA level was increased at least until day 21, then dropped to the level of day 14. UCP1 protein expression was investigated by Western blot, either when the white or when the PPAR γ -driven differentiation process was carried out. We found that UCP1 protein was slightly expressed in browned cells after 14 days of differentiation. Long-term rosiglitazone induction led to further robust upregulation of UCP1 at protein level. When the PPAR γ stimulus was omitted after 2 weeks of browning differentiation program, the expression level of UCP1 protein was slightly increased by the end of the third week, and it was still detectable one week later at a lower level (**Figure 23**).

At the end of the fourth week of differentiation process, we detected a six-fold higher UCP1 protein content by immunohistochemistry as a result of the browning cocktail as compared to white. When the PPAR γ -agonist was replaced by the white differentiation protocol for the last 2 weeks, the UCP1 protein content per cells did not change robustly as compared to adipocytes maintained continuously in the presence of the PPAR γ -driven differentiation regimen. Paralelly, similar texture sum variance was detected in both cell populations (**Figure 25**).

In paralell, we examined brown-fat specific genes: *Cidea* and *Elovl3*; similarly to *Ucp1*, further upregulation was observed when we continued the administration of the browning protocol; when PPAR γ -stimulation was eliminated, their expression levels remained elevated as compared to B14.

The replacement of the cocktails from browning to white without rosiglitazone did not induce de novo white adipogenesis, marked by the continuous low expression of *Lep* (Figure 24).

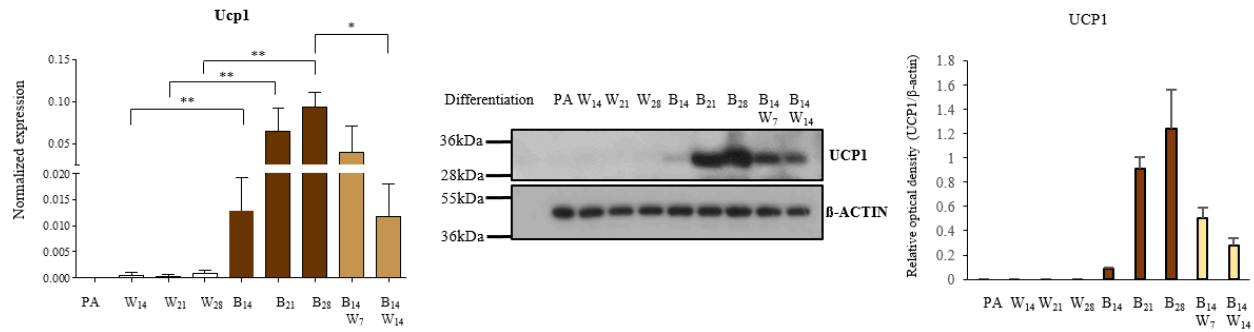


Figure 23. PPAR γ -driven differentiation can be maintained in long-term cultures of browning adipocytes. SGBS preadipocytes were differentiated to white (W) or beige (B) for two, three and four weeks (indicated by the number of days), respectively. At day 14, the PPAR γ -driven browning cocktail was replaced by the white without rosiglitazone for additional one (B14,W7) or two weeks (B14,W14). Expression of UCP1 at mRNA and protein level. Normalized expression of *Ucp1* gene by RT-qPCR and target genes were normalized to *Gapdh*. For multiple comparisons of groups statistical significance was evaluated by one-way ANOVA followed by Tukey post-hoc test. $n=4$; $p<0.05$; $**p<0.01$

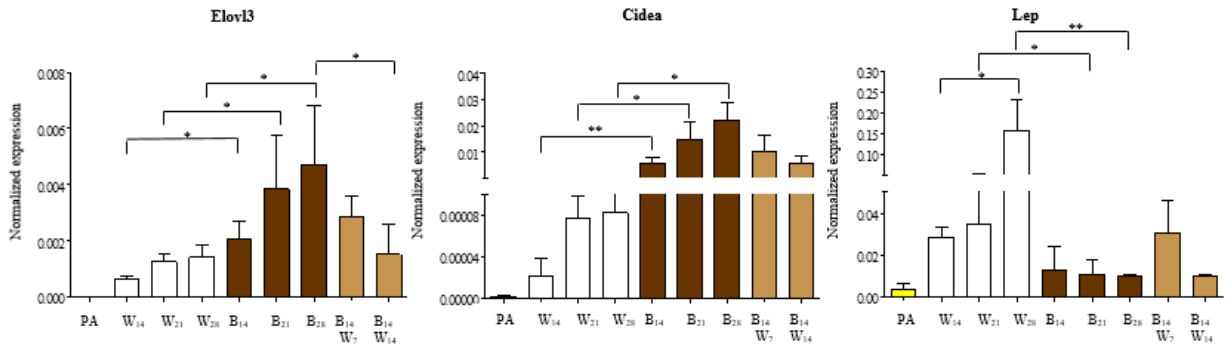


Figure 24. PPAR γ -driven differentiation can be maintained in long-term cultures of browning adipocytes. SGBS preadipocytes were differentiated as in Figure 23. Normalized expression of *Cidea*, *Elov13* and *Lep* genes by RT-qPCR and target genes were normalized to *Gapdh*. For multiple comparisons of groups statistical significance was evaluated by one-way ANOVA followed by Tukey post-hoc test. $n=4$; $p<0.05$; $**p<0.01$

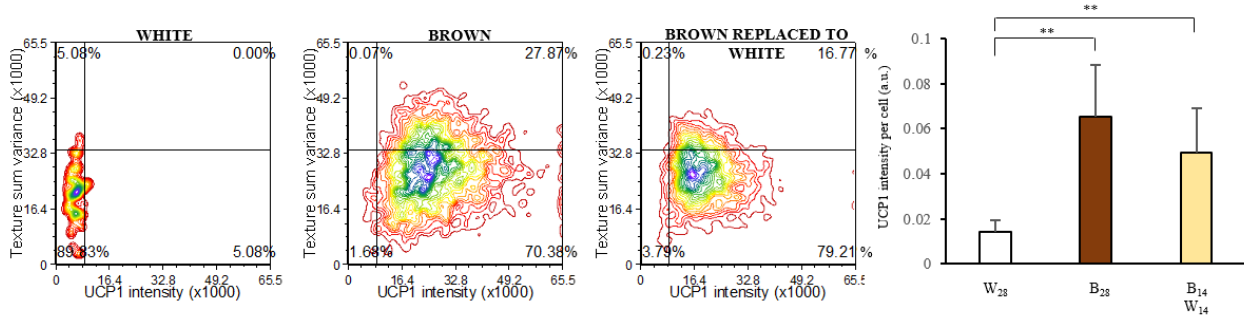


Figure 25. PPAR γ -driven differentiation can be maintained in long-term cultures of browning adipocytes. SGBS preadipocytes were differentiated as in Figure 23. Density plot figures show texture sum variance and UCP1 protein content of differentiated cells detected by Laser-scanning cytometry in one representative SGBS replicate; $n=3$, 1000-2000 cells per each sample. $*p<0.05$; $**p<0.01$ Density plot figures was carried out by Dr. Zsolt Bacsó.

Mitochondrial oxidative phosphorylation (OXPHOS) plays a fundamental role in the energy production of brown/beige adipocytes (Hüttemann et al., 2007). We found that protein expression of mitochondrial respiratory components in complex II, III and IV followed the same pattern of UCP1 expression in SGBS adipocytes. We detected higher expression of respiratory chain proteins in browned adipocytes as compared to control white adipocytes indicating stimulated mitochondrial biogenesis (**Figure 26**). The omitted PPAR γ agonist resulted in only a slight reduction in the level of these proteins, suggesting the clearance of a small fraction of the mitochondria. These results suggest that the signaling pathways driving the beige phenotype in SGBS cells can be maintained at least for two consecutive weeks, even when rosiglitazone is eliminated from the differentiation media.

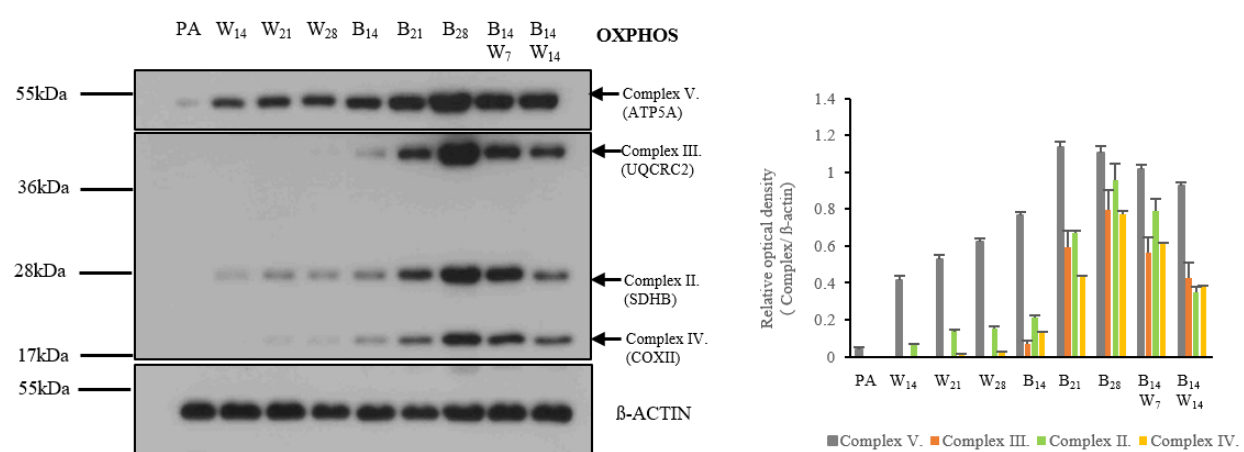


Figure 26. Expression of mitochondrial complex subunits detected by immunoblotting. *SGBS preadipocytes were differentiated as in Figures 23-25. Relative optical density was determined by Image J software. β -actin was used as endogenous control, $n=3$. All gels were run under the same conditions.*

5.6. Browning cocktail resulted in increased expression of IL-8, IL-6 and MCP1 cytokines compared to white adipocytes.

Additionally, we investigated the secretion of cytokines by human SGBS cells. Differentiation media were collected during the regular replacement of the adipogenic cocktails and IL-8, IL-6, IL1 β , TNF α and MCP-1 were measured by ELISA after samples stored on the 1st and 2nd weeks of differentiation were pooled. Neither undifferentiated nor differentiated adipocytes secreted TNF α and IL-1 β .

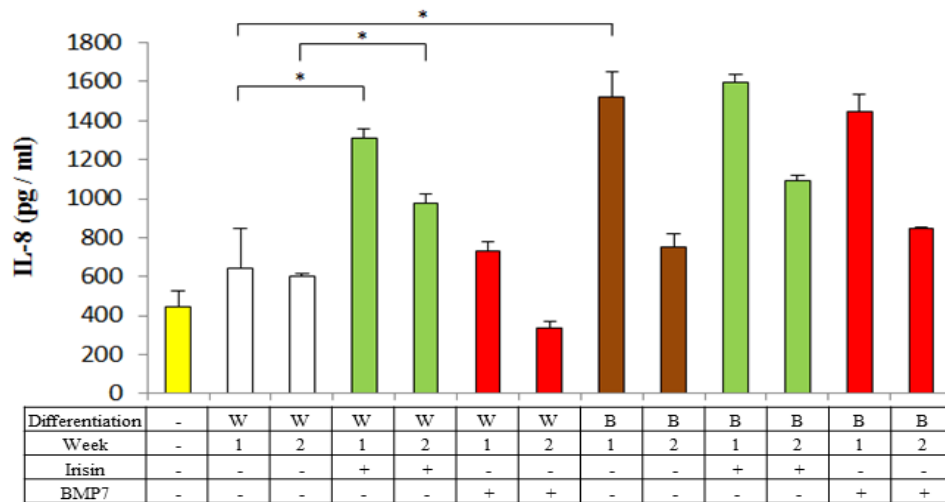


Figure 27. IL-8 secretion by differentiated SGBS treated with irisin or BMP7. SGBS cells were differentiated for two weeks as described in Figure 11. Supernatants were collected and pooled during the 1st and 2nd week of differentiation and secreted IL-8 was measured by sandwich ELISA. Data are expressed as the mean \pm SD for 3 independent experiments. For multiple comparison of groups statistical significance was evaluated by one-way ANOVA followed by Tukey post-hoc test. * $p < 0.05$, $n = 3$

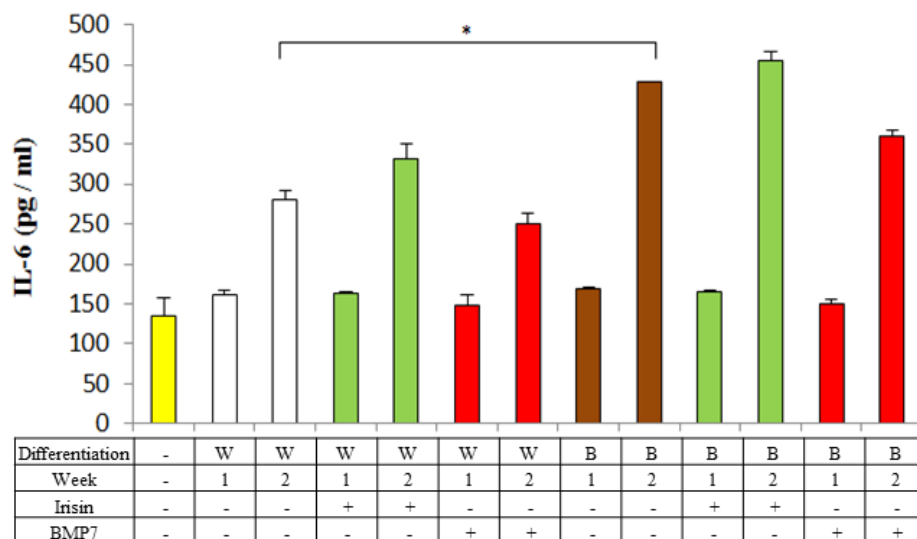


Figure 28. IL-6 secretion by differentiated SGBS treated with irisin or BMP7. SGBS cells were differentiated for two weeks as described in Figure 11. Supernatants were collected and pooled during the 1st and 2nd week of differentiation and secreted IL-6 was measured by sandwich ELISA. Data are expressed as the mean \pm SD for 3 independent experiments. For multiple comparison of groups statistical significance was evaluated by one-way ANOVA followed by Tukey post-hoc test. * $p < 0.05$, $n = 3$

In undifferentiated preadipocytes, IL-8, IL-6 and monocyte chemoattractant protein-1 (MCP1) were detected at a comparatively high level. Interestingly, the secretion of these cytokines was significantly higher by browned adipocytes as compared to white adipocytes (**Figure 27-29**). In contrast to BMP7 administration, irisin treatment resulted in an increased total IL-8 production.

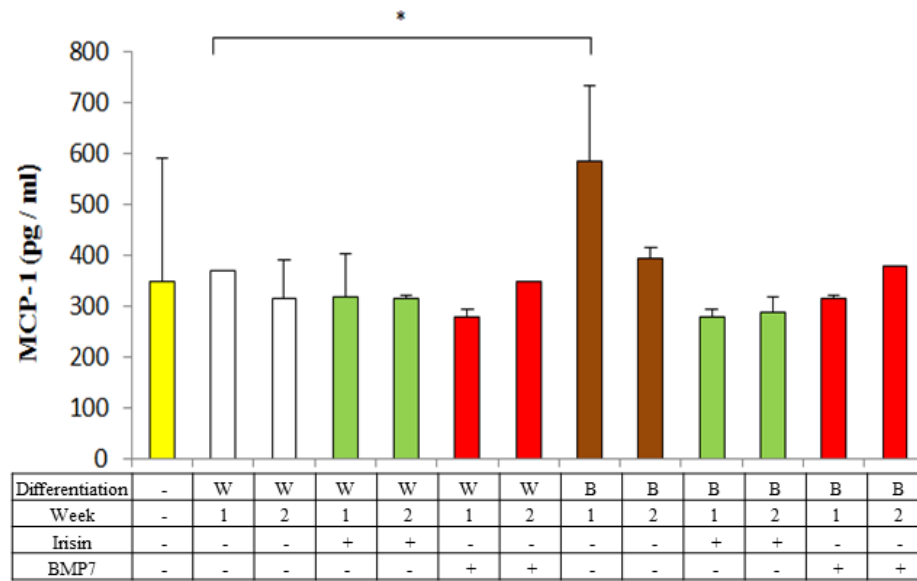


Figure 29. MCP1 secretion by differentiated SGBS treated with irisin or BMP7. SGBS cells were differentiated for two weeks as described in Figure 11. Supernatants were collected and pooled during the 1st and 2nd week of differentiation and secreted MCP1 was measured by sandwich ELISA. Data are expressed as the mean \pm SD for 3 independent experiments. For multiple comparison of groups statistical significance was evaluated by one-way ANOVA followed by Tukey post-hoc test. * $p < 0.05$, $n = 3$

5.7. Continuous inhibition of the IL-6 receptor resulted in a downregulation of UCP1 and extracellular acidification during browning differentiation.

Thermogenic, noradrenergic activation of brown adipocytes is in line with increased IL-6 expression (Burysek et al., 1997). In mice, it has been shown that IL-6 is necessary for the induction of browning of WAT as a result of cold exposure, as shown by inhibited UCP1 protein induction in IL-6-null mice (Knudsen et al., 2014). In contrast to IL-6-null-mice, overexpression of this cytokine led to reduced body weight in all regions (Peters et al., 1997). Recently we examined the cytokine secretion of human adipose tissue samples and primary adipocytes and we found the IL-

6 secretion was maintained until the end of the differentiation program (Kristóf et al., 2019). Therefore, we investigated the effect of a continuous blocking of IL-6 receptor alpha (encoded by IL6A gene) with an antibody (Munir et al., 2016) in hADMSCs. To examine the changes in the morphological characteristics of browned adipocytes as a result of IL-6-receptor inhibition, the previously introduced slide-based image-cytometry approach was used (Doan-Xuan et al., 2013; Kristóf et al., 2016). With this method we could detect the texture and UCP1 protein content in single adipocytes. When the blocking antibody was applied on top of the PPAR γ -driven browning protocol, it resulted in increased texture sum variance (**Figure 30.A**), which associated with larger lipid droplets, meanwhile the mean Ucp1 intensity decreased (**Figure 30.B**). These results suggest that the differentiation shifted towards producing more white adipocytes (**Figure 30.C**).

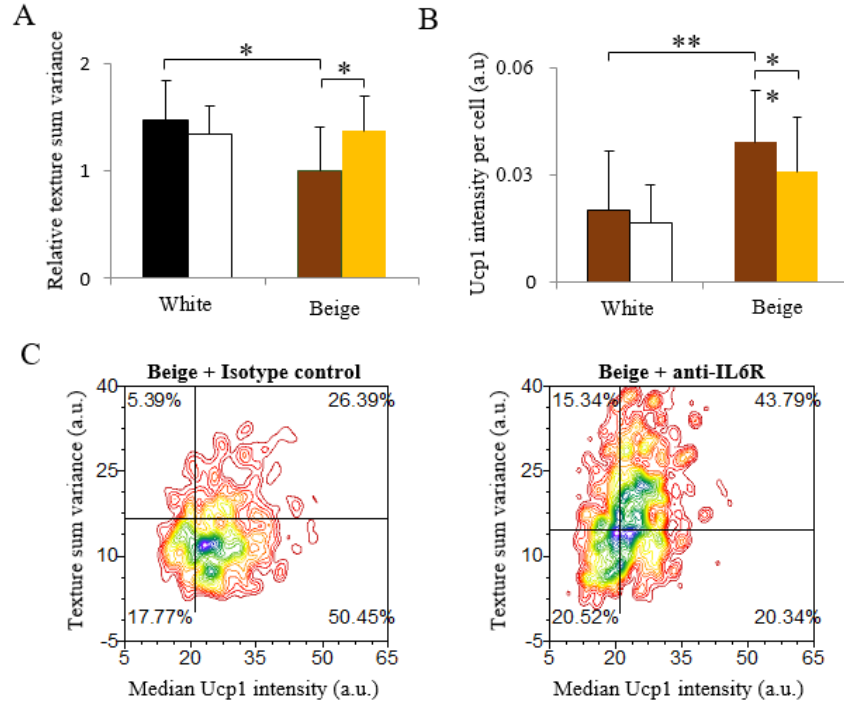


Figure 30. Morphological features of the primary adipocytes differentiated in the presence of anti-IL-6 receptor. Abdominal subcutaneous hADMSCs were differentiated to white (W) or beige (B) for two weeks; human IL-6R alpha or IgG Isotype control antibody was applied at 5µg/ml every day during the whole differentiation. The experiment was repeated five times with ADMSCs from independent healthy donors. (A) Texture sum variance (as compared to untreated beige adipocytes). (B) Median Ucp1 protein content of adipocytes per cell. (C) Contour plot figures which show single cell data of texture sum variance and Ucp1 protein content of differentiated adipocytes of one representative donor based on browning adipocytes, which contain small lipid droplets and high levels of Ucp1, are identified. For multiple comparisons of groups statistical significance was evaluated by one-way ANOVA followed by Tukey post-hoc test. ** $p < 0.01$, * $p < 0.05$. 2000 cells / each sample. Density plot figures was carried out by Dr. Zsolt Bacsó.

As a next experiment, functional capacity of adipocytes treated with anti-IL-6 receptor was measured (**Figure 31**). The sensitivity to cAMP and basal, stimulated or proton leak OCR was not reduced significantly (**Figure 32**). However, the basal and cAMP-stimulated ECAR were significantly decreased in response to sustained IL-6 receptor inhibition (**Figure 33**).

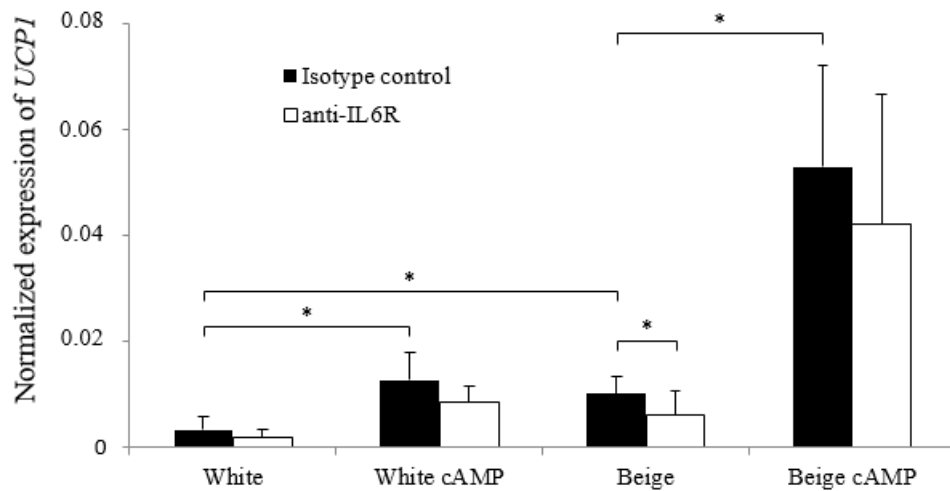


Figure 31. *Ucp1* expression of the primary adipocytes differentiated in the presence of *anti-IL-6-receptor*. Abdominal subcutaneous hADMSCs were differentiated as in Figure 30. Effect of short-term cAMP treatment on the expression of *Ucp1* gene in adipocytes. Cells received a single bolus of dibutyryl-cAMP at 500 μ M concentration for 4 h. The experiment was repeated five times with ADMSCs from independent healthy donors. Normalized gene expression was determined by RT-qPCR, target gene was normalized to *Gapdh*. For multiple comparisons of groups statistical significance was evaluated by one-way ANOVA followed by Tukey post-hoc test. * $p < 0.05$.

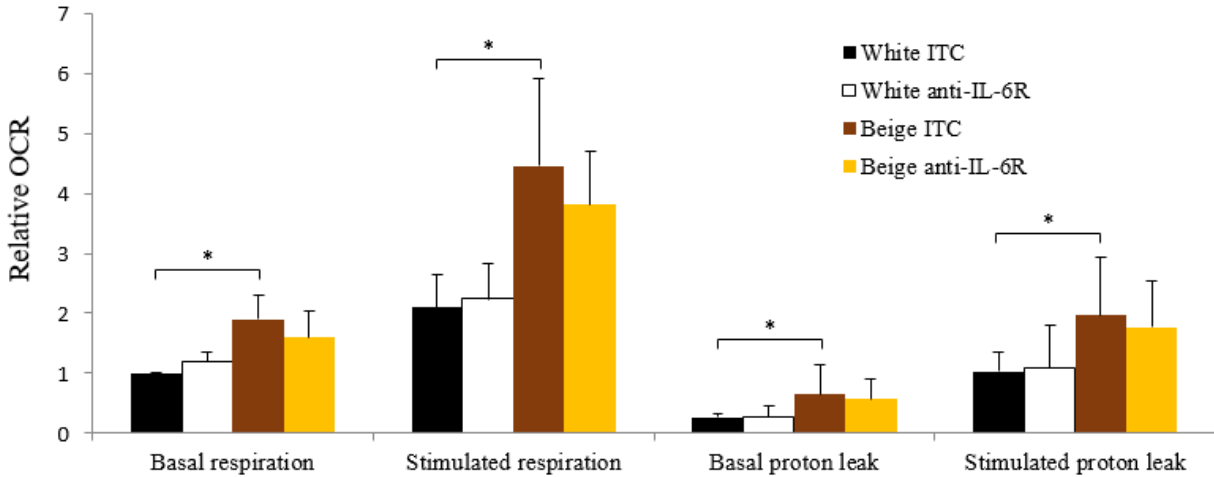


Figure 32. Oxygen consumption of the primary adipocytes differentiated in the presence of anti-IL-6-receptor Abdominal subcutaneous hADMSCs were differentiated as in Figures 30-31. Basal, cAMP stimulated and oligomycin inhibited oxygen consumption (OCR) levels (as compared to basal OCR of white adipocytes) in 4 different hADMSC-derived adipocyte donors. OC of adipocytes was measured with an XF96 oxymeter. After recording the baseline OC, cells received a single bolus dose of dibutyryl-cAMP. Proton leak respiration was determined after adding oligomycin to block ATP synthase activity. For multiple comparisons of groups statistical significance was evaluated by one-way ANOVA followed by Tukey post-hoc test. * $p < 0.05$.

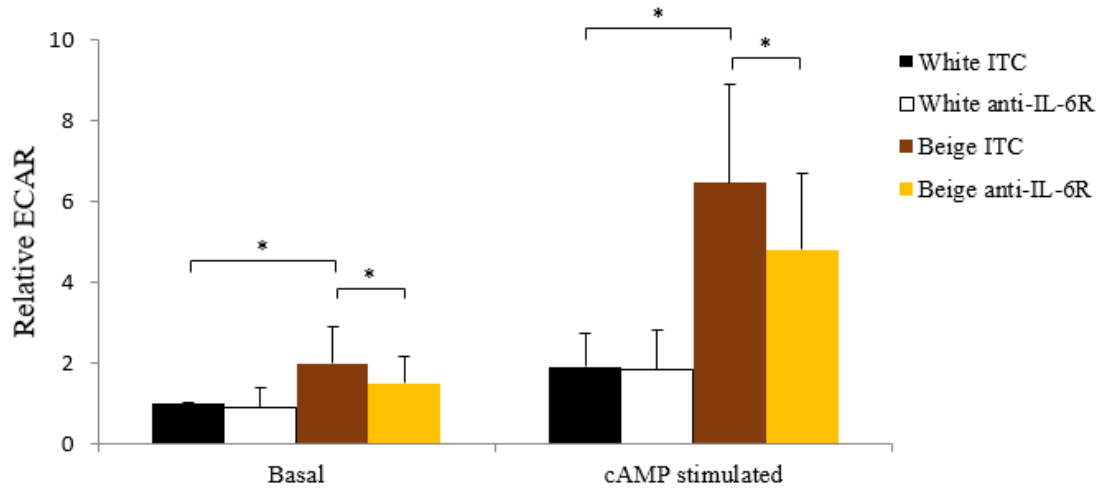


Figure 33. Extracellular acidification of the primary adipocytes differentiated in the presence of anti-IL-6-receptor. Abdominal subcutaneous hADMSCs were differentiated as in Figures 30-31. Basal and cAMP-stimulated extracellular acidification levels (as compared to basal ECAR of isotype control (ITC)-treated white adipocytes) in 4 different adipocyte donors measured with an XF96 oxymeter. For multiple comparisons of groups statistical significance was evaluated by one-way ANOVA followed by Tukey post-hoc test. * $p < 0.05$.

5.8. TG2 is expressed at a higher level in browned adipocytes and as a result of its inhibition both TG2 and UCP1 expression decreased.

We also analyzed the gene and protein expression of TG2 during the long-term experiment. Our results show that *Tg2* is expressed at a higher level in browned SGBS adipocytes (**Figure 34**). Furthermore, TG2 expression is correlating with UCP1 expression at mRNA and protein level as well (**Figures 23** and **34**). NC9 is a penetrating, irreversible, site-specific inhibitor of TG2, which inhibits both transamidase and guanosine triphosphate-binding activities. NC9 can transform TG2 from its closed conformation to its open form, modulating both its activity and conformation (Keillor et al., 2008; Caron et al., 2012). To test the short-term effect of NC9 we applied it for 9 hours after 14 days of white and PPAR γ -driven browning differentiation. For long-term

examination we administered NC9 during the whole differentiation (21 days) both to white and browning cocktail, in every fourth day when the medium was changed. As a result of NC9 treatment, either for 9 hours or 21 days in differentiated brown SGBS adipocytes, that both *Tg2* and *Pm20d1* gene expression were significantly decreased (**Figure 35**) as compared to untreated browned adipocytes. 21-day-long NC9 treatment on browned adipocytes led to significantly lower expression of *Ucp1*. In case of white adipocytes we did not observe any significant difference between the NC9 treated and untreated cells. Moreover, we could not determine any difference between differentiated SGBS cells in the presence or absence of NC9 in *Tg5* expression which means there is no compensatory upregulation as a result of NC9 (**Figure 37**). In case of differentiated white adipocytes, we could not see any effect of NC9 on the gene expression profile of *Ucp1*, *Tg2*, *Tg5* or *Pm20d1*.

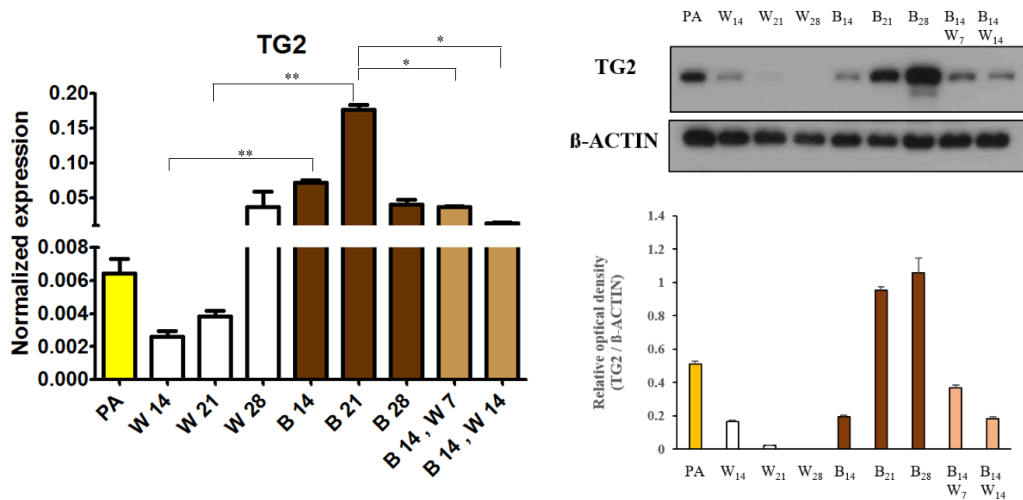


Figure 34. TG2 gene and protein expression in white and browned SGBS cells. SGBS preadipocytes were differentiated as in Figures 31-33. *Tg2* gene was normalized to *Gapdh*. For multiple comparisons of groups statistical significance was evaluated by one-way ANOVA followed by Tukey post-hoc test. Relative optical density was determined by Image J software. β -actin was used as endogenous control. All gels were run under the same conditions. $n=3$ * $p<0.05$; ** $p<0.01$

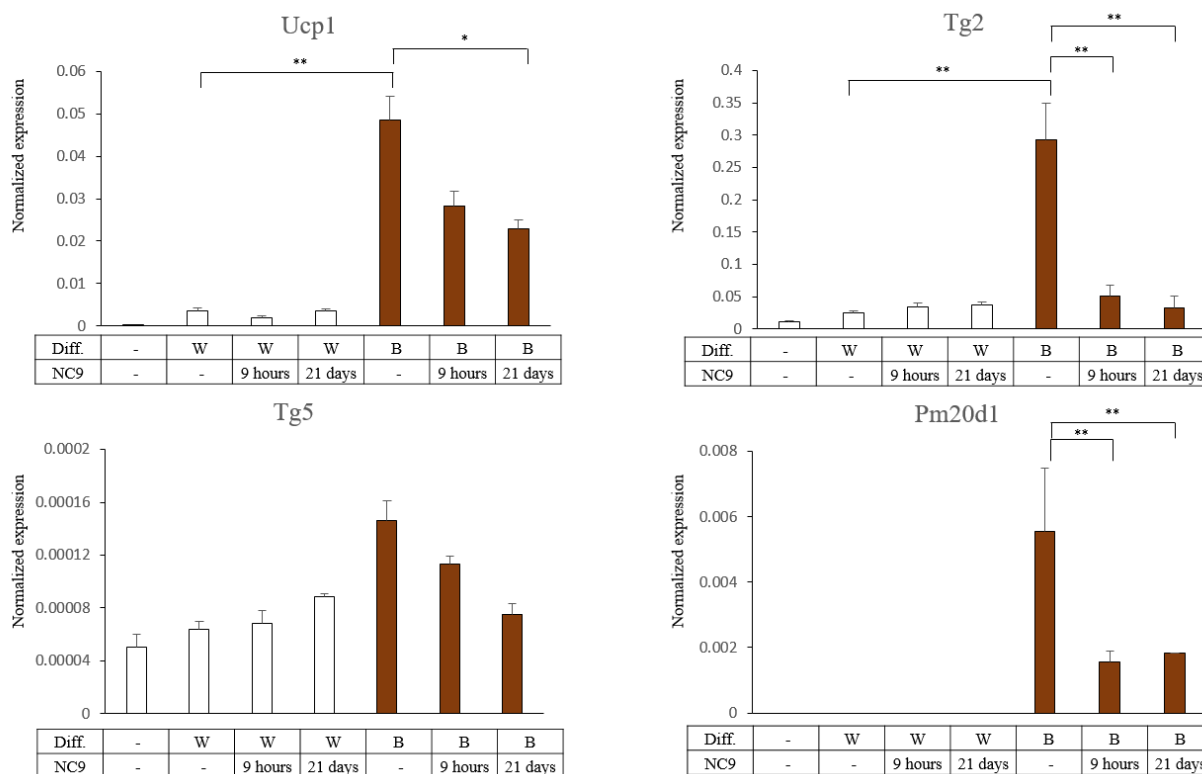


Figure 35. Browning of SGBS cells is decreased as a result of 9 hours or 21 days long NC9 treatment. Normalized expression of *Ucp1*, *Tg2*, *Tg5*, *Pm20d1* genes in SGBS adipocytes. SGBS cells were differentiated with white and browning differentiation cocktail for 21 days with NC9 supplementation. (Gene expression was determined by RT-qPCR and target genes were normalized to *Gapdh*.) For multiple comparisons of groups statistical significance was evaluated by one-way ANOVA followed by Tukey post-hoc test. $n=3$ * $p<0.05$; ** $p<0.01$

We also tested the changes of protein expression in TG2 (**Figure 36**) and UCP1 (**Figure 37**) in response to the white and browning differentiation cocktail in the presence or absence of NC9 treatment for 9 hours or 21 days, respectively. In line with the results of gene expression we found that the 21-day-long NC9 administration resulted in significantly decreased TG2 protein expression on differentiated browned adipocytes (**Figure 36**). However, we did not observe significant changes as a result of 9 hours long NC9 treatment in either white or browned adipocytes. A similar

trend was found in the case of UCP1 protein expression, which showed a robust reduction in response to the 21-days long NC9 treatment of browned adipocytes (**Figure 37**), although, 9 hours treatment did not influence notably the expression level of UCP1 either in white or in browned SGBS cells.

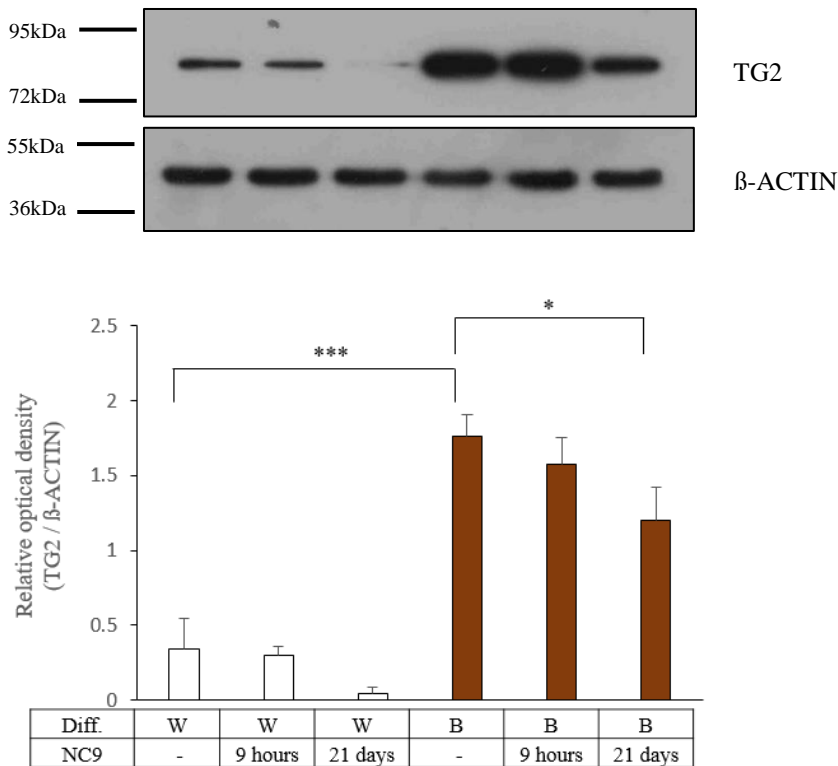


Figure 36. TG2 protein expression of differentiated SGBS cells after 9 hours or 21 days long NC9 treatment. SGBS cells were differentiated and treated as in Figure 35. The expression level of TG2 in SGBS cells in the presence or absence of NC9 treatment was detected using Western Blot analysis. Relative optical density was assessed by densitometry using Image J softwares. The loading control was β-actin. Data are mean \pm SEM of 3 independent measurements.

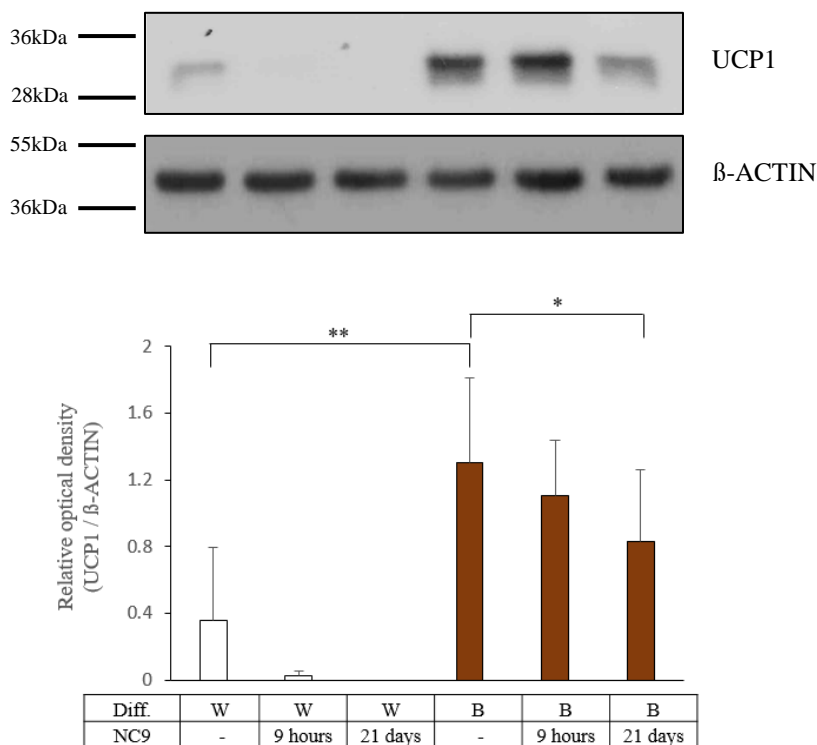


Figure 37. UCP1 protein expression of differentiated SGBS cells after 9 hours or 21 days long NC9 treatment. SGBS cells were differentiated and treated as in Figures 35-36. The expression level of UCP1 in SGBS cells in the presence or absence of NC9 treatment was detected using Western Blot analysis. Relative optical density was assessed by densitometry using Image J softwares. The loading control was β-actin. Data are mean \pm SEM of 3 independent measurements.

Finally, we investigated the functional capacity of human SGBS cells differentiated in the presence of NC9. In line with the previous results, PPAR γ -driven differentiation cocktail led to higher basal OCR than white (**Figure 38**). The presence or absence of NC9 during the differentiation did not affect significantly the basal OCR of adipocytes. After the cells received a single bolus dose of dibutyryl-cAMP adrenergic stimulation, we found that browned adipocytes differentiated in the presence or absence of NC9 had significantly increased stimulated mitochondrial respiration as compared to white. ATP synthase activity was inhibited after adding oligomycin. β-GPA (creatine

analogue which reduces creatine levels in the cells) resulted in decreased OCR both in white and browned adipocytes, in treated and untreated cells. Surprisingly, as a result of NC9 treatment we did not observe any significant changes in the functional capacity either in white or in browned cells (**Figure 38**). Basal and cAMP-stimulated extracellular acidification levels were measured and Figure 41. shows that ECAR was significantly increased in case of browned SGBS cells both in basal and stimulated cells. However, NC9 treatment did not affect robustly the ECAR of the differentiated SGBS cells (**Figure 39**). In case of the browned SGBS cells, the creatine-cycle related OCR was appreciably increased in contrast to untreated white adipocytes, and the same trend was observed as a result of NC9, but the difference was not statistically significant (**Figure 39**).

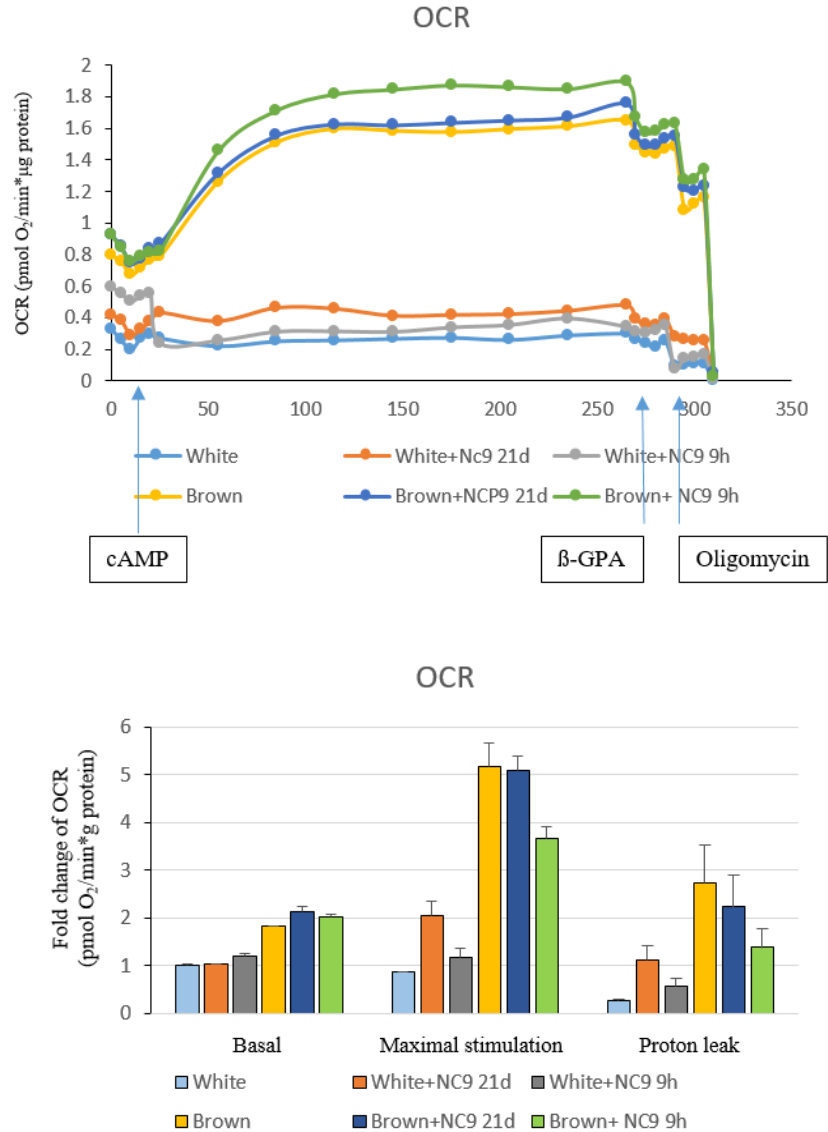


Figure 38. Functional measurements detect high oxygen consumption in browning adipocytes and no significant effect of the NC9 treatment. SGBS preadipocytes were differentiated and treated as in Figures 35-37. Mitochondrial oxygen consumption rate (OCR) of differentiated SGBS cells of one representative measurement determined by a Seahorse XF96 analyzer. Basal, dibutyl-*c*-AMP-stimulated and oligomycin-inhibited oxygen consumption levels in SGBS cells, as compared to basal OCR of white-directed adipocytes. *n*=3

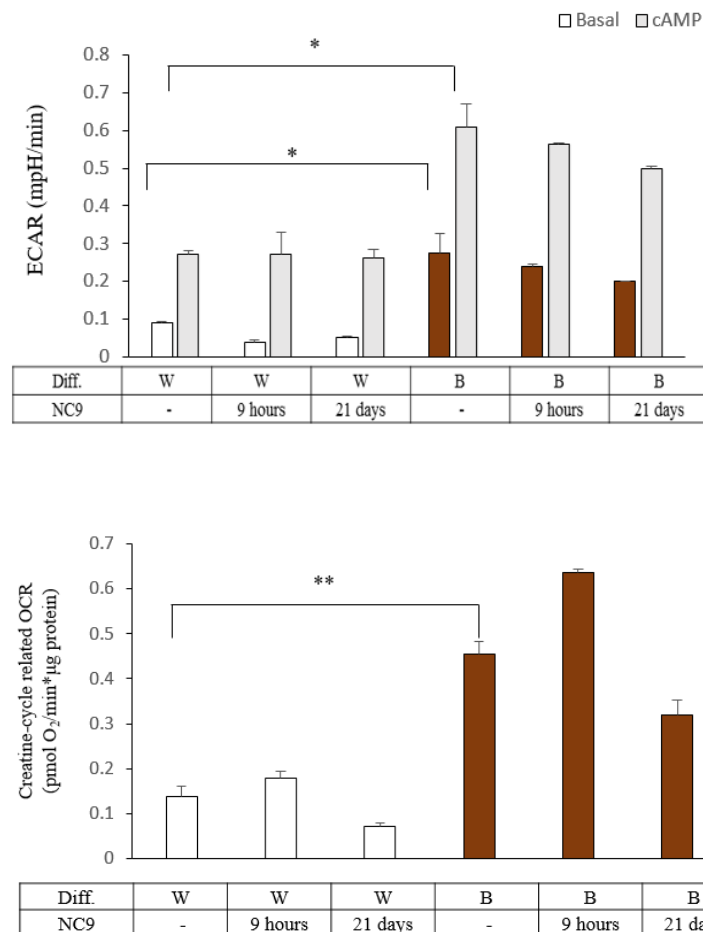


Figure 39. Functional analysis of differentiated SGBS cells treated with NC9. SGBS preadipocytes were differentiated and treated as in Figures 35-38. Extracellular acidification rate (ECAR) of differentiated SGBS cells measured by a Seahorse XF96 analyzer. Inhibitory effect of β -guanidiopropionic acid (β -GPA) (at 100mg/ml concentration) on the oxygen consumption of SGBS adipocytes. For multiple comparisons of groups statistical significance was evaluated by one-way ANOVA followed by Tukey post-hoc test. $n=5$ * $p<0.05$; ** $p<0.01$

6. DISCUSSION

1. Distribution of BAT in the human body and studying browning of hADMSCs.

BAT allows mammals to maintain their body temperature by non-shivering thermogenesis. BAT is highly abundant in human newborns and essential for their survival in the absence of other thermogenic means (Cannon et al., 2004). It can be found in human adults as well, where its presence is associated with lower body weight (Lichtenbelt et al., 2009). Besides participating in the regulation of energy homeostasis and body temperature, the activity of BAT has an important effect on systemic metabolism (Stanford et al., 2012; Chondronikola et al., 2014); for instance, it increases glucose tolerance and insulin sensitivity, while reducing body weight. BAT can be a target tissue to treat obesity and obesity-associated diseases (Chouchani et al., 2019).

The key mediator of heat production of brown and beige adipocytes is UCP1, which is located in the IMM, where it dissociates cellular respiration from the ATP generation. As a result of certain stimuli, such as cold exposure, NE activates β 3-adrenergic signaling on brown adipocytes, which triggers the release of FFA and subsequent activation of UCP1 (Cannon et al., 2004; Fedorenko et al., 2012). In the mitochondria of beige adipocytes an effective UCP1-independent thermogenic mechanism was described recently, which is mediated by a futile cycle of creatine metabolism (Kazak et al., 2015). Although the presence of BAT is limited in humans, it is functionally active not only in neonates but also in adults (Tews et al., 2011). Since the beginning of the last decade, ^{18}F -FDG-PET/CT has been used to image BAT activity, especially in human adults, which clearly demonstrates cold-activated BAT (Lichtenbelt et al., 2009; Virtanen et al., 2009; Saito et al., 2009; Cypess et al., 2009).

Having a better understanding of human adipocyte browning, hADMSCs isolated from SVFs are the most widely used *ex vivo* system (Raschke et al., 2013; Lee et al., 2014; Kristóf et al., 2015; and 2016). Recently, we showed that hADMSCs isolated from abdominal subcutaneous fat could be differentiated into beige adipocytes; moreover, brown-specific marker proteins (UCP1, CIDEA) were highly expressed in single adipocytes detected by laser-scanning cytometry (LSC). In the current study, we applied this tool to quantify the amount of browned SGBS adipocytes as well.

In line with the expectations from mouse data, our previous findings suggest that irisin could induce beige type of browning when administered during white adipocyte differentiation as indicated by *Tbx1* induction; while BMP7 treatment led to *Zic1* induction pointing to the possibility of the classical brown adipocyte differentiation pathway (Kristóf et al., 2015). However, there are many limitations of using hADMSCs, due to the limited availability of biopsy materials and the huge variability between donors, which can make it difficult to reproduce experiments.

2. Human preadipocyte cell lines exist and have some features consistent with having browning capacity.

Recently, several experiments were reported to overcome the limitations described above. PAZ6 cells, which were obtained from SVF of human infant BAT, and transformed with SV40 T and t antigens were able to differentiate into brown adipocytes *in vitro* (Zilberfarb et al., 1997). PAZ6 is regarded as a brown preadipocyte cell line, because UCP1 was highly expressed in differentiated PAZ6 cells which could be further induced as a result of NE (Kazantzis et al., 2012). Another research group, Xue et al. generated human preadipocyte cell lines by immortalization process, from the supraclavicular region of four healthy patients. Preadipocyte clones from the deep neck area were capable of differentiating to functional thermogenic adipocytes and responded to BMP7

administration, in contrast to those which were isolated and generated from subcutaneous WAT (Xue et al., 2015).

In another study, Shinoda et al. compared the differentiation of 65 clonal preadipocyte lines originated from supraclavicular fat biopsies with 35 lines which were generated from the SVF of subcutaneous WAT. RNA sequencing was performed from three clonal brown and white adipocyte cultures, differentiated from supraclavicular and subcutaneous progenitor clones, respectively. They found that the majority of the adipocytes derived from single cell clones of SVF from supraclavicular regions exhibited gene expression signatures which resembled the beige type of thermogenic adipocytes, marked by upregulated UCP1 and KCNK3 expression (Shinoda et al., 2015).

3. Interpretation of SGBS adipocyte browning observed by other groups.

In the present study, we demonstrated that mature SGBS and primary human subcutaneous adipocytes have similar features; however, they display distinct metabolic signatures. The SGBS human preadipocyte cell line is often used as a representative model of studying human adipocyte biology and previously it was described as a representative model of white adipocyte differentiation (Fischer-Posovszky et al., 2008; Wabitsch et al., 2011; Allott et al., 2012; Schlottmann et al., 2014). The first results were described in 2013, showing the possibility that SGBS cells can differentiate into thermogenic adipocytes. 2-oxoglutarate dependent dioxygenase (encoded by the proposed *Fto* gene) deficient SGBS preadipocytes differentiated to white adipocytes had increased UCP1 expression and uncoupled respiration, without any changes in mitochondrial mass or structure (Tews et al., 2013). Later, Tews et al. (2017) found that TENM2 (teneurin-2), which may inhibit the classical brown marker, *Zic1* (Bagutti et al., 2003), is enriched in white adipocyte progenitor

cells from subcutaneous neck WAT as compared to deep neck ones. They examined SGBS cells with TENM2 knockdown by siRNA, which led to increased UCP1 at mRNA and protein level as well. Moreover, basal and proton leak mitochondrial respiration were enhanced.

Interestingly, TENM2 deficient SGBS adipocytes had the same amount of mitochondria as the wild type ones and gained larger lipid droplets than the control cells. These results suggest that TENM2 knockdown in SGBS adipocytes results in a beige type of thermogenic gene expression program (the expression of *Zic1* did not change) without increased mitochondrial biogenesis and accumulation of small lipid droplets in a multilocular arrangement (Tews et al., 2017). In these studies, SGBS cells were differentiated to white adipocytes for two weeks, expressing UCP1 at a low, but detectable level, which we could confirm in our present study. In response to the knockdown of 2-oxoglutarate dependent dioxygenase or TENM2, the browning potential of the SGBS cells could be significantly increased. The administration of the atypical antipsychotic, clozapine, resulted in significant upregulation of *Elovl3*, *Cidea*, *Cycl*, *Pgc1a*, *Tbx1* but not *Zic1*, suggesting the induction of beige and not the classical brown phenotype of SGBS adipocytes (Kristóf et al., 2016).

Contrary to these studies and to the results presented here, Guennoun et al. found that the SGBS adipocytes switch their phenotype during a four weeks-long differentiation program. Within two weeks, they demonstrated high UCP1 expression and a thermogenic phenotype even as a result of the white differentiation protocol without adding any browning inducer or stimulus. Then, the expression of UCP1 greatly declined as a result of the continuation of the white differentiation for additional two weeks (Guennoun et al., 2015). Another study seemingly strengthened these results by comparing the gene expression pattern of the differentiated SGBS and primary hADMSC-derived subcutaneous adipocytes (Yeo et al., 2018). Of note, hADMSCs in this case were obtained

from obese, non-healthy patients and there might be a difference between the differentiation capacity of these and healthy hADMSCs and SGBS preadipocytes. They also observed that UCP1 protein expression was high in SGBS cells differentiated for 12 days even when either rosiglitazone or T3 were omitted from the media. In these experiments, they demonstrated a band on immunoblots below the molecular mass of 25 kDa. This band, most probably, does not correspond to UCP1 which has a predicted molecular weight at 33 kDa. In our experiments, we could demonstrate UCP1 protein expression in response to long-term rosiglitazone and T3 administration (browning protocol) at ~ 33 kDa, but not when the white cocktail was applied. In addition, we also found bands below 25 kDa as Yeo et al. have seen. In order to confirm our assumptions, three kinds of anti-UCP1 (both monoclonal and polyclonal) antibodies were used to investigate the UCP1 protein expression (**Figure 40**). The application of polyclonal antibodies (U6382, PA1-24894) (**Figure 40.a,b**) resulted in two distinct bands at ~33 kDa and below 25 kDa. However, when a monoclonal antibody (MAB6158) (**Figure 40.c**) was applied, we could clearly demonstrate which line corresponds to the UCP1 protein, supported by its occurrence at the predicted molecular weight. Furthermore, UCP1 expressed in a mouse BAT lysate, which served as a positive control, was detected at the exact same molecular weight of the band appeared in the browning SGBS adipocyte samples.

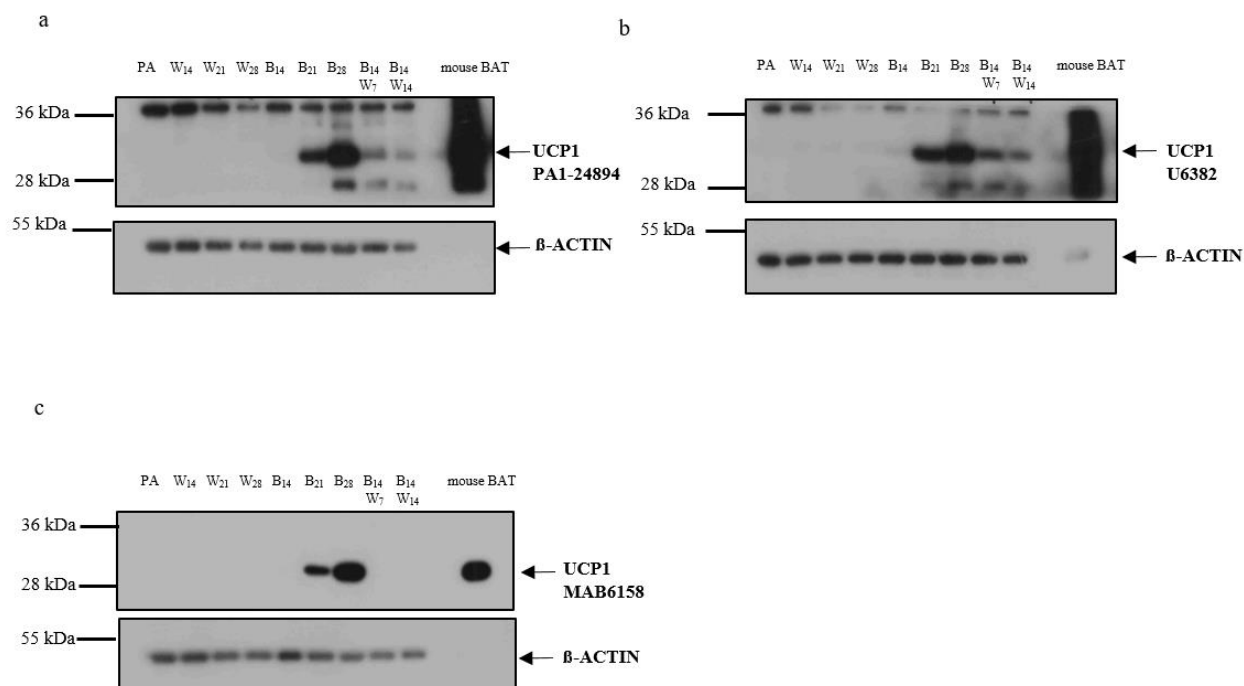


Figure 40. The analysis of UCP1 expression by Western blotting using three different antibodies in one representative SGBS replicate. *SGBS cells were differentiated and treated as in Figure 23. The expression level of UCP1 in SGBS cells and mouse BAT was detected using Western Blot analysis. Relative optical density was assessed by densitometry using Image J softwares. The loading control was β -actin. 3 independent measurements were carried out.*

Currently, our collaborator partners, Tews et al. published that basal/resting glucose uptake can be improved by elevating the UCP1 protein level alone in human white adipocytes (Tews et al., 2019). They generated a stable knock-out and overexpression of UCP1 in SGBS cells. In line with the previous publication (Hankir et al., 2017), knocking out of UCP1 had no effect on glucose utilization. However, UCP1 overexpressing cells significantly improved their glucose uptake and lactate production by 40%, in line with reduced glycerol release. These results correlate well with other studies performed with human samples, showing increased glycolytic activity in BAT (Weir et al., 2018). They also displayed that UCP1 is functionally active in SGBS adipocytes under basal

as well as lipolytic conditions. It has been recently demonstrated that glucose uptake is mediated either by GLUT1 alone, or GLUT1 and GLUT4 together in brown adipocytes (Winther et al., 2017). As a next step, Tews et al. selectively inhibited GLUT1 which resulted in completely diminished differences between UCP1 overexpressing and control cells in glucose uptake. These results suggest that GLUT1 can be identified as a possible gate keeper of glycolytic flux. Taken together, they generated a unique model system to study UCP1 overexpressing human adipocytes which allows us to further study human UCP1 function and its effect on cellular metabolism.

To further support our abovementioned results, Tews et al. kindly provided us UCP1 KO and overexpressing (GOF) samples. We conducted additional immunoblots using the U6382 anti-UCP1 polyclonal antibody on the following samples: preadipocyte (PA), white differentiated for 14 days (W₁₄), brown differentiated for 14 days (B₁₄), brown differentiated for 28 days (B₂₈), brown differentiated for 14 days then replaced to white (B₁₄W₁₄), UCP1 KO differentiated for 14 days (UCP1 KO₁₄), UCP1 overexpressed differentiated for 14 days (UCP1 GOF₁₄). These data further suggest that Yeo et al. displayed unspecific bands for UCP1 previously using the polyclonal antibody (PA1-24894). Furthermore, it can not be excluded that the origin of the applied SGBS cells were different in the two studies.

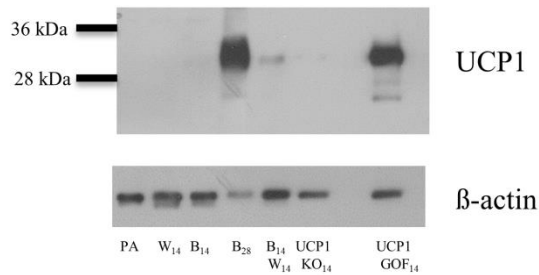


Figure 41. The analysis of UCP1 expression using Western blotting in one representative SGBS replicate. *SGBS cells were differentiated and treated as in Figure 23. The expression level of UCP1 in SGBS cells was detected using Western Blot analysis. Relative optical density was assessed by densitometry using Image J softwares. The loading control was β -actin.*

4. SGBS cells are able to differentiate into brown or beige adipocytes, and respond to either rosiglitazone, irisin or BMP7.

Using laser-scanning cytometry (Kristóf et al., 2015) and applying functional assays we aimed to examine whether classical brown or beige adipocyte differentiation (browning) can be induced in SGBS cells and if these adipocytes can maintain their morphology during long-term culturing. To give insight into the browning of human adipocytes, thermogenic competency of SGBS cells was induced by multiple approaches: sustained PPAR γ stimulation, irisin and BMP7 treatment. Irisin induces browning of subcutaneous white adipocytes *ex vivo* (Boström et al., 2012; Lee et al., 2014; Kristóf et al., 2015). Of note, irisin was applied in a concentration that can be found in the blood plasma of exercise trained rodents (Boström et al., 2012; Jedrychowski et al., 2015). However, in humans much less irisin is secreted into the bloodstream (Jedrychowski et al., 2015). Our experiments clearly shows that the PPAR γ -driven browning protocol (including rosiglitazone) and irisin treatment could be successfully used to induce browning of SGBS adipocytes, which resulted in a beige phenotype. Our data imply that irisin induces browning of already committed “beige” preadipocytes or multipotent progenitors.

Meanwhile, BMP7 drives brown fat cell differentiation of both mesenchymal progenitor cells and committed brown preadipocytes. *In vivo*, BMP7 is able to enhance brown fat mass and thermogenic energy expenditure in mice (Tseng et al., 2008). In our current study, administration of BMP7 had a more moderate effect and induced a distinct gene expression program without the upregulation of the beige-selective markers, *Tbx1* and *Cited1*. Both in primary subcutaneous and in SGBS adipocytes, BMP7 treatment results in an increased gene expression of *Pparg* and *Zic1* suggesting that this mediator induces a classic brown-like differentiation instead (Kristóf et al., 2015).

The functional studies detected UCP1-dependent proton leak (heat production) and high extracellular acidification in the case of browned adipocytes induced by either rosiglitazone or irisin. Besides UCP1-dependent thermogenesis, UCP1-independent heat-producing mechanisms were described as a beige specific feature. In our experiments, the involvement of the creatine-phosphate futile cycle (Kazak et al., 2015) was investigated in the heat production of SGBS beige adipocytes. Using a specific compound (β -GPA) which depletes creatine and inhibits the cycle, we demonstrated the induction of this futile cycle in response to a β -adrenergic cue in beige SGBS adipocytes. The importance of this pathway of creatin-metabolism was demonstrated formerly in mice (Kazak et al., 2015; Stockebrand et al., 2016) and in human cell lines (Kazak et al., 2015; Müller et al., 2016), but our laboratory detected firstly in human primary adipocytes, according to our knowledge (Kristóf et al., 2016).

We can conclude that it is still unclear whether the thermogenic fat depots in human adults contain the classical brown or beige type of adipocytes. Using an *ex vivo* human cellular model to determine the heterogeneity of cultured and differentiated adipocytes in response to anti-obesity treatment would be a possible tool to understand the development of classical brown or beige or “masked

beige” adipocytes and strengthen the data from mice. Our results suggest that SGBS cell line is an excellent, stable and suitable model for studying human adipocyte browning.

5. FTO locus is connected to beige or “masked beige” potential of adipocytes.

Another point to consider is that in human studies each individual has different life-style, dietary and genetic background - for example the presence of the risk-allele of the FTO locus which has an effect of adipocyte browning and represents genetic association with obesity (Claussnitzer et al., 2015). Genome-wide association studies can be used to identify disease-relevant genomic regions. The FTO (fat mass and obesity-associated protein) region harbors the strongest genetic association with obesity. Three genotypes exist of FTO rs1421085, namely the T/T healthy, T/C heterozygous and C/C obesity-risk. The presence of the C risk-allele of the FTO locus at rs1421085 position results in increased *Irx3* and *Irx5* expression levels during early adipocyte differentiation. This can be caused by the lack of ARID5B binding and repression which leads to cell autonomous shift towards white adipocytes in the gene expression program, and results in decreased thermogenesis (Claussnitzer et al., 2015). Therefore, the potential of mitochondrial thermogenesis is reduced in those individuals who carry the C risk allele which occurs at a high frequency (approx. 44%) in the European population (Claussnitzer et al., 2015). A CC to TT rescue by genome editing of primary adipocytes resulted in 2-fold-elevated *Ucp1* expression and an increased stimulated oxygen consumption by seven fold (Claussnitzer et al., 2015). According to our knowledge, no data is available how a heterozygous composition affects these parameters. In the literature, so far no information has been known about the status of this allele in SGBS cells. In this study, we described that the SGBS cell line carries one copy of the C risk allele; however, these preadipocytes were able to differentiate into functional beige adipocytes if browning stimuli (e.g. rosiglitazone or irisin treatment) were continuously present during their differentiation.

6. Cytokine secretion of SGBS cells and hADMSCs.

The importance of BAT activity in controlling the energy homeostasis of the entire body of adult humans has been revealed several years ago, highlighting a promising, possible therapeutic application of BAT stimulation in the treatment of obesity and T2D. In line with SGBS cells, our laboratory also investigated the effect of browning inducers to hADMSCs. Firstly, hADMSCs were isolated from abdominal subcutaneous fat and differentiated to white and PPAR γ -driven differentiation according to the previously described protocols.

Comparing the action of Irisin on hADMSCs vs. SGBS cells, the treatment had an increasing effect on IL-6, MCP-1 and IL-8 production on hADMSCs (Kristóf et al., 2019), and on IL-8 production of SGBS cells as compared to white control adipocytes (**Figure 27**). Earlier, cytokine secretion of hADMSCs were investigated and we detected IL-6, IL-8 and MCP-1 release from human adipose tissue samples and differentiating primary adipocytes without the secretion of the general pro-inflammatory cytokines, TNF α and IL-1 β (Kristóf et al., 2019). Only IL-6 was produced and maintained till the end of the differentiation by the adipocytes, but not by the undifferentiated cells. Based on the literature we know that IL-6 knock-out mice develop obesity during aging because of the missing effects of the cytokine in the CNS (Wallenius et al., 2002). Last year it was shown that as a result of long-term cold exposure, these mice have decreased core body temperature and energy expenditure (Egecioglu et al., 2018). In contrast, mice overexpressing IL-6 have a decreased body weight which includes reduced body fat in all regions as compared to WT mice (Peters et al., 1997). It was also shown that IL-6 secretion of brown adipocytes was required for the profound effects of BAT on the insulin sensitivity and glucose homeostasis (Stanford et al., 2013). In mice, daily intraperitoneal injections of IL-6 resulted in upregulation of *Ucp1* expression in subcutaneous white depots (Knudsen et al., 2014). In humans, the blockage of IL-6 is used as a therapy to treat

Crohn's disease or rheumatoid arthritis (Younis et al., 2013). In patients, the pharmacological blockade of IL-6 resulted in weight gain during the treatment by tocilizumab, which slightly penetrates the blood-brain barrier, hence, has an effect outside of the CNS (Younis et al., 2013). The weight gain can be partially explained with the reduced browning, enhanced by auto/paracrine IL-6 signaling.

In line with the aforementioned *in vivo* studies, we investigated the morphological characteristics and functional capacity of beige adipocytes and inhibition of the auto/paracrine effect of IL-6 receptor. Our findings suggest that the inhibition of IL-6 receptor led to a decreased beige phenotype of human adipocytes.

7. The role of transglutaminase 2 and its inhibitor in SGBS adipocyte differentiation.

Limited data is available in humans about the role and function of TG2. Studies focusing on gene expression profile of human adipose tissues revealed that in BAT *Tg2* expression is 6-fold higher than in WAT, presumably it suggests that *Tg2* is involved in thermogenic functions of adipose tissue (Svensson et al., 2010). Recently, the potential effect of TG2 on the formation and function of adipose tissue (Myneni et al., 2015) in mice was investigated in our laboratory (Mádi et al., 2017). Without treatments, they did not find any significant difference between TG2 KO or wild-type (WT) animals. However, when cold exposure was applied, TG2 ^{-/-} animals showed decreased tolerance to cold as compared to WT ones. This phenomenon can be due to the hampered utilization of their gonadal WAT, which was very likely caused by augmented browning process of adipose tissue in the TG2 KO mice. They also showed lower expression of browning markers, including UCP1 (**Figure 42**).

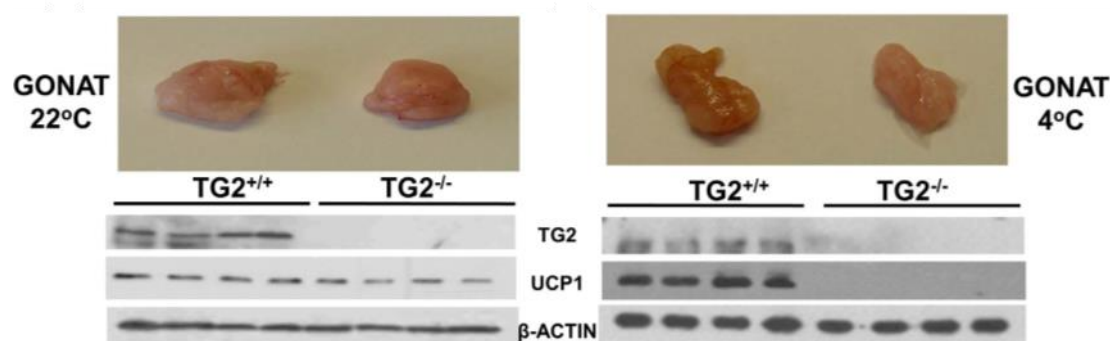


Figure 42. Browning is inhibited in the GONAT of TG2^{-/-} mice. *Representative images on the portions of WAT specimens and their TG2, UCP1 contents on Western blot Figure adopted from: Mádi et al., 2017*

Earlier, researchers in our laboratory investigated the gene expression profile of *Tg2* in human deep neck (DN) and subcutaneous neck (SCN) adipose tissue. They found that *Tg2* gene expression is higher in deep neck than in subcutaneous neck adipose tissue (unpublished data). During our long-term experiment (**Figure 23**) we investigated the expression of TG2 (**Figure 34**) as well. Our data show that TG2 is expressed at a higher level in browned SGBS adipocytes either at mRNA and protein level as compared to white adipocytes, which correlates with the expression data of *Tg2* from our previous study. Moreover, we examined the expression of *Tg1*, *Tg3*, *Tg4*, *Tg5*, *Tg6*, *Tg8* and *FXIII* in differentiated SGBS cells - other transglutaminases were not detected, or only slightly expressed. These results suggest that other transglutaminases might not influence the effect of TG2 for browning.

Finally, to study the effect of TG2 during the browning process, we tested the effect of NC9 (a-N-carbobenzyloxy-c-N-acryloyl-L-lysine(2-(2-dansylaminoethoxy)ethoxy)ethanamide), which is an irreversible inhibitor of the transglutaminase family that reacts with the active site of the enzyme and it is used to generate the open conformation crystal structure of TG2 (Pinkas et al., 2007). NC9 has been hypothesized to stabilize the protein in an open conformation (Colak et al., 2011; Keillor

et al., 2008). NC9 could be successfully use to inhibit the effect of TG2 in cell experiments (Jambrovics et al., 2019). Our data suggest that either 9 hours or 21 days NC9 treatment had a decreasing effect on gene expression of *Tg2* and *Pm20d1*. Additionally, *Ucp1* gene expression level also showed reduction in response to long-term effect of NC9 in browned SGBS cells. The importance of this pathway in the metabolism of beige adipocytes is still unclear; however, our data clearly shows that TG2 plays an important role in browned adipocytes, and NC9 has an effect on them.

7. SUMMARY

- SGBS preadipocytes represent an uncommitted preadipocyte stage with one FTO risk allele, which is able to differentiate either white or browned adipocytes.
- Our findings show that SGBS cells can be used as an easily applicable and valuable model for studying human adipocyte biology *in vitro*.
- We could follow SGBS adipocyte differentiation at different time points and detect single browning adipocytes in a high-throughput manner. Our measurement combined texture analysis with the size and number of lipid droplets and detection of UCP1 protein content.
- As a result of rosiglitazone or irisin treatment, the induction of browning was successful in SGBS cells, which followed the beige pathway. The induction of beige phenomenon could be detected by the enhanced expression of brown and beige marker genes (*Ucp1*, *Cidea*, *Elovl3*, *Ppar γ* , *Cycl*, *Tbx1*, *Pm20d1*), enrichment of mitochondria and multilocular morphology, and these features are strongly associated with high oxygen consumption as a result of cAMP treatment.
- Administration of BMP7 during white adipocyte differentiation led to upregulation of *Ucp1*, *Cidea*, *Pgc1 α* , *Ppar γ* and *Zic1* gene expression suggesting appearance of classical brown adipocyte features.
- We could observe significant involvement of the creatine-phosphate futile cycle in heat production of browned SGBS adipocytes, induced either by rosiglitazone, irisin or BMP7; detected by appreciably elevated OCR in response to β -adrenergic stimulus.
- In long-term experiments we could demonstrate that when the browning-inducer, rosiglitazone was omitted from the differentiation media, the expression of UCP1 and mitochondrial enrichment could be partially maintained.

- Beige (browned) SGBS adipocytes secrete increased levels of IL-6, IL-8 and MCP1 cytokines.
- Continuous inhibition of the IL-6 receptor resulted in decreased beige phenotype of human primary adipocytes (downregulation of the browning marker genes). Basal, stimulated or proton-leak oxygen consumption did not decrease markedly, but the extracellular acidification was significantly lower in the inhibited cells.
- Transglutaminase 2 is expressed at a higher level in browned SGBS adipocytes, which correlates with UCP1 expression at gene and protein level as well. Transglutaminase inhibitor treatment for short or long-term resulted in decreased *Tg2* gene expression. Long-term inhibition of TG2 led to significantly lower expression of *Ucp1* in browned SGBS cells. In line with the results of gene expression, significantly decreased TG2 and UCP1 protein expression were observed in response to long-term administration of the inhibitor. However, in browning functional test we could not observe significant effect of transglutaminase inhibition.

ÖSSZEFOGLALÁS

- Eredményeink arra utalnak, hogy az SGBS-sejtek könnyen és értékes modellként alkalmazhatók a human zsírsejtek *in vitro* tanulmányozáshoz.
- Az SGBS preadipociták egy nem-elköteleződött preadipocita stádiumot képviselnek egy FTO rizikó alléllal, amelyek képesek fehér vagy barnult adipocitákká differenciálódni.
- A rosiglitazon vagy irisin kezelés eredményeként a “browning” indukciója sikeres volt az SGBS sejtekben, amelyek a “beige” útvonalat követik. A “beige” jelenség indukcióját a barna és a “beige” marker gének (*Ucp1*, *Cidea*, *Elovl3*, *Ppar γ* , *Cycl*, *Tbx1*, *Pm20d1*) fokozott expressziója, a mitokondriumok felhalmozódása, a multilokuláris morfológia bizonyítja, és ezek a tulajdonságok szorosan kapcsolódnak cAMP hatására kialakuló magas oxigénfogyasztással
- Különböző időpontokban követhetjük az SGBS adipocita differenciálódását, és “browning” folyamatát lézer pásztázó citométer segítségével. Mérésünk kombinálta a lipidcseppek méretét és számát, valamint az UCP1 fehérje tartalmát.
- A BMP7 adása azonban az *Ucp1*, *Cidea*, *Pgc1a*, *Ppar γ* és *Zic1* génexpressziójának felregulálódásához vezetett a kezeletlen sejtekhez képest, amely a klasszikus barna adipociták tulajdonságainak megjelenését idézi elő.
- A kreatin-foszfát ciklus hőtermelésben való szignifikáns részvételét figyeltük meg barnult SGBS adipocitákban, melyet a rosiglitazon, irisin vagy BMP7 kezeléssel értünk el, jelentősen emelkedett oxigén fogyasztást detektáltunk β -adrenerg stimulus eredményeként.
- Hosszú távú kísérleteink során bebizonyítottuk, hogy ha a “browning” induktor, a rosiglitazon kihagyásra kerül a differenciációs tápfolyadékból, az UCP1 expressziója és a mitokondriális feldúsulás részben fenntartható.
- A “beige” (barnult) SGBS zsírsejtek több IL-6, IL-8 és MCP1 citokint szekretálnak.

- Az IL-6 receptor folyamatos gátlása csökkentette a human primer adipociták “beige” fenotípusát, a blokkolása eredményeként azt találtuk, hogy sem az alap, sem a stimulált, sem a protonszivárgásos oxigénfogyasztás nem csökkent jelentősen. Ennek ellenére az ECAR szignifikánsan alacsonyabb volt a gátolt sejtekben.
- A Transzglutamináz-2 magasabb szinten expresszálódik a barnult SGBS adipocitákban, ami korrelál az UCP1 expresszióval gén és fehérje szintjén is.
- A transzglutamináz inhibitor rövid vagy hosszú távú alkalmazása csökkentette a *Tg2* gén expresszióját. A TG2 hosszú távú gátlása az *Ucp1* expressziójának szignifikánsan alacsonyabb szintjét eredményezi a barnult SGBS sejtekben.
- A génexpresszió eredményeivel összhangban a hosszú távú inhibitorral történő kezelés során szignifikánsan csökkent TG2 és UCP1 fehérje expresszió volt megfigyelhető. A funkcionális tesztben azonban nem tudunk észlelni jelentős változásokat a transzglutamináz gátlószerének hatására.

8. REFERENCES

1. Abdul-Rahman, O., Kristóf, E., Doan-Xuan, Q. M., Vida, A., Nagy, L., Horváth, A., ... & Debreceni, T. (2016). AMP-activated kinase (AMPK) activation by AICAR in human white adipocytes derived from pericardial white adipose tissue stem cells induces a partial beige-like phenotype. *PLoS One*, *11*(6), e0157644.
2. Admiraal, W. M., Holleman, F., Bahler, L., Soeters, M. R., Hoekstra, J. B., & Verberne, H. J. (2013). Combining 123I-metaiodobenzylguanidine SPECT/CT and 18F-FDG PET/CT for the assessment of brown adipose tissue activity in humans during cold exposure. *Journal of Nuclear Medicine*, *54*(2), 208-212..
3. Aldiss, P., Betts, J., Sale, C., Pope, M., Budge, H., & Symonds, M. E. (2018). Exercise-induced 'browning' of adipose tissues. *Metabolism*, *81*, 63-70.
4. Allott, E. H., Oliver, E., Lysaght, J., Gray, S. G., Reynolds, J. V., Roche, H. M., & Pidgeon, G. P. (2012). The SGBS cell strain as a model for the in vitro study of obesity and cancer. *Clinical and Translational Oncology*, *14*(10), 774-782.
5. Anunciado-Koza, R., Ukropec, J., Koza, R. A., & Kozak, L. P. (2008). Inactivation of UCP1 and the glycerol phosphate cycle synergistically increases energy expenditure to resist diet-induced obesity. *Journal of Biological Chemistry*, *283*(41), 27688-27697.
6. Arroyo-Johnson, C., & Mincey, K. D. (2016). Obesity epidemiology worldwide. *Gastroenterology Clinics*, *45*(4), 571-579.
7. Asahi, M., Otsu, K., Nakayama, H., Hikoso, S., Takeda, T., Gramolini, A. O., ... & Hirano, S. (2004). Cardiac-specific overexpression of sarcolipin inhibits sarco (endo) plasmic reticulum Ca²⁺ ATPase (SERCA2a) activity and impairs cardiac function in mice. *Proceedings of the National Academy of Sciences*, *101*(25), 9199-9204.
8. Asahi, M., Sugita, Y., Kurzydowski, K., De Leon, S., Tada, M., Toyoshima, C., & MacLennan, D. H. (2003). Sarcolipin regulates sarco (endo) plasmic reticulum Ca²⁺-ATPase (SERCA) by binding to transmembrane helices alone or in association with phospholamban. *Proceedings of the National Academy of Sciences*, *100*(9), 5040-5045.
9. Asano, A., Kimura, K., & Saito, M. (1999). Cold-induced mRNA expression of angiogenic factors in rat brown adipose tissue. *Journal of veterinary medical science*, *61*(4), 403-409.
10. Atit, R., Sgaier, S. K., Mohamed, O. A., Taketo, M. M., Dufort, D., Joyner, A. L., ... & Conlon, R. A. (2006). β -catenin activation is necessary and sufficient to specify the dorsal dermal fate in the mouse. *Developmental biology*, *296*(1), 164-176.
11. Babu, G. J., Bhupathy, P., Petrashevskaya, N. N., Wang, H., Raman, S., Wheeler, D., ... & Ziolo, M. T. (2006). Targeted overexpression of sarcolipin in the mouse heart decreases sarcoplasmic reticulum calcium transport and cardiac contractility. *Journal of Biological Chemistry*, *281*(7), 3972-3979.
12. Babu, G. J., Bhupathy, P., Timofeyev, V., Petrashevskaya, N. N., Reiser, P. J., Chiamvimonvat, N., & Periasamy, M. (2007). Ablation of sarcolipin enhances sarcoplasmic reticulum calcium transport and atrial contractility. *Proceedings of the National Academy of Sciences*, *104*(45), 17867-17872.

13. Babu, G. J., Zheng, Z., Natarajan, P., Wheeler, D., Janssen, P. M., & Periasamy, M. (2005). Overexpression of sarcolipin decreases myocyte contractility and calcium transient. *Cardiovascular research*, 65(1), 177-186.
14. Bagutti, C., Forro, G., Ferralli, J., Rubin, B., & Chiquet-Ehrismann, R. (2003). The intracellular domain of teneurin-2 has a nuclear function and represses zic-1-mediated transcription. *Journal of cell science*, 116(14), 2957-2966.
15. Bal, N. C., Maurya, S. K., Sopariwala, D. H., Sahoo, S. K., Gupta, S. C., Shaikh, S. A., ... & Tupling, A. R. (2012). Sarcolipin is a newly identified regulator of muscle-based thermogenesis in mammals. *Nature medicine*, 18(10), 1575.
16. Balajthy, Z., Csomós, K., Vámosi, G., Szántó, A., Lanotte, M., & Fésüs, L. (2006). Tissue-transglutaminase contributes to neutrophil granulocyte differentiation and functions. *Blood*, 108(6), 2045-2054.
17. Barak, Y., Nelson, M. C., Ong, E. S., Jones, Y. Z., Ruiz-Lozano, P., Chien, K. R., ... & Evans, R. M. (1999). PPAR γ is required for placental, cardiac, and adipose tissue development. *Molecular cell*, 4(4), 585-595.
18. Barness, L. A., Opitz, J. M., & Gilbert-Barness, E. (2007). Obesity: genetic, molecular, and environmental aspects. *American Journal of Medical Genetics Part A*, 143(24), 3016-3034.
19. Bartelt, A., Bruns, O. T., Reimer, R., Hohenberg, H., Ittrich, H., Peldschus, K., ... & Eychemüller, A. (2011). Brown adipose tissue activity controls triglyceride clearance. *Nature medicine*, 17(2), 200.
20. Bartsaghi, S., Hallen, S., Huang, L., Svensson, P. A., Momo, R. A., Wallin, S., ... & Peng, X. R. (2015). Thermogenic activity of UCP1 in human white fat-derived beige adipocytes. *Molecular Endocrinology*, 29(1), 130-139.
21. Bartness, T. J., Shrestha, Y. B., Vaughan, C. H., Schwartz, G. J., & Song, C. K. (2010). Sensory and sympathetic nervous system control of white adipose tissue lipolysis. *Molecular and cellular endocrinology*, 318(1-2), 34-43.
22. Belkin, A. M. (2011). Extracellular TG2: emerging functions and regulation. *The FEBS journal*, 278(24), 4704-4716.
23. Berlet, H. H., Bonsmann, I., & Birringer, H. (1976). Occurrence of free creatine, phosphocreatine and creatine phosphokinase in adipose tissue. *Biochimica et Biophysica Acta (BBA)-General Subjects*, 437(1), 166-174.
24. Bernassola, F., FEDERICI, M., Corazzari, M., Terrinoni, A., Hribal, M. L., De Laurenzi, V., ... & Citro, G. (2002). Role of transglutaminase 2 in glucose tolerance: knockout mice studies and a putative mutation in a MODY patient. *The FASEB Journal*, 16(11), 1371-1378.
25. Berry, R., & Rodeheffer, M. S. (2013). Characterization of the adipocyte cellular lineage in vivo. *Nature cell biology*, 15(3), 302.

26. Bhowmik, A. D., & Dalal, A. (2015). Whole exome sequencing identifies a novel frameshift mutation in GPC3 gene in a patient with overgrowth syndrome. *Gene*, 572(2), 303-306.
27. Bordicchia, M., Liu, D., Amri, E. Z., Ailhaud, G., Dessì-Fulgheri, P., Zhang, C., ... & Collins, S. (2012). Cardiac natriuretic peptides act via p38 MAPK to induce the brown fat thermogenic program in mouse and human adipocytes. *The Journal of clinical investigation*, 122(3), 1022-1036.
28. Boström, P., Wu, J., Jedrychowski, M. P., Korde, A., Ye, L., Lo, J. C., ... & Kajimura, S. (2012). A PGC1- α -dependent myokine that drives brown-fat-like development of white fat and thermogenesis. *Nature*, 481(7382), 463.
29. Bouřová, L., Peřanová, Z., Novotný, J., Bengtsson, T., & Svoboda, P. (2000). Differentiation of cultured brown adipocytes is associated with a selective increase in the short variant of Gs α protein. Evidence for higher functional activity of Gs α S. *Molecular and cellular endocrinology*, 167(1-2), 23-31.
30. Brandt, C., & Pedersen, B. K. (2010). The role of exercise-induced myokines in muscle homeostasis and the defense against chronic diseases. *BioMed Research International*, 2010.
31. Burýšek, L., & Houštěk, J. (1997). β -Adrenergic stimulation of interleukin-1 α and interleukin-6 expression in mouse brown adipocytes. *FEBS letters*, 411(1), 83-86.
32. Cannon, B., & Nedergaard, J. A. N. (2004). Brown adipose tissue: function and physiological significance. *Physiological reviews*, 84(1), 277-359.
33. Cannon, B., & Vogel, G. (1977). The mitochondrial ATPase of brown adipose tissue Purification and comparison with the mitochondrial ATPase from beef heart. *FEBS letters*, 76(2), 284-289.
34. Cao, W., Medvedev, A. V., Daniel, K. W., & Collins, S. (2001). β -adrenergic activation of p38 MAP kinase in adipocytes cAMP induction of the uncoupling protein 1 (UCP1) gene requires p38 map kinase. *Journal of Biological Chemistry*, 276(29), 27077-27082.
35. Caron, N. S., Munsie, L. N., Keillor, J. W., & Truant, R. (2012). Using FLIM-FRET to measure conformational changes of transglutaminase type 2 in live cells. *PloS one*, 7(8), e44159.
36. Cederberg, A., Grønning, L. M., Åhrén, B., Taskén, K., Carlsson, P., & Enerbäck, S. (2001). FOXC2 is a winged helix gene that counteracts obesity, hypertriglyceridemia, and diet-induced insulin resistance. *Cell*, 106(5), 563-573.
37. Chartoumpekis, D. V., Habeos, I. G., Ziros, P. G., Psyrogiannis, A. I., Kyriazopoulou, V. E., & Papavassiliou, A. G. (2011). Brown adipose tissue responds to cold and adrenergic stimulation by induction of FGF21. *Molecular medicine*, 17(7-8), 736-740.
38. Chaudhry, A. R. C. H. A. N. A., Muffler, L. A., Yao, R. U. I. H. O. N. G., & Granneman, J. G. (1996). Perinatal expression of adenylyl cyclase subtypes in rat brown adipose

- tissue. *American Journal of Physiology-Regulatory, Integrative and Comparative Physiology*, 270(4), R755-R760.
39. Chaudhry, A., & Granneman, J. G. (1999). Differential regulation of functional responses by β -adrenergic receptor subtypes in brown adipocytes. *American Journal of Physiology-Regulatory, Integrative and Comparative Physiology*, 277(1), R147-R153.
 40. Cheng, Y., Jiang, L., Keipert, S., Zhang, S., Hauser, A., Graf, E., ... & Perocchi, F. (2018). Prediction of adipose browning capacity by systematic integration of transcriptional profiles. *Cell reports*, 23(10), 3112-3125.
 41. Chondronikola, M., Volpi, E., Børsheim, E., Porter, C., Annamalai, P., Enerbäck, S., ... & Yfanti, C. (2014). Brown adipose tissue improves whole-body glucose homeostasis and insulin sensitivity in humans. *Diabetes*, 63(12), 4089-4099.
 42. Chouchani, E. T., Kazak, L., Jedrychowski, M. P., Lu, G. Z., Erickson, B. K., Szpyt, J., ... & Robinson, A. J. (2016). Mitochondrial ROS regulate thermogenic energy expenditure and sulfenylation of UCP1. *Nature*, 532(7597), 112.
 43. Chouchani, E. T., Kazak, L., & Spiegelman, B. M. (2018). New advances in adaptive thermogenesis: UCP1 and beyond. *Cell metabolism*.
 44. Cinti, S., & Vettor, R. (2009). The adipose organ. In *Adipose Tissue and Inflammation* (pp. 11-31). CRC Press.
 45. Claussnitzer, M., Dankel, S. N., Kim, K. H., Quon, G., Meuleman, W., Haugen, C., ... & Abdennur, N. A. (2015). FTO obesity variant circuitry and adipocyte browning in humans. *New England Journal of Medicine*, 373(10), 895-907.
 46. Clément, K., Viguerie, N., Poitou, C., Carette, C., Pelloux, V., Curat, C. A., ... & Vidal, H. (2004). Weight loss regulates inflammation-related genes in white adipose tissue of obese subjects. *The FASEB Journal*, 18(14), 1657-1669.
 47. Cohen, P., Levy, J. D., Zhang, Y., Frontini, A., Kolodin, D. P., Svensson, K. J., ... & Wu, J. (2014). Ablation of PRDM16 and beige adipose causes metabolic dysfunction and a subcutaneous to visceral fat switch. *Cell*, 156(1-2), 304-316.
 48. Colak, G., Keillor, J. W., & Johnson, G. V. (2011). Cytosolic guanine nucleotide binding deficient form of transglutaminase 2 (R580a) potentiates cell death in oxygen glucose deprivation. *PLoS One*, 6(1), e16665
 49. Collins, S. (2014). A heart–adipose tissue connection in the regulation of energy metabolism. *Nature Reviews Endocrinology*, 10(3), 157.
 50. Collins, S., Daniel, K. W., Petro, A. E., & Surwit, R. S. (1997). Strain-Specific Response to β 3-Adrenergic Receptor Agonist Treatment of Diet-Induced Obesity in Mice. *Endocrinology*, 138(1), 405-413.
 51. Commins, S. P., Watson, P. M., Frampton, I. C., & Gettys, T. W. (2001). Leptin selectively reduces white adipose tissue in mice via a UCP1-dependent mechanism in brown adipose tissue. *American Journal of Physiology-Endocrinology And Metabolism*, 280(2), E372-E377.

52. Contreras, C., Gonzalez, F., Fernø, J., Diéguez, C., Rahmouni, K., Nogueiras, R., & López, M. (2015). The brain and brown fat. *Annals of medicine*, 47(2), 150-168.
53. Cypess, A. M., Lehman, S., Williams, G., Tal, I., Rodman, D., Goldfine, A. B., ... & Kolodny, G. M. (2009). Identification and importance of brown adipose tissue in adult humans. *New England Journal of Medicine*, 360(15), 1509-1517.
54. Cypess, A. M., White, A. P., Vernochet, C., Schulz, T. J., Xue, R., Sass, C. A., ... & Chacko, A. T. (2013). Anatomical localization, gene expression profiling and functional characterization of adult human neck brown fat. *Nature medicine*, 19(5), 635.
55. Csomós, K., Német, I., Fésüs, L., & Balajthy, Z. (2010). Tissue transglutaminase contributes to the all-trans-retinoic acid-induced differentiation syndrome phenotype in the NB4 model of acute promyelocytic leukemia. *Blood*, 116(19), 3933-3943.
56. De Laurenzi, V., & Melino, G. (2001). Gene disruption of tissue transglutaminase. *Molecular and Cellular Biology*, 21(1), 148-155.
57. De Matteis, R., Lucertini, F., Guescini, M., Polidori, E., Zeppa, S., Stocchi, V., ... & Cuppini, R. (2013). Exercise as a new physiological stimulus for brown adipose tissue activity. *Nutrition, metabolism and cardiovascular diseases*, 23(6), 582-590.
58. Doan-Xuan, Q. M., Sarvari, A. K., Fischer-Posovszky, P., Wabitsch, M., Balajthy, Z., Fesus, L., & Bacso, Z. (2013). High content analysis of differentiation and cell death in human adipocytes. *Cytometry Part A*, 83(10), 933-943.
59. Eckert, R. L., Kaartinen, M. T., Nurminskaya, M., Belkin, A. M., Colak, G., Johnson, G. V., & Mehta, K. (2014). Transglutaminase regulation of cell function. *Physiological reviews*, 94(2), 383-417.
60. Egecioglu, E., Anesten, F., Schéle, E., & Palsdottir, V. (2018). Interleukin-6 is important for regulation of core body temperature during long-term cold exposure in mice. *Biomedical reports*, 9(3), 206-212.
61. Elabd, C., Chiellini, C., Carmona, M., Galitzky, J., Cochet, O., Petersen, R., ... & Dani, C. (2009). Human multipotent adipose-derived stem cells differentiate into functional brown adipocytes. *Stem cells*, 27(11), 2753-2760.
62. Ellingsgaard, H., Hauselmann, I., Schuler, B., Habib, A. M., Baggio, L. L., Meier, D. T., ... & Hansen, A. M. K. (2011). Interleukin-6 enhances insulin secretion by increasing glucagon-like peptide-1 secretion from L cells and alpha cells. *Nature medicine*, 17(11), 1481.
63. English, J. T., Patel, S. K., & Flanagan, M. J. (1973). Association of pheochromocytomas with brown fat tumors. *Radiology*, 107(2), 279-281.
64. Febbraio, M. A., & Pedersen, B. K. (2002). Muscle-derived interleukin-6: mechanisms for activation and possible biological roles. *The FASEB journal*, 16(11), 1335-1347.

65. Federico, A., D'Aiuto, E., Borriello, F., Barra, G., Gravina, A. G., Romano, M., & De Palma, R. (2010). Fat: a matter of disturbance for the immune system. *World journal of gastroenterology: WJG*, 16(38), 4762.
66. Fedorenko, A., Lishko, P. V., & Kirichok, Y. (2012). Mechanism of fatty-acid-dependent UCP1 uncoupling in brown fat mitochondria. *Cell*, 151(2), 400-413.
67. Fesus, L., & Piacentini, M. (2002). Transglutaminase 2: an enigmatic enzyme with diverse functions. *Trends in biochemical sciences*, 27(10), 534-539.
68. Fesus L. (2014). Lipids and the medical practice. *Biochemistry I*.
69. Fischer-Posovszky, P., Newell, F. S., Wabitsch, M., & Tornqvist, H. E. (2008). Human SGBS cells—a unique tool for studies of human fat cell biology. *Obesity facts*, 1(4), 184-189.
70. Fischer-Posovszky, P., Wabitsch, M., & Hochberg, Z. (2007). Endocrinology of adipose tissue—an update. *Hormone and Metabolic Research*, 39(05), 314-321.
71. Folk, J. E., & Finlayson, J. S. (1977). The ϵ -(γ -glutamyl) lysine crosslink and the catalytic role of transglutaminases. In *Advances in protein chemistry* (Vol. 31, pp. 1-133). Academic Press.
72. Frayling, T. M., Timpson, N. J., Weedon, M. N., Zeggini, E., Freathy, R. M., Lindgren, C. M., ... & Shields, B. (2007). A common variant in the FTO gene is associated with body mass index and predisposes to childhood and adult obesity. *Science*, 316(5826), 889-894.
73. Freytag, S. O., Paielli, D. L., & Gilbert, J. D. (1994). Ectopic expression of the CCAAT/enhancer-binding protein alpha promotes the adipogenic program in a variety of mouse fibroblastic cells. *Genes & development*, 8(14), 1654-1663.
74. Fu, Z., Yao, F., Abou-Samra, A. B., & Zhang, R. (2013). Lipasin, thermoregulated in brown fat, is a novel but atypical member of the angiopoietin-like protein family. *Biochemical and biophysical research communications*, 430(3), 1126-1131.
75. Gamas, L., Matafome, P., & Seica, R. (2015). Irisin and myonectin regulation in the insulin resistant muscle: implications to adipose tissue: muscle crosstalk. *Journal of diabetes research*, 2015.
76. GBD 2015 Obesity Collaborators. (2017). Health effects of overweight and obesity in 195 countries over 25 years. *New England Journal of Medicine*, 377(1), 13-27.
77. Gesta, S., Tseng, Y. H., & Kahn, C. R. (2007). Developmental origin of fat: tracking obesity to its source. *Cell*, 131(2), 242-256.
78. Giralt, M., Gavalda-Navarro, A., & Villarroya, F. (2015). Fibroblast growth factor-21, energy balance and obesity. *Molecular and cellular endocrinology*, 418, 66-73.
79. Granneman, J. G. (1988). Norepinephrine infusions increase adenylate cyclase responsiveness in brown adipose tissue. *Journal of Pharmacology and Experimental Therapeutics*, 245(3), 1075-1080.
80. Green, D. E. (1936). α -Glycerophosphate dehydrogenase. *Biochemical Journal*, 30(4), 629.

81. Greenberg, C. S., Birckbichler, P. J., & Rice, R. H. (1991). Transglutaminases: multifunctional cross-linking enzymes that stabilize tissues. *The FASEB Journal*, 5(15), 3071-3077.
82. Griffin, M., Casadio, R., & Bergamini, C. M. (2002). Transglutaminases: nature's biological glues. *Biochemical Journal*, 368(2), 377-396.
83. Guennoun, A., Kazantzis, M., Thomas, R., Wabitsch, M., Tews, D., Sastry, K. S., ... & Chouchane, L. (2015). Comprehensive molecular characterization of human adipocytes reveals a transient brown phenotype. *Journal of translational medicine*, 13(1), 135.
84. Guerra, C., Koza, R. A., Yamashita, H., Walsh, K., & Kozak, L. P. (1998). Emergence of brown adipocytes in white fat in mice is under genetic control. Effects on body weight and adiposity. *The Journal of clinical investigation*, 102(2), 412-420.
85. Handschin, C., & Spiegelman, B. M. (2008). The role of exercise and PGC1 α in inflammation and chronic disease. *Nature*, 454(7203), 463.
86. Hankir, M. K., Kranz, M., Keipert, S., Weiner, J., Andreasen, S. G., Kern, M., ... & Hesse, S. (2017). Dissociation Between Brown Adipose Tissue 18F-FDG Uptake and Thermogenesis in Uncoupling Protein 1-Deficient Mice. *Journal of Nuclear Medicine*, 58(7), 1100-1103.
87. Harms, M., & Seale, P. (2013). Brown and beige fat: development, function and therapeutic potential. *Nature medicine*, 19(10), 1252.
88. Haslam, D., & James, W. (2005). Obesity IJ J. *Lancet*, 366(9492)
89. Hauner, H. (2005). Secretory factors from human adipose tissue and their functional role. *Proceedings of the Nutrition Society*, 64(2), 163-169.
90. Hayward, J. S., & Lisson, P. A. (1992). Evolution of brown fat: its absence in marsupials and monotremes. *Canadian Journal of Zoology*, 70(1), 171-179.
91. Heilbronn, L., Smith, S. R., & Ravussin, E. (2004). Failure of fat cell proliferation, mitochondrial function and fat oxidation results in ectopic fat storage, insulin resistance and type II diabetes mellitus. *International journal of obesity*, 28(S4), S12.
92. Himms-Hagen, J., Melnyk, A., Zingaretti, M. C., Ceresi, E., Barbatelli, G., & Cinti, S. (2000). Multilocular fat cells in WAT of CL-316243-treated rats derive directly from white adipocytes. *American Journal of Physiology-Cell Physiology*, 279(3), C670-C681.
93. Holm, C., Fredrikson, G., Cannon, B., & Belfrage, P. (1987). Hormone-sensitive lipase in brown adipose tissue: identification and effect of cold exposure. *Bioscience reports*, 7(11), 897-904.
94. Hondares, E., Iglesias, R., Giralt, A., Gonzalez, F. J., Giralt, M., Mampel, T., & Villarroya, F. (2011). Thermogenic activation induces FGF21 expression and release in brown adipose tissue. *Journal of Biological Chemistry*, 286(15), 12983-12990.
95. Hondares, E., Mora, O., Yubero, P., de la Concepción, M. R., Iglesias, R., Giralt, M., & Villarroya, F. (2006). Thiazolidinediones and rexinoids induce peroxisome proliferator-

- activated receptor-coactivator (PGC)-1 α gene transcription: an autoregulatory loop controls PGC-1 α expression in adipocytes via peroxisome proliferator-activated receptor- γ coactivation. *Endocrinology*, 147(6), 2829-2838.
96. Hondares, E., Rosell, M., Gonzalez, F. J., Giralt, M., Iglesias, R., & Villarroya, F. (2010). Hepatic FGF21 expression is induced at birth via PPAR α in response to milk intake and contributes to thermogenic activation of neonatal brown fat. *Cell metabolism*, 11(3), 206-212.
 97. Houstek, J., Andersson, U., Tvrdík, P., Nedergaard, J., & Cannon, B. (1995). The expression of subunit c correlates with and thus may limit the biosynthesis of the mitochondrial F₀F₁-ATPase in brown adipose tissue. *Journal of Biological Chemistry*, 270(13), 7689-7694.
 98. Huttunen, P., Hirvonen, J., & Kinnula, V. (1981). The occurrence of brown adipose tissue in outdoor workers. *European journal of applied physiology and occupational physiology*, 46(4), 339-345.
 99. Hüttemann, M., Lee, I., Samavati, L., Yu, H., & Doan, J. W. (2007). Regulation of mitochondrial oxidative phosphorylation through cell signaling. *Biochimica et Biophysica Acta (BBA)-Molecular Cell Research*, 1773(12), 1701-1720.
 100. Iismaa, S. E., Mearns, B. M., Lorand, L., & Graham, R. M. (2009). Transglutaminases and disease: lessons from genetically engineered mouse models and inherited disorders. *Physiological reviews*, 89(3), 991-1023.
 101. Ikeda, K., Kang, Q., Yoneshiro, T., Camporez, J. P., Maki, H., Homma, M., ... & Tajima, K. (2017). UCP1-independent signaling involving SERCA2b-mediated calcium cycling regulates beige fat thermogenesis and systemic glucose homeostasis. *Nature medicine*, 23(12), 1454.
 102. Ikeda, S. I., Tamura, Y., Kakehi, S., Sanada, H., Kawamori, R., & Watada, H. (2016). Exercise-induced increase in IL-6 level enhances GLUT4 expression and insulin sensitivity in mouse skeletal muscle. *Biochemical and biophysical research communications*, 473(4), 947-952.
 103. Ishibashi, J., & Seale, P. (2010). Beige can be slimming. *Science*, 328(5982), 1113-1114.
 104. Jacobsson, A., Stadler, U., Glotzer, M. A., & Kozak, L. P. (1985). Mitochondrial uncoupling protein from mouse brown fat. Molecular cloning, genetic mapping, and mRNA expression. *Journal of Biological Chemistry*, 260(30), 16250-16254.
 105. Jacobus, W. E., & Lehninger, A. L. (1973). Creatine kinase of rat heart mitochondria coupling of creatine phosphorylation to electron transport. *Journal of Biological Chemistry*, 248(13), 4803-4810.
 106. Jambrovics, K., Uray, I. P., Keresztessy, Z., Keillor, J. W., Fésüs, L., & Balajthy, Z. (2019). Transglutaminase 2 programs differentiating acute promyelocytic leukemia cells in all-trans retinoic acid treatment to inflammatory stage through NF- κ B activation. *haematologica*, 104(3), 505-515.

107. Jedrychowski, M. P., Wrann, C. D., Paulo, J. A., Gerber, K. K., Szpyt, J., Robinson, M. M., ... & Spiegelman, B. M. (2015). Detection and quantitation of circulating human irisin by tandem mass spectrometry. *Cell metabolism*, 22(4), 734-740.
108. Jespersen, N. Z., Larsen, T. J., Peijs, L., Dagaard, S., Homøe, P., Loft, A., ... & Pedersen, B. K. (2013). A classical brown adipose tissue mRNA signature partly overlaps with brite in the supraclavicular region of adult humans. *Cell metabolism*, 17(5), 798-805.
109. Kajimura, S., Seale, P., Kubota, K., Lunsford, E., Frangioni, J. V., Gygi, S. P., & Spiegelman, B. M. (2009). Initiation of myoblast to brown fat switch by a PRDM16–C/EBP- β transcriptional complex. *Nature*, 460(7259), 1154.
110. Kajimura, S., Seale, P., Tomaru, T., Erdjument-Bromage, H., Cooper, M. P., Ruas, J. L., ... & Spiegelman, B. M. (2008). Regulation of the brown and white fat gene programs through a PRDM16/CtBP transcriptional complex. *Genes & development*, 22(10), 1397-1409.
111. Kajimura, S., Spiegelman, B. M., & Seale, P. (2015). Brown and beige fat: physiological roles beyond heat generation. *Cell metabolism*, 22(4), 546-559.
112. Kazak, L., Chouchani, E. T., Jedrychowski, M. P., Erickson, B. K., Shinoda, K., Cohen, P., ... & Kajimura, S. (2015). A creatine-driven substrate cycle enhances energy expenditure and thermogenesis in beige fat. *Cell*, 163(3), 643-655.
113. Kazak, L., Chouchani, E. T., Lu, G. Z., Jedrychowski, M. P., Bare, C. J., Mina, A. I., ... & Dzeja, P. (2017). Genetic depletion of adipocyte creatine metabolism inhibits diet-induced thermogenesis and drives obesity. *Cell metabolism*, 26(4), 660-671.
114. Kazantzis, M., Takahashi, V., Hinkle, J., Kota, S., Zilberfarb, V., Issad, T., ... & Strosberg, A. D. (2012). PAZ6 cells constitute a representative model for human brown pre-adipocytes. *Frontiers in endocrinology*, 3, 13.
115. Keillor, J. W., Chica, R. A., Chabot, N., Vinci, V., Pardin, C., Fortin, E., ... & Lubell, W. D. (2008). The bioorganic chemistry of transglutaminase—from mechanism to inhibition and engineering. *Canadian Journal of Chemistry*, 86(4), 271-276.
116. Keillor, J. W., Chica, R. A., Chabot, N., Vinci, V., Pardin, C., Fortin, E., ... & Lubell, W. D. (2008). The bioorganic chemistry of transglutaminase—from mechanism to inhibition and engineering. *Canadian Journal of Chemistry*, 86(4), 271-276.
117. Kelly, M., Gauthier, M. S., Saha, A. K., & Ruderman, N. B. (2009). Activation of AMP-activated protein kinase by interleukin-6 in rat skeletal muscle: association with changes in cAMP, energy state, and endogenous fuel mobilization. *Diabetes*, 58(9), 1953-1960.
118. Kim, H., Wrann, C. D., Jedrychowski, M., Vidoni, S., Kitase, Y., Nagano, K., ... & Strutzenberg, T. S. (2018). Irisin mediates effects on bone and fat via α V integrin receptors. *Cell*, 175(7), 1756-1768.
119. Kim, J. K., Kim, H. J., Park, S. Y., Cederberg, A., Westergren, R., Nilsson, D., ... & Cline, G. W. (2005). Adipocyte-specific overexpression of FOXC2 prevents diet-induced

- increases in intramuscular fatty acyl CoA and insulin resistance. *Diabetes*, 54(6), 1657-1663.
120. Király, R., Thangaraju, K., Nagy, Z., Collighan, R., Nemes, Z., Griffin, M., & Fésüs, L. (2016). Isopeptidase activity of human transglutaminase 2: disconnection from transamidation and characterization by kinetic parameters. *Amino acids*, 48(1), 31-40.
 121. Kleiner, S., Douris, N., Fox, E. C., Mepani, R. J., Verdeguer, F., Wu, J., ... & Spiegelman, B. M. (2012). FGF21 regulates PGC-1 α and browning of white adipose tissues in adaptive thermogenesis. *Genes & development*, 26(3), 271-281.
 122. Knudsen, J. G., Murholm, M., Carey, A. L., Biensø, R. S., Basse, A. L., Allen, T. L., ... & Pilegaard, H. (2014). Role of IL-6 in exercise training-and cold-induced UCP1 expression in subcutaneous white adipose tissue. *PloS one*, 9(1), e84910.
 123. Kong, X., Banks, A., Liu, T., Kazak, L., Rao, R. R., Cohen, P., ... & Cypess, A. M. (2014). IRF4 is a key thermogenic transcriptional partner of PGC-1 α . *Cell*, 158(1), 69-83.
 124. Koza, R. A., Kozak, U. C., Brown, L. J., Leiter, E. H., MacDonald, M. J., & Kozak, L. P. (1996). Sequence and tissue-dependent RNA expression of mouse FAD-linked glycerol-3-phosphate dehydrogenase. *Archives of biochemistry and biophysics*, 336(1), 97-104.
 125. Kozak, L. P., & Young, M. E. (2012). Heat from calcium cycling melts fat. *Nature medicine*, 18(10), 1458.
 126. Kramarova, T. V., Shabalina, I. G., Andersson, U., Westerberg, R., Carlberg, I., Houstek, J., ... & Cannon, B. (2008). Mitochondrial ATP synthase levels in brown adipose tissue are governed by the c-Fo subunit P1 isoform. *The FASEB Journal*, 22(1), 55-63.
 127. Kristóf, E., Doan-Xuan, Q. M., Bai, P., Bacso, Z., & Fésüs, L. (2015). Laser-scanning cytometry can quantify human adipocyte browning and proves effectiveness of irisin. *Scientific reports*, 5, 12540.
 128. Kristóf, E., Doan-Xuan, Q. M., Bai, P., Bacso, Z., & Fésüs, L. (2015). Laser-scanning cytometry can quantify human adipocyte browning and proves effectiveness of irisin. *Scientific reports*, 5, 12540.
 129. Kristóf, E., Klusóczki, Á., Veress, R., Shaw, A., Combi, Z. S., Varga, K., ... & Fésüs, L. (2019). Interleukin-6 released from differentiating human beige adipocytes improves browning. *Experimental cell research*, 377(1-2), 47-55.
 130. Kwok, K. H., Lam, K. S., & Xu, A. (2016). Heterogeneity of white adipose tissue: molecular basis and clinical implications. *Experimental & molecular medicine*, 48(3), e215.
 131. Lapunzina, P. (2005, August). Risk of tumorigenesis in overgrowth syndromes: a comprehensive review. In *American Journal of Medical Genetics Part C: Seminars in Medical Genetics* (Vol. 137, No. 1, pp. 53-71). Hoboken: Wiley Subscription Services, Inc., A Wiley Company.

132. Lardy, H., & Shrago, E. (1990). Biochemical aspects of obesity. *Annual review of biochemistry*, 59(1), 689-710.
133. Lee, P., Werner, C. D., Kebebew, E., & Celi, F. S. (2014). Functional thermogenic beige adipogenesis is inducible in human neck fat. *International journal of obesity*, 38(2), 170.
134. Lee, Y. H., Petkova, A. P., Mottillo, E. P., & Granneman, J. G. (2012). In vivo identification of bipotential adipocyte progenitors recruited by β 3-adrenoceptor activation and high-fat feeding. *Cell metabolism*, 15(4), 480-491.
135. Lepper, C., & Fan, C. M. (2010). Inducible lineage tracing of Pax7-descendant cells reveals embryonic origin of adult satellite cells. *genesis*, 48(7), 424-436.
136. Lidell, M. E., Betz, M. J., Leinhard, O. D., Heglind, M., Elander, L., Slawik, M., ... & Virtanen, K. A. (2013). Evidence for two types of brown adipose tissue in humans. *Nature medicine*, 19(5), 631.
137. Lidell, M. E., Seifert, E. L., Westergren, R., Heglind, M., Gowing, A., Sukonina, V., ... & Fernandez-Rodriguez, J. (2011). The adipocyte-expressed forkhead transcription factor Foxc2 regulates metabolism through altered mitochondrial function. *Diabetes*, 60(2), 427-435.
138. Lin, C. S., & Klingenberg, M. (1980). Isolation of the uncoupling protein from brown adipose tissue mitochondria. *FEBS letters*, 113(2), 299-303.
139. Lindberg, O., De Pierre, J., Rylander, E., & Afzelius, B. A. (1967). Studies of the mitochondrial energy-transfer system of brown adipose tissue. *The Journal of cell biology*, 34(1), 293-310.
140. Lindquist, J. M., Fredriksson, J. M., Rehnmark, S., Cannon, B., & Nedergaard, J. (2000). β 3- and α 1-adrenergic Erk1/2 activation is Src-but not Gi-mediated in Brown adipocytes. *Journal of Biological Chemistry*, 275(30), 22670-22677.
141. Long, J. Z., Svensson, K. J., Bateman, L. A., Lin, H., Kamenecka, T., Lokurkar, I. A., ... & Paulo, J. A. (2016). The secreted enzyme PM20D1 regulates lipidated amino acid uncouplers of mitochondria. *Cell*, 166(2), 424-435.
142. Lorand, L., & Graham, R. M. (2003). Transglutaminases: crosslinking enzymes with pleiotropic functions. *Nature reviews Molecular cell biology*, 4(2), 140.
143. Lynes, M. D., & Tseng, Y. H. (2015). The thermogenic circuit: regulators of thermogenic competency and differentiation. *Genes & diseases*, 2(2), 164-172.
144. Mádi, A., Cuaranta-Monroy, I., Lénárt, K., Pap, A., Mezei, Z. A., Kristóf, E., ... & Fésüs, L. (2017). Browning deficiency and low mobilization of fatty acids in gonadal white adipose tissue leads to decreased cold-tolerance of transglutaminase 2 knock-out mice. *Biochimica et Biophysica Acta (BBA)-Molecular and Cell Biology of Lipids*, 1862(12), 1575-1586.

145. Mårin, P., Andersson, B., Ottosson, M., Olbe, L., Chowdhury, B., Kvist, H., ... & Björntorp, P. (1992). The morphology and metabolism of intraabdominal adipose tissue in men. *Metabolism*, 41(11), 1242-1248.
146. Markan, K. R., Naber, M. C., Ameka, M. K., Anderegg, M. D., Mangelsdorf, D. J., Kliewer, S. A., ... & Potthoff, M. J. (2014). Circulating FGF21 is liver derived and enhances glucose uptake during refeeding and overfeeding. *Diabetes*, 63(12), 4057-4063.
147. Mathur, N., & Pedersen, B. K. (2008). Exercise as a mean to control low-grade systemic inflammation. *Mediators of inflammation*, 2008.
148. Matsushita, M., Yoneshiro, T., Aita, S., Kameya, T., Sugie, H., & Saito, M. (2014). Impact of brown adipose tissue on body fatness and glucose metabolism in healthy humans. *International journal of obesity*, 38(6), 812.
149. Matthias, A., Ohlson, K. B., Fredriksson, J. M., Jacobsson, A., Nedergaard, J., & Cannon, B. (2000). Thermogenic responses in brown fat cells are fully Ucp1-dependent UCP2 or UCP3 do not substitute for UCP1 in adrenergically or fatty acid-induced thermogenesis. *Journal of Biological Chemistry*, 275(33), 25073-25081.
150. Minokoshi, Y., Haque, M. S., & Shimazu, T. (1999). Microinjection of leptin into the ventromedial hypothalamus increases glucose uptake in peripheral tissues in rats. *Diabetes*, 48(2), 287-291.
151. Morrison, S. F., Madden, C. J., & Tupone, D. (2012). Central control of brown adipose tissue thermogenesis. *Frontiers in endocrinology*, 3, 5.
152. Munir, H., Luu, N. T., Clarke, L. S., Nash, G. B., & McGettrick, H. M. (2016). Comparative ability of mesenchymal stromal cells from different tissues to limit neutrophil recruitment to inflamed endothelium. *PLoS One*, 11(5), e0155161.
153. Müller, S., Balaz, M., Stefanicka, P., Varga, L., Amri, E. Z., Ukropec, J., ... & Wolfrum, C. (2016). Proteomic analysis of human brown adipose tissue reveals utilization of coupled and uncoupled energy expenditure pathways. *Scientific reports*, 6, 30030.
154. Myneni, V. D., Melino, G., & Kaartinen, M. T. (2015). Transglutaminase 2—a novel inhibitor of adipogenesis. *Cell death & disease*, 6(8), e1868.
155. Nakaoka, H., Perez, D. M., Baek, K. J., Das, T., Husain, A., Misono, K., ... & Graham, R. M. (1994). Gh: a GTP-binding protein with transglutaminase activity and receptor signaling function. *Science*, 264(5165), 1593-1596.
156. Néchad, M., Ruka, E., & Thibault, J. (1994). Production of nerve growth factor by brown fat in culture: relation with the in vivo developmental stage of the tissue. *Comparative Biochemistry and Physiology Part A: Physiology*, 107(2), 381-388.
157. Nedergaard, J., Petrovic, N., Lindgren, E. M., Jacobsson, A., & Cannon, B. (2005). PPAR γ in the control of brown adipocyte differentiation. *Biochimica et Biophysica Acta (BBA)-Molecular Basis of Disease*, 1740(2), 293-304.

158. Nguyen, K. D., Qiu, Y., Cui, X., Goh, Y. S., Mwangi, J., David, T., ... & Chawla, A. (2011). Alternatively activated macrophages produce catecholamines to sustain adaptive thermogenesis. *Nature*, 480(7375), 104.
159. Nicholls, D. G. (1976). The bioenergetics of brown adipose tissue mitochondria. *FEBS letters*, 61(2), 103-110.
160. Nicholls, D. G., & Locke, R. M. (1984). Thermogenic mechanisms in brown fat. *Physiological reviews*, 64(1), 1-64.
161. Nisoli, E. N. Z. O., Tonello, C. R. I. S. T. I. N. A., Benarese, M. A. R. I. N. A., Liberini, P. A. O. L. O., & Carruba, M. O. (1996). Expression of nerve growth factor in brown adipose tissue: implications for thermogenesis and obesity. *Endocrinology*, 137(2), 495-503.
162. Oelkrug, R., Goetze, N., Exner, C., Lee, Y., Ganjam, G. K., Kutschke, M., ... & Heldmaier, G. (2013). Brown fat in a protoendothermic mammal fuels eutherian evolution. *Nature communications*, 4, 2140.
163. .
164. Ohno, H., Shinoda, K., Spiegelman, B. M., & Kajimura, S. (2012). PPAR γ agonists induce a white-to-brown fat conversion through stabilization of PRDM16 protein. *Cell metabolism*, 15(3), 395-404.
165. Ortega, M. T., Xie, L., Mora, S., & Chapes, S. K. (2011). Evaluation of macrophage plasticity in brown and white adipose tissue. *Cellular immunology*, 271(1), 124-133.
166. Ouellet, V., Labbé, S. M., Blondin, D. P., Phoenix, S., Guérin, B., Haman, F., ... & Carpentier, A. C. (2012). Brown adipose tissue oxidative metabolism contributes to energy expenditure during acute cold exposure in humans. *The Journal of clinical investigation*, 122(2), 545-552.
167. Ouellet, V., Routhier-Labadie, A., Bellemare, W., Lakhel-Chaieb, L., Turcotte, E., Carpentier, A. C., & Richard, D. (2011). Outdoor temperature, age, sex, body mass index, and diabetic status determine the prevalence, mass, and glucose-uptake activity of 18F-FDG-detected BAT in humans. *The Journal of Clinical Endocrinology & Metabolism*, 96(1), 192-199.
168. Palominos, M. M., Dünner, N. H., Wabitsch, M., & Rojas, C. V. (2015). Angiotensin II directly impairs adipogenic differentiation of human preadipose cells. *Molecular and cellular biochemistry*, 408(1-2), 115-122.
169. Pedersen, B. K., & Febbraio, M. A. (2012). Muscles, exercise and obesity: skeletal muscle as a secretory organ. *Nature Reviews Endocrinology*, 8(8), 457.
170. Peppler, W. T., Townsend, L. K., Knuth, C. M., Foster, M. T., & Wright, D. C. (2017). Subcutaneous inguinal white adipose tissue is responsive to, but dispensable for, the metabolic health benefits of exercise. *American Journal of Physiology-Endocrinology and Metabolism*, 314(1), E66-E77.

171. Perdikari, A., Leparc, G. G., Balaz, M., Pires, N. D., Lidell, M. E., Sun, W., ... & Balazova, L. (2018). Batlas: deconvoluting brown adipose tissue. *Cell reports*, 25(3), 784-797.
172. Peters, M., Schirmacher, P., Goldschmitt, J., Odenthal, M., Peschel, C., Fattori, E., ... & Rose-John, S. (1997). Extramedullary expansion of hematopoietic progenitor cells in interleukin (IL)-6-sIL-6R double transgenic mice. *Journal of Experimental Medicine*, 185(4), 755-766.
173. Peters, M., Schirmacher, P., Goldschmitt, J., Odenthal, M., Peschel, C., Fattori, E., ... & Rose-John, S. (1997). Extramedullary expansion of hematopoietic progenitor cells in interleukin (IL)-6-sIL-6R double transgenic mice. *Journal of Experimental Medicine*, 185(4), 755-766.
174. Petrovic, N., Walden, T. B., Shabalina, I. G., Timmons, J. A., Cannon, B., & Nedergaard, J. (2010). Chronic peroxisome proliferator-activated receptor γ (PPAR γ) activation of epididymally derived white adipocyte cultures reveals a population of thermogenically competent, UCP1-containing adipocytes molecularly distinct from classic brown adipocytes. *Journal of Biological Chemistry*, 285(10), 7153-7164.
175. Pinkas, D. M., Strop, P., Brunger, A. T., & Khosla, C. (2007). Transglutaminase 2 undergoes a large conformational change upon activation. *PLoS biology*, 5(12), e327.
176. Pinkas, D. M., Strop, P., Brunger, A. T., & Khosla, C. (2007). Transglutaminase 2 undergoes a large conformational change upon activation. *PLoS biology*, 5(12), e327.
177. Poher, A. L., Altirriba, J., Veyrat-Durebex, C., & Rohner-Jeanrenaud, F. (2015). Brown adipose tissue activity as a target for the treatment of obesity/insulin resistance. *Frontiers in physiology*, 6, 4.
178. Prusiner, S. B., Cannon, B., & Lindberg, O. (1968). Oxidative Metabolism in Cells Isolated from Brown Adipose Tissue: 1. Catecholamine and Fatty Acid Stimulation of Respiration. *European journal of biochemistry*, 6(1), 15-22.
179. Puigserver, P., Wu, Z., Park, C. W., Graves, R., Wright, M., & Spiegelman, B. M. (1998). A cold-inducible coactivator of nuclear receptors linked to adaptive thermogenesis. *Cell*, 92(6), 829-839.
180. Qiang, L., Wang, L., Kon, N., Zhao, W., Lee, S., Zhang, Y., ... & Accili, D. (2012). Brown remodeling of white adipose tissue by SirT1-dependent deacetylation of Ppar γ . *Cell*, 150(3), 620-632.
181. Raschke, S., Elsen, M., Gassenhuber, H., Sommerfeld, M., Schwahn, U., Brockmann, B., ... & Hallén, J. (2013). Evidence against a beneficial effect of irisin in humans. *PloS one*, 8(9), e73680.
182. Ratner, P. L., Fisher, M., Burkart, D., Cook, J. R., & Kozak, L. P. (1981). The role of mRNA levels and cellular localization in controlling sn-glycerol-3-phosphate dehydrogenase expression in tissues of the mouse. *Journal of Biological Chemistry*, 256(7), 3576-3579.

183. Ravussin, E., & Smith, S. R. (2002). Increased fat intake, impaired fat oxidation, and failure of fat cell proliferation result in ectopic fat storage, insulin resistance, and type 2 diabetes mellitus. *Annals of the New York Academy of Sciences*, 967(1), 363-378.
184. Ricquier, D. (2011). Uncoupling protein 1 of brown adipocytes, the only uncoupler: a historical perspective. *Frontiers in endocrinology*, 2, 85.
185. Ricquier, D., Mory, G., & Hemon, P. (1979). Changes induced by cold adaptation in the brown adipose tissue from several species of rodents, with special reference to the mitochondrial components. *Canadian journal of biochemistry*, 57(11), 1262-1266
186. Rosell, M., Kaforou, M., Frontini, A., Okolo, A., Chan, Y. W., Nikolopoulou, E., ... & Moore, J. D. (2014). Brown and white adipose tissues: intrinsic differences in gene expression and response to cold exposure in mice. *American Journal of Physiology-Endocrinology and Metabolism*, 306(8), E945-E964.
187. Rosen, E. D., & Spiegelman, B. M. (2000). Molecular regulation of adipogenesis. *Annual review of cell and developmental biology*, 16(1), 145-171.
188. Rosen, E. D., & Spiegelman, B. M. (2001). PPAR γ : a nuclear regulator of metabolism, differentiation, and cell growth. *Journal of Biological Chemistry*, 276(41), 37731-37734.
189. Rosen, E. D., & Spiegelman, B. M. (2014). What we talk about when we talk about fat. *Cell*, 156(1-2), 20-44.
190. Rosen, E. D., Sarraf, P., Troy, A. E., Bradwin, G., Moore, K., Milstone, D. S., ... & Mortensen, R. M. (1999). PPAR γ is required for the differentiation of adipose tissue in vivo and in vitro. *Molecular cell*, 4(4), 611-617.
191. Rosenwald, M., Perdikari, A., Röllicke, T., & Wolfrum, C. (2013). Bi-directional interconversion of brite and white adipocytes. *Nature cell biology*, 15(6), 659.
192. Rowland, L. A., Bal, N. C., Kozak, L. P., & Periasamy, M. (2015). Uncoupling protein 1 and sarcolipin are required to maintain optimal thermogenesis, and loss of both systems compromises survival of mice under cold stress. *Journal of Biological Chemistry*, 290(19), 12282-12289.
193. Ryu, V., Garretson, J. T., Liu, Y., Vaughan, C. H., & Bartness, T. J. (2015). Brown adipose tissue has sympathetic-sensory feedback circuits. *Journal of Neuroscience*, 35(5), 2181-2190.
194. Saito, M., Okamatsu-Ogura, Y., Matsushita, M., Watanabe, K., Yoneshiro, T., Nio-Kobayashi, J., ... & Kawai, Y. (2009). High incidence of metabolically active brown adipose tissue in healthy adult humans: effects of cold exposure and adiposity. *Diabetes*, 58(7), 1526-1531.
195. Sakurai, T., Ogasawara, J., Kizaki, T., Sato, S., Ishibashi, Y., Takahashi, M., ... & Ishida, H. (2013). The effects of exercise training on obesity-induced dysregulated expression of adipokines in white adipose tissue. *International journal of endocrinology*, 2013.

196. Sanchez-Gurmaches, J., Hung, C. M., Sparks, C. A., Tang, Y., Li, H., & Guertin, D. A. (2012). PTEN loss in the Myf5 lineage redistributes body fat and reveals subsets of white adipocytes that arise from Myf5 precursors. *Cell metabolism*, 16(3), 348-362.
197. Sarang, Z., Köröskényi, K., Pallai, A., Duró, E., Melino, G., Griffin, M., ... & Szondy, Z. (2011). Transglutaminase 2 null macrophages respond to lipopolysaccharide stimulation by elevated proinflammatory cytokine production due to an enhanced $\alpha\beta3$ integrin-induced Src tyrosine kinase signaling. *Immunology letters*, 138(1), 71-78.
198. Sarang, Z., Madi, A., Koy, C., Varga, S., Glocker, M. O., Ucker, D. S., ... & Szondy, Z. (2007). Tissue transglutaminase (TG2) facilitates phosphatidylserine exposure and calpain activity in calcium-induced death of erythrocytes. *Cell death and differentiation*, 14(10), 1842.
199. Sarang, Z., Tóth, B., Balajthy, Z., Köröskényi, K., Garabuczi, E., Fésüs, L., & Szondy, Z. (2009). Some lessons from the tissue transglutaminase knockout mouse. *Amino acids*, 36(4), 625.
200. Sárvári, A. K., Doan-Xuan, Q. M., Bacsó, Z., Csomós, I., Balajthy, Z., & Fésüs, L. (2015). Interaction of differentiated human adipocytes with macrophages leads to trogocytosis and selective IL-6 secretion. *Cell death & disease*, 6(1), e1613.
201. Sárvári, A. K., Doan-Xuan, Q. M., Bacsó, Z., Csomós, I., Balajthy, Z., & Fésüs, L. (2015). Interaction of differentiated human adipocytes with macrophages leads to trogocytosis and selective IL-6 secretion. *Cell death & disease*, 6(1), e1613.
202. Sárvári, A. K., Veréb, Z., Uray, I. P., Fésüs, L., & Balajthy, Z. (2014). Atypical antipsychotics induce both proinflammatory and adipogenic gene expression in human adipocytes in vitro. *Biochemical and biophysical research communications*, 450(4), 1383-1389.
203. Schlottmann, I., Ehrhart-Bornstein, M., Wabitsch, M., Bornstein, S. R., & Lamounier-Zepter, V. (2014). Calcium-dependent release of adipocyte fatty acid binding protein from human adipocytes. *International journal of obesity*, 38(9), 1221.
204. Schulz, T. J., Huang, P., Huang, T. L., Xue, R., McDougall, L. E., Townsend, K. L., ... & Tseng, Y. H. (2013). Brown-fat paucity due to impaired BMP signalling induces compensatory browning of white fat. *Nature*, 495(7441), 379.
205. Schulz, T. J., Huang, T. L., Tran, T. T., Zhang, H., Townsend, K. L., Shadrach, J. L., ... & Schrier, D. (2011). Identification of inducible brown adipocyte progenitors residing in skeletal muscle and white fat. *Proceedings of the National Academy of Sciences*, 108(1), 143-148.
206. Scuteri, A., Sanna, S., Chen, W. M., Uda, M., Albai, G., Strait, J., ... & Dei, M. (2007). Genome-wide association scan shows genetic variants in the FTO gene are associated with obesity-related traits. *PLoS genetics*, 3(7), e115.
207. Seale, P., Bjork, B., Yang, W., Kajimura, S., Chin, S., Kuang, S., ... & Tempst, P. (2008). PRDM16 controls a brown fat/skeletal muscle switch. *Nature*, 454(7207), 961.

208. Seale, P., Conroe, H. M., Estall, J., Kajimura, S., Frontini, A., Ishibashi, J., ... & Spiegelman, B. M. (2011). Prdm16 determines the thermogenic program of subcutaneous white adipose tissue in mice. *The Journal of clinical investigation*, 121(1), 96-105.
209. Seale, P., Kajimura, S., Yang, W., Chin, S., Rohas, L. M., Uldry, M., ... & Spiegelman, B. M. (2007). Transcriptional control of brown fat determination by PRDM16. *Cell metabolism*, 6(1), 38-54.
210. Shan, T., Liang, X., Bi, P., Zhang, P., Liu, W., & Kuang, S. (2013). Distinct populations of adipogenic and myogenic Myf5-lineage progenitors in white adipose tissues. *Journal of lipid research*, 54(8), 2214-2224.
211. Sharp, L. Z., Shinoda, K., Ohno, H., Scheel, D. W., Tomoda, E., Ruiz, L., ... & Kajimura, S. (2012). Human BAT possesses molecular signatures that resemble beige/brite cells. *PloS one*, 7(11), e49452.
212. Shih, M. F., & Taberner, P. V. (1995). Selective activation of brown adipocyte hormone-sensitive lipase and cAMP production in the mouse by β 3-adrenoceptor agonists. *Biochemical pharmacology*, 50(5), 601-608.
213. Shinoda, K., Luijten, I. H., Hasegawa, Y., Hong, H., Sonne, S. B., Kim, M., ... & Nedergaard, J. (2015). Genetic and functional characterization of clonally derived adult human brown adipocytes. *Nature medicine*, 21(4), 389.
214. Shinoda, K., Luijten, I. H., Hasegawa, Y., Hong, H., Sonne, S. B., Kim, M., ... & Nedergaard, J. (2015). Genetic and functional characterization of clonally derived adult human brown adipocytes. *Nature medicine*, 21(4), 389.
215. Shoelson, S. E., Herrero, L., & Naaz, A. (2007). Obesity, inflammation, and insulin resistance. *Gastroenterology*, 132(6), 2169-2180.
216. Stanford, K. I., Middelbeek, R. J., Townsend, K. L., An, D., Nygaard, E. B., Hitchcox, K. M., ... & Goodyear, L. J. (2012). Brown adipose tissue regulates glucose homeostasis and insulin sensitivity. *The Journal of clinical investigation*, 123(1).
217. Steensberg, A., Van Hall, G., Osada, T., Sacchetti, M., Saltin, B., & Pedersen, B. K. (2000). Production of interleukin-6 in contracting human skeletal muscles can account for the exercise-induced increase in plasma interleukin-6. *The Journal of physiology*, 529(1), 237-242.
218. Stine, R. R., Shapira, S. N., Lim, H. W., Ishibashi, J., Harms, M., Won, K. J., & Seale, P. (2016). EBF2 promotes the recruitment of beige adipocytes in white adipose tissue. *Molecular metabolism*, 5(1), 57-65.
219. Stine, R. R., Shapira, S. N., Lim, H. W., Ishibashi, J., Harms, M., Won, K. J., & Seale, P. (2016). EBF2 promotes the recruitment of beige adipocytes in white adipose tissue. *Molecular metabolism*, 5(1), 57-65.
220. Stockebrand, M., Nejad, A. S., Neu, A., Kharbanda, K. K., Sauter, K., Schillemeit, S., ... & Choe, C. U. (2016). Transcriptomic and metabolic analyses reveal salvage pathways in creatine-deficient AGAT^{-/-} mice. *Amino acids*, 48(8), 2025-2039

221. Svensson, P. A., Jernås, M., Sjöholm, K., Hoffmann, J. M., Nilsson, B. E., Hansson, M., & Carlsson, L. (2011). Gene expression in human brown adipose tissue. *International journal of molecular medicine*, 27(2), 227-232.
222. Szántó, M., Rutkai, I., Hegedűs, C., Czikora, Á., Rózsahegyí, M., Kiss, B., ... & Bai, P. (2011). Poly (ADP-ribose) polymerase-2 depletion reduces doxorubicin-induced damage through SIRT1 induction. *Cardiovascular research*, 92(3), 430-438.
223. Szondy, Z., Sarang, Z., Molnár, P., Németh, T., Piacentini, M., Mastroberardino, P. G., ... & Szegezdi, É. (2003). Transglutaminase 2-/-mice reveal a phagocytosis-associated crosstalk between macrophages and apoptotic cells. *Proceedings of the National Academy of Sciences*, 100(13), 7812-7817.
224. Taube, M., Andersson-Assarsson, J. C., Lindberg, K., Pereira, M. J., Gäbel, M., Svensson, M. K., ... & Svensson, P. A. (2015). Evaluation of reference genes for gene expression studies in human brown adipose tissue. *Adipocyte*, 4(4), 280-285.
225. Tenorio, J., Arias, P., Martínez-Glez, V., Santos, F., García-Miñaur, S., Nevado, J., & Lapunzina, P. (2014). Simpson-Golabi-Behmel syndrome types I and II. *Orphanet journal of rare diseases*, 9(1), 138.
226. Terblanche, S. E., Masondo, T. C., & Nel, W. (1998). Effects of cold acclimation on the activity levels of creatine kinase, lactate dehydrogenase and lactate dehydrogenase isoenzymes in various tissues of the rat. *Cell biology international*, 22(9-10), 701-707.
227. Tews, D., & Wabitsch, M. (2011). Renaissance of brown adipose tissue. *Hormone research in paediatrics*, 75(4), 231-239.
228. Tews, D., Fischer-Posovszky, P., Fromme, T., Klingenspor, M., Fischer, J., Rüther, U., ... & Wabitsch, M. (2013). FTO deficiency induces UCP-1 expression and mitochondrial uncoupling in adipocytes. *Endocrinology*, 154(9), 3141-3151.
229. Tews, D., Fromme, T., Keuper, M., Hofmann, S. M., Debatin, K. M., Klingenspor, M., ... & Fischer-Posovszky, P. (2017). Teneurin-2 (TENM2) deficiency induces UCP1 expression in differentiating human fat cells. *Molecular and cellular endocrinology*, 443, 106-113.
230. Tews, D., Pula, T., Funcke, J. B., Jastroch, M., Keuper, M., Debatin, K. M., ... & Fischer-Posovszky, P. (2019). Elevated UCP1 levels are sufficient to improve glucose uptake in human white adipocytes. *Redox biology*, 26, 101286.
231. Thomas, C., Gioiello, A., Noriega, L., Strehle, A., Oury, J., Rizzo, G., ... & Pellicciari, R. (2009). TGR5-mediated bile acid sensing controls glucose homeostasis. *Cell metabolism*, 10(3), 167-177.
232. Timmons, J. A., Wennmalm, K., Larsson, O., Walden, T. B., Lassmann, T., Petrovic, N., ... & Nedergaard, J. (2007). Myogenic gene expression signature establishes that brown and white adipocytes originate from distinct cell lineages. *Proceedings of the National Academy of Sciences*, 104(11), 4401-4406.
233. Tontonoz, P., Hu, E., & Spiegelman, B. M. (1994). Stimulation of adipogenesis in fibroblasts by PPAR γ 2, a lipid-activated transcription factor. *Cell*, 79(7), 1147-1156.

234. Tóth, B., Garabuczi, É., Sarang, Z., Vereb, G., Vámosi, G., Aeschlimann, D., ... & Zhang, A. (2009). Transglutaminase 2 is needed for the formation of an efficient phagocyte portal in macrophages engulfing apoptotic cells. *The Journal of Immunology*, 182(4), 2084-2092.
235. Trayhurn, P., & Beattie, J. H. (2001). Physiological role of adipose tissue: white adipose tissue as an endocrine and secretory organ. *Proceedings of the Nutrition Society*, 60(3), 329-339.
236. Trayhurn, P., & Wood, I. S. (2004). Adipokines: inflammation and the pleiotropic role of white adipose tissue. *British journal of nutrition*, 92(3), 347-355.
237. Tseng, Y. H., Kokkotou, E., Schulz, T. J., Huang, T. L., Winnay, J. N., Taniguchi, C. M., ... & Ahrens, M. J. (2008). New role of bone morphogenetic protein 7 in brown adipogenesis and energy expenditure. *Nature*, 454(7207), 1000.
238. van Marken Lichtenbelt, W. D., & Schrauwen, P. (2011). Implications of non-shivering thermogenesis for energy balance regulation in humans. *American Journal of Physiology-Heart and Circulatory Physiology*
239. van Marken Lichtenbelt, Wouter D., et al. "Cold-activated brown adipose tissue in healthy men." *New England Journal of Medicine* 360.15 (2009): 1500-1508.
240. Vaughan, C. H., & Bartness, T. J. (2012). Anterograde transneuronal viral tract tracing reveals central sensory circuits from brown fat and sensory denervation alters its thermogenic responses. *American Journal of Physiology-Regulatory, Integrative and Comparative Physiology*, 302(9), R1049-R1058.
241. Vegiopoulos, A., Müller-Decker, K., Strzoda, D., Schmitt, I., Chichelnitskiy, E., Ostertag, A., ... & Meyer, C. W. (2010). Cyclooxygenase-2 controls energy homeostasis in mice by de novo recruitment of brown adipocytes. *Science*, 328(5982), 1158-1161.
242. Villanueva, C. J., Vergnes, L., Wang, J., Drew, B. G., Hong, C., Tu, Y., ... & Wroblewski, K. (2013). Adipose subtype-selective recruitment of TLE3 or Prdm16 by PPAR γ specifies lipid storage versus thermogenic gene programs. *Cell metabolism*, 17(3), 423-435.
243. Villarroya, F., & Vidal-Puig, A. (2013). Beyond the sympathetic tone: the new brown fat activators. *Cell metabolism*, 17(5), 638-643.
244. Villarroya, F., Cereijo, R., Villarroya, J., & Giralt, M. (2017). Brown adipose tissue as a secretory organ. *Nature Reviews Endocrinology*, 13(1), 26.
245. Virtanen, K. A., Lidell, M. E., Orava, J., Heglind, M., Westergren, R., Niemi, T., ... & Nuutila, P. (2009). Functional brown adipose tissue in healthy adults. *New England Journal of Medicine*, 360(15), 1518-1525.
246. Vitali, A., Murano, I., Zingaretti, M. C., Frontini, A., Ricquier, D., & Cinti, S. (2012). The adipose organ of obesity-prone C57BL/6J mice is composed of mixed white and brown adipocytes. *Journal of lipid research*, 53(4), 619-629.

247. Wabitsch, M., Brenner, R. E., Melzner, I., Braun, M., Möller, P., Heinze, E., ... & Hauner, H. (2001). Characterization of a human preadipocyte cell strain with high capacity for adipose differentiation. *International journal of obesity*, 25(1), 8.
248. Wajchenberg, B. L. (2000). Subcutaneous and visceral adipose tissue: their relation to the metabolic syndrome. *Endocrine reviews*, 21(6), 697-738.
249. Wallenius, V., Wallenius, K., Ahrén, B., Rudling, M., Carlsten, H., Dickson, S. L., ... & Jansson, J. O. (2002). Interleukin-6-deficient mice develop mature-onset obesity. *Nature medicine*, 8(1), 75.
250. Wallenius, V., Wallenius, K., Ahrén, B., Rudling, M., Carlsten, H., Dickson, S. L., ... & Jansson, J. O. (2002). Interleukin-6-deficient mice develop mature-onset obesity. *Nature medicine*, 8(1), 75.
251. Wang, G. X., Zhao, X. Y., Meng, Z. X., Kern, M., Dietrich, A., Chen, Z., ... & Li, S. (2014). The brown fat-enriched secreted factor Nrg4 preserves metabolic homeostasis through attenuation of hepatic lipogenesis. *Nature medicine*, 20(12), 1436.
252. Wang, Q. A., Tao, C., Gupta, R. K., & Scherer, P. E. (2013). Tracking adipogenesis during white adipose tissue development, expansion and regeneration. *Nature medicine*, 19(10), 1338.
253. Wang, S. P., Laurin, N., Himms-Hagen, J., Rudnicki, M. A., Levy, E., Robert, M. F., ... & Mitchell, G. A. (2001). The adipose tissue phenotype of hormone-sensitive lipase deficiency in mice. *Obesity research*, 9(2), 119-128.
254. Wang, W., Kissig, M., Rajakumari, S., Huang, L., Lim, H. W., Won, K. J., & Seale, P. (2014). Ebf2 is a selective marker of brown and beige adipogenic precursor cells. *Proceedings of the National Academy of Sciences*, 111(40), 14466-14471.
255. Wang, W., Kissig, M., Rajakumari, S., Huang, L., Lim, H. W., Won, K. J., & Seale, P. (2014). Ebf2 is a selective marker of brown and beige adipogenic precursor cells. *Proceedings of the National Academy of Sciences*, 111(40), 14466-14471.
256. Wang, Z., & Griffin, M. (2012). TG2, a novel extracellular protein with multiple functions. *Amino acids*, 42(2-3), 939-949.
257. Watanabe, M., Houten, S. M., Matakai, C., Christoffolete, M. A., Kim, B. W., Sato, H., ... & Schoonjans, K. (2006). Bile acids induce energy expenditure by promoting intracellular thyroid hormone activation. *Nature*, 439(7075), 484.
258. Weir, G., Ramage, L. E., Akyol, M., Rhodes, J. K., Kyle, C. J., Fletcher, A. M., ... & Ashton, C. (2018). Substantial metabolic activity of human brown adipose tissue during warm conditions and cold-induced lipolysis of local triglycerides. *Cell metabolism*, 27(6), 1348-1355.
259. White, P. J., St-Pierre, P., Charbonneau, A., Mitchell, P. L., St-Amand, E., Marcotte, B., & Marette, A. (2014). Protectin DX alleviates insulin resistance by activating a myokine-liver gluco-regulatory axis. *Nature medicine*, 20(6), 664.

260. Whittle, A. J., Carobbio, S., Martins, L., Slawik, M., Hondares, E., Vázquez, M. J., ... & Dale, M. (2012). BMP8B increases brown adipose tissue thermogenesis through both central and peripheral actions. *Cell*, 149(4), 871-885.
261. Wilkin, T. J., & Voss, L. D. (2004). Metabolic syndrome: maladaptation to a modern world. *Journal of the Royal Society of Medicine*, 97(11), 511-520
262. Winther, S., Isidor, M. S., Basse, A. L., Skjoldborg, N., Cheung, A., Quistorff, B., & Hansen, J. B. (2017). Restricting glycolysis impairs brown adipocyte glucose and oxygen consumption. *American Journal of Physiology-Endocrinology and Metabolism*, 314(3), E214-E223.
263. World Health Organization. (2000). *Obesity: preventing and managing the global epidemic* (No. 894). World Health Organization.
264. Wu, J., Boström, P., Sparks, L. M., Ye, L., Choi, J. H., Giang, A. H., ... & Huang, K. (2012). Beige adipocytes are a distinct type of thermogenic fat cell in mouse and human. *Cell*, 150(2), 366-376.
265. Wu, J., Boström, P., Sparks, L. M., Ye, L., Choi, J. H., Giang, A. H., ... & Huang, K. (2012). Beige adipocytes are a distinct type of thermogenic fat cell in mouse and human. *Cell*, 150(2), 366-376.
266. Wu, Z., & Boss, O. (2007). Targeting PGC-1 α to control energy homeostasis. *Expert opinion on therapeutic targets*, 11(10), 1329-1338.
267. Xue, R., Lynes, M. D., Dreyfuss, J. M., Shamsi, F., Schulz, T. J., Zhang, H., ... & Weiner, L. S. (2015). Clonal analyses and gene profiling identify genetic biomarkers of the thermogenic potential of human brown and white preadipocytes. *Nature medicine*, 21(7), 760.
268. Xue, Y., Petrovic, N., Cao, R., Larsson, O., Lim, S., Chen, S., ... & Cannon, B. (2009). Hypoxia-independent angiogenesis in adipose tissues during cold acclimation. *Cell metabolism*, 9(1), 99-109.
269. Yamashita, H., Sato, Y., Kizaki, T., Oh-ishi, S., Nagasawa, J. I., & Ohno, H. (1994). Basic fibroblast growth factor (bFGF) contributes to the enlargement of brown adipose tissue during cold acclimation. *Pflügers Archiv*, 428(3-4), 352-356.
270. Yeo, C. R., Agrawal, M., Hoon, S., Shabbir, A., Shrivastava, M. K., Huang, S., ... & Vidal-Puig, A. (2017). SGBS cells as a model of human adipocyte browning: A comprehensive comparative study with primary human white subcutaneous adipocytes. *Scientific reports*, 7(1), 4031.
271. Young, P. J. R. S., Arch, J. R. S., & Ashwell, M. (1984). Brown adipose tissue in the parametrial fat pad of the mouse. *FEBS letters*, 167(1), 10-14.
272. Younis, S., Rosner, I., Rimar, D., Boulman, N., Rozenbaum, M., Odeh, M., & Slobodin, G. (2013). Weight change during pharmacological blockade of interleukin-6 or tumor necrosis factor- α in patients with inflammatory rheumatic disorders: a 16-week comparative study. *Cytokine*, 61(2), 353-355.

273. Younis, S., Rosner, I., Rimar, D., Boulman, N., Rozenbaum, M., Odeh, M., & Slobodin, G. (2013). Interleukin 6 Blockade–Associated Weight Gain With Abdominal Enlargement in a Patient With Rheumatoid Arthritis. *JCR: Journal of Clinical Rheumatology*, 19(1), 48-49.
274. Zhang, Y., Proenca, R., Maffei, M., Barone, M., Leopold, L., & Friedman, J. M. (1994). Positional cloning of the mouse obese gene and its human homologue. *Nature*, 372(6505), 425.
275. Zilberfarb, V., Piétri-Rouxel, F., Jockers, R., Krief, S., Delouis, C., Issad, T., & Strosberg, A. D. (1997). Human immortalized brown adipocytes express functional beta3-adrenoceptor coupled to lipolysis. *Journal of Cell Science*, 110(7), 801-807.

9. KEYWORDS

SGBS adipocyte, human preadipocyte, rosiglitazone, irisin, browning, beige, thermogenesis
differentiation, obesity, cytokine

9. TÁRGYSZAVAK

SGBS adipociták, human preadipocita, roziglitazon, irisin, browning, beige, termogenezis,
differenciáció, elhízás, citokinek

10. ACKNOWLEDGEMENTS

First of all, I would like to express my sincere gratitude to my supervisor, Prof. Dr. László Fésüs, for the excellent training, continuous support and motivation, and the scientific discussions during my Ph.D. studies. I am very grateful that he gave me the opportunity to learn and work in his research group. Secondly, I am especially thankful to Dr. Endre Kristóf for helping me with his constructive advices and scientific discussions.

Many thanks to all the past and present member of the Cellular Biochemistry Research Group for the friendly working atmosphere. Special thanks to Dr. Mária Szatmári-Tóth for her continuous help and sharing her knowledge and experience with me. I also would like to thank to Jennifer Nagy, Attiláné Klem and Anikó Nagy for their technical assistance.

I am really grateful to our long-term collaborators in Hungary: Dr. Zsolt Bacsó, Dr. Péter Bai and Dr. Zoltán Veréb for their excellent help in Laser-scanning image acquisition and analysis or in cellular respiration measurements or multiparametric analysis; and our collaborators in Germany: Prof. Dr. Martin Wabitsch and Prof. Dr. Pamela Fischer-Posovszky for providing us the SGBS cell line and samples.

I am also thankful to former undergraduate students (Zsolt Combi, Attila Vámos, Boglárka Vinnai) who worked with me on experiments related to human adipocyte browning.

I am also thankful for Prof. Dr. József Tőzsér, the Head of the Department of Biochemistry and Molecular Biology, for the opportunity to work in a well-equipped institute. Furthermore, I would like to thank all my colleagues from the Department of Biochemistry and Molecular Biology.

I wish to express my deepest gratitude to my colleagues and dear friends for their kindness and great emotional support.

Most importantly and dearly, I would like to thank my beloved family and to all of my dear friends helping me get through the difficult times and for their continuous encouragement. My deepest gratitude I wish to express to my mother who supported me in each situation and with her help I could write my thesis after giving birth to my child.



UNIVERSITY of
DEBRECEN

UNIVERSITY AND NATIONAL LIBRARY
UNIVERSITY OF DEBRECEN

H-4002 Egyetem tér 1, Debrecen

Phone: +3652/410-443, email: publikaciok@lib.unideb.hu

Registry number:
Subject:

DEENK/348/2019.PL
PhD Publikációs Lista

Candidate: Ágnes Klusóczki

Neptun ID: E5EAEN

Doctoral School: Doctoral School of Molecular Cellular and Immune Biology

MTMT ID: 10056744

List of publications related to the dissertation

1. **Klusóczki, Á.**, Veréb, Z., Vámos, A., Fischer-Posovszky, P., Wabitsch, M., Bacsó, Z., Fésüs, L., Kristóf, E.: Differentiating SGBS adipocytes respond to PPAR γ stimulation, irisin and BMP7 by functional browning and beige characteristics.
Sci. Rep. 9 (1), 1-35, 2019.
DOI: <http://dx.doi.org/10.1038/s41598-019-42256-0>
IF: 4.011 (2018)
2. Kristóf, E., **Klusóczki, Á.**, Veress, R., Shaw, A., Combi, Z., Varga, K., Györy, F., Balajthy, Z., Bai, P., Bacsó, Z., Fésüs, L.: Interleukin-6 released from differentiating human beige adipocytes improves browning.
Exp. Cell Res. 377 (1-2), 47-55, 2019.
DOI: <http://dx.doi.org/10.1016/j.yexcr.2019.02.015>
IF: 3.329 (2018)





List of other publications

3. Kristóf, E., Doan-Xuan, Q. M., Sárvári, A. K., **Klusóczki, Á.**, Fischer-Posovszky, P., Wabitsch, M., Bacsó, Z., Bai, P., Balajthy, Z., Fésüs, L.: Clozapine modifies the differentiation program of human adipocytes inducing browning.
Transl. Psychiatry. 6 (11), 1-12, 2016.
IF: 4.73

Total IF of journals (all publications): 12,07

Total IF of journals (publications related to the dissertation): 7,34

The Candidate's publication data submitted to the iDEa Tudóstér have been validated by DEENK on the basis of the Journal Citation Report (Impact Factor) database.

18 October, 2019

